Statistical methods to assess the hydrodynamic boundary conditions for risk based design approaches in coastal engineering

Methods and application to the German North Sea coastline

Vom Department für Bauingenieurwesen der Naturwissenschaftlich-Technischen Fakultät der Universität Siegen angenommene

Dissertation

zur Erlangung des akademischen Grades

Doktor der Ingenieurwissenschaften (Dr.-Ing.)

von

Dipl.-Ing. Thomas Wahl

Geboren am 16.06.1981 in Siegen

Referent: **Univ.-Prof. Dr.-Ing. Jürgen Jensen**
                   Universität Siegen

Korreferent: **Prof. Robert Nicholls BSc PhD**
                   University of Southampton

Siegen, im Februar 2012 | Tag der mündlichen Prüfung: 11.06.2012

About the cover picture:

The cover picture shows a compilation of some of the most important coastal defence structures, which can be found along the German North Sea coastline. From left to right: a flood protection wall as part of the coastal defence line of the "Polder Hamburg Süd" in the harbour of Hamburg; a segment of the dike next to the harbour of Hoernum in the southeast of Sylt Island; the barrage "Schmidtkanal" in Hamburg-Wilhelmsburg as part of the complex flood protection system of the city of Hamburg.

Contact: Thomas Wahl | e-Mail: thomas-wahl@web.de

Acknowledgements

A number of reviewers provided helpful comments (mostly anonymous) on the manuscripts of the journal articles, which form the basis for this thesis. Sylvin Müller-Navarra (BSH) commented on the manuscript which became Sect. 2 of the thesis. Ivan Haigh (University of Western Australia) served as a reviewer for one of the manuscripts (Sect. 4 of the thesis) and provided helpful comments on my research. We became good friends during our cooperation, which I hope will continue in the future.

Data sets were provided by the Shipping Administration of the Federal Government (WSA), the Government-Owned Company for Coastal Protection, National Parks and Ocean Protection (LKN), Svetlana Jevrejeva (Proudman Oceanographic Laboratory), Aimée Slangen (Utrecht University) and were downloaded from the website of the Permanent Service for Mean Sea Level (PSMSL).

Finally, I want to thank my parents Uwe and Irene Wahl for being the best parents in the world and my fiancée Janina for her support, inspiration, patience and love.

Abstract

Worldwide, coastal areas are considered important settlement and industrial areas and host some of the most valuable ecological systems of our planet. At the same time, they are particularly vulnerable to natural catastrophes; this includes the low lying areas along the German North Sea coastline. In the past, and partly even today, coastal structures were most often designed with simple deterministic approaches. Nowadays, risk based design methods become more and more important in modern coastal engineering applications. Thereby, one of the main challenges consists in estimating the input variables or relevant loading parameters for coastal defence structures, respectively. These parameters need to be determined for current and possible future climate conditions in order to guarantee high safety standards throughout the expected lifetime of a structure (e.g. 100 years). This thesis deals with the important loading parameters for coastal defence structures, i.e. mean sea level (MSL), storm surges and wind waves, as well as with their statistical assessment, representing an integral part of any risk analysis.

In order to analyse past changes in MSL along the German North Sea coastline, methods to generate long and high quality observational MSL time series are further developed and new analysis techniques are introduced. With these methods and based on tide gauge data dating back to the mid 19th century, observed changes in mean sea level are reconstructed and analysed in detail. To achieve meaningful results from risk assessments it is furthermore indispensable to consider a large sample of storm surge scenarios. Such scenarios can be derived with hydrodynamic model simulations or with empirical approaches, whereas both methods are very time consuming and therefore restrict the number of scenarios. Here, a stochastic approach to simulate storm surge scenarios is introduced. The results can be used as input data for risk analyses or other applications, but can also be considered as a basis for statistical assessments. In this thesis, multivariate statistical models based on Copula functions are developed and applied. With these statistical models it is for the first time possible to take all relevant loading parameters (i.e. selected storm surge and wave parameters) into account. Hence, the exceedance probabilities to be used within risk assessments can be calculated more reliably than before, as demonstrated in the German Bight study area.

Kurzfassung

Weltweit gelten Küstengebiete als wichtige Siedlungs- und Wirtschaftsräume und stellen sich als Räume mit einigen der wertvollsten Ökosysteme unseres Planeten dar. Gleichzeitig sind sie durch Naturkatastrophen besonders gefährdet, dies schließt die tiefliegenden Gebiete entlang der deutschen Nordseeküste ein. Wurden Küstenschutzanlagen in der Vergangenheit, und teilweise noch heute, mithilfe vereinfachter deterministischer Verfahren bemessen, so gewinnen risikobasierte Bemessungsverfahren im modernen Küsteningenieurwesen immer mehr an Bedeutung. Eine besondere Herausforderung besteht in der Ermittlung der Eingangsgrößen bzw. der maßgebenden Belastungsparameter für Küstenschutzanlagen. Diese müssen nicht nur für heutige, sondern auch für mögliche zukünftige klimatische Bedingungen ermittelt werden um eine ausreichend hohe Sicherheit für die angedachte Lebensdauer eines Bauwerkes (z.B. 100 Jahre) zu gewährleisten. Die vorliegende Arbeit befasst sich mit den wichtigen Belastungsparamatern für Küstenschutzanlagen, dem mittleren Meeresspiegel (MSL), Sturmfluten und Windwellen, sowie deren statistischer Analyse, die Bestandteil jeder Risikobetrachtung ist.

Zur Untersuchung der in der Vergangenheit stattgefundenen MSL-Änderungen entlang der deutschen Nordseeküste werden Verfahren zur Generierung langer und qualitativ hochwertiger Beobachtungszeitreihen weiterentwickelt und neue Analysemethoden erarbeitet. Mithilfe dieser Verfahren und auf der Basis von bis ins 19. Jahrhundert zurückreichenden Pegeldaten werden die beobachteten Änderungen des MSL erstmalig im Detail nachvollzogen. Um belastbare Ergebnisse in der Risikoanalyse zu erzielen, ist des Weiteren eine große Anzahl an Sturmflutszenarien zu berücksichtigen, welche sich durch numerische Modellsimulationen oder auf Basis empirischer Ansätze nur in einem begrenzten Umfang und sehr zeitaufwendig generieren lassen. Hier wird ein stochastischer Ansatz zur Simulation von Sturmflutszenarien vorgestellt, wobei diese sowohl als Eingangsdaten für Risikobetrachtungen oder andere Anwendungen, aber auch als Grundlage für statistische Analysen herangezogen werden können. In der vorliegenden Arbeit werden multivariate statistische Modelle auf der Basis von Copula-Funktionen erarbeitet und vorgestellt, die es erstmalig erlauben alle wichtigen Belastungsparameter (d.h. ausgewählte Sturmflut- und Seegangsparameter) in die statistischen Betrachtungen einzubeziehen. Somit können Eintrittswahrscheinlichkeiten zur Berücksichtigung in der Risikoanalyse, wie hier am Beispiel der Deutschen Bucht gezeigt, mit größerer Genauigkeit berechnet werden, als es bisher der Fall war.

List of Papers

The main sections (i.e. Sects. 2 to 5) of this cumulative doctoral thesis are primarily based on four papers, which have been published in different international peer-reviewed journals.

Section 2: Wahl, T., Jensen, J. and Frank, T.: On analysing sea level rise in the German Bight since 1844, *Nat. Hazards Earth Syst. Sci.*, 10, 171–179, doi:10.5194/nhess-10-171-2010, 2010.

Section 3: Wahl, T., Jensen, J., Frank, T. and Haigh, I.D.: Improved estimates of mean sea level changes in the German Bight over the last 166 years, *Ocean Dynamics*, 61 (5), 701–715, doi: 10.1007/s10236-011-0383-x, 2011.

Section 4: Wahl, T., Mudersbach, C. and Jensen J.: Assessing the hydrodynamic boundary conditions for risk analyses in coastal areas: A stochastic storm surge model, *Nat. Hazards Earth Syst. Sci.*, 11, 2925-2939, doi:10.5194/nhess-11-2925-2011, 2011.

Section 5: Wahl, T., Mudersbach, C. and Jensen J.: Assessing the hydrodynamic boundary conditions for risk analyses in coastal areas: A multivariate statistical approach based on Copula functions, *Nat. Hazards Earth Syst. Sci.*, 12, 495-510, doi:10.5194/nhess-12-495-2012, 2012.

Although the papers have three or four authors, the main work was done by the first author. The co-authors were involved in the research projects where most of the presented methods and results were developed. They participated in helpful technical discussions and gave valuable advices and comments while preparing the manuscripts for the journal articles. Due to the cumulative character of the thesis, minor repetitions may occur in the individual sections.

List of Contents

List of Figures

List of Tables

Abbreviations and Symbols

Token	Unit	Description
a	[a]	year
a	[cmNN]	location parameter
AMSeL		research project: Mean Sea Level and Tidal Analysis along the German North Sea coastline
b	[cm]	scale parameter
BSH		Federal Maritime and Hydrographic Agency
C		cumulative distribution function of a Copula
c		probability density function of a Copula
CGCM		Coupled General Circulation Model
CGPS		Continuous Global Positioning System
NN		Normal Null (German ordnance datum)
D	[€]	risk analysis: damage
	[a]	mean sea level analyses: embedding dimension
EOF		empirical orthogonal function
EU		European Union
F	[cm*min/1000]	storm surge intensity
$F_X(x)$		cumulative distribution function
$f_X(x)$		probability density function
FLOODsite		research project: Integrated Flood Risk Analysis and Management Methodologies
FNAC		fully nested Archimedean Copula construction
GEV and *GEV(x)*		Generalized Extreme Value distribution
GIA		glacial isostatic adjustment
GoF		goodness of fit

Token	Unit	Description
GPD and *GP(x)*		Generalized Pareto distribution
H_s	[cm]	significant wave height
HW	[cmNN]	tidal high water
i		index variable
IKÜS		research project: Integrated Height Monitoring System in Coastal Regions
IPCC		Intergovernmental Panel on Climate Change
j		index variable
k		mean sea level analyses: *k*-factor (i.e. form parameter for the tide curve)
		statistics: shape parameter of a distribution
KDF or *K(x)*		Kernel Density Function
KS-test		Kolmogorov-Smirnov test
KTA		Nuclear Safety Standard Commission
logN(x)		LogNormal distribution
MA		moving average
MCAP		Monte-Carlo autoregressive padding
MHW and *MHW(t)*	[cmNN]	mean high water
MLW	[cmNN]	mean low water
MRL		mean residual life
MSE	[cm]	mean squared error
MSL and *MSL(t)*	[cm] or [cmNN]	mean sea level
MTL and *MTL(t)*	[cmNN]	mean tide level
MTR and *MTR(t)*	[cm]	mean tidal range
N		sample size (i.e. number of events)
n		number of occurrences
N(x)		Normal distribution

Token	Unit	Description
P_{10}	[cm]	parameter 10 (from paramterising observed storm surge events)
P_e	[1/a]	(joint) exceedance probability
P_{flood}	[1/a]	probability of flooding
PAC		pairwise Archimedean Copula construction
PLP		plotting position (i.e. empirical probability)
PNAC		partially nested Archimedean Copula construction
POT		peaks over threshold
PSMSL		Permanent Service for Mean Sea Level
r		Pearson's correlation coefficient
R_d		resistance
RMSE	[cm]	root mean squared error
RMSL	[cm] or [cmNN]	relative mean sea level
S	[cmNN]	highest turning point (i.e. maximum storm surge water level)
S_d		stress
SLR		sea level rise
SPR concept		Source-Pathway-Receptor concept
SRES		Special Report on Emission Scenarios
SSA		Singular System Analysis
STM		stability method
t	e.g. [s], [min]	time
THESEUS		research project: Innovative technologies for safer European coasts in a changing climate
u	[cm]	threshold value
U		uniformly distributed random variable
UK		United Kingdom

Token	Unit	Description
UNESCO		United Nations Educational, Scientific and Cultural Organization
V		uniformly distributed random variable
W	[cm]	water level
$WBL(x)$		Weibull distribution
XtremRisK		research project: Extreme Storm Surges at Open Coasts and Estuarine Areas – Risk Assessment and Mitigation under Climate Change Aspects
z_t		first order autoregressive model
α	e.g. [mm/a]	slope of a linear equation (i.e. linear trend)
β	[cm]	y-intercept of a linear equation
γ		linear equation
ε_t		white noise process
θ		mean sea level analyses: autocorrelation parameter
		multivariate statistics: Copula parameter
σ	[cm]	sigma
τ		Kendall's rank correlation
φ		Copula generator
χ^2		chi-squared

1   General introduction

Many of the world's coastlines are highly threatened by mean sea level rise and severe storm surges. The risk of flooding is expected to increase as sea levels are projected to rise at an accelerated rate throughout the 21st century and beyond (e.g. Meehl et al., 2007). At the same time, coastal regions are densely populated and host high monetary and ecological assets. Today, about 200 million people are already vulnerable to flooding by extreme sea levels (e.g. Hoozemans et al., 1993) and the number could grow to 800 million or even higher by the 2080s (Nicholls, 2004). A comprehensive review of possible implications and responses (i.e. mitigation and adaptation) to these changes was provided by Nicholls (2011). A summary of possible impacts for Europe's coastlines was presented by Nicholls and de La Vega-Leinert (2008). Bosello et al. (2011) estimated economic impacts due to sea level rise in Europe and found that Poland ($483 million) and Germany ($390 million) have to expect the highest economic losses (under a high sea level rise scenario by 2085 and without adaptation). To cope with these challenges, reliable design methods for coastal defence structures need to be established. Many different design approaches are described in the literature and most countries set up their own guidelines. Sometimes the considered approaches are not even consistent on a country-wide scale, as for example in Germany, where the federal states are responsible for coastal protection and every state has its own guideline.

In general, structures can be designed with deterministic or probabilistic approaches, whereas the latter are often divided into different categories. Following Plate (1993) and Mai (2004), Mudersbach (2010) used four categories (i.e. Level I to Level IV), which are described in the following. Further approaches to categorise probabilistic design approaches (or reliability methods) are described in the literature (e.g. Reeve, 2010), but are not discussed here. According to Mudersbach (2010) Level I methods compare the resistance R_d (for example the height of a dike) and the stress S_d (for example a storm surge

water level with a specified exceedance probability), whereas the structure has to be designed in a way that $R_d > S_d$. Partial safety factors have been developed to consider the uncertainties in the estimates of R_d and S_d. Mudersbach (2010) counts deterministic approaches among Level I methods, as deterministic approaches could also include probabilistic aspects (see also Plate, 1993). The difference between Level II and Level III methods is small and related to the level of detail, which is considered for the statistical analyses. With Level II/Level III methods probability density functions are calculated for both parameters R_d and S_d. By comparing these density functions, failure probabilities of existent flood defence structures can be determined. While Level II methods are based on the assumption that all parameters used to calculate R_d and S_d are normally distributed, Level III methods allow a free specification of the probability density functions (see also Mai, 2004). With Level IV methods, failure probabilities are calculated in the same way as with Level III methods, but the potential losses in the hinterland are also quantified and multiplied with the failure probabilities. Hence, Level IV methods include the most detailed analyses and the flood risk for a selected investigation area is calculated as:

$$risk = probability\ of\ failure \cdot potential\ losses \tag{1-1}$$

In recent years, different research projects focussed on performing vulnerability studies and risk assessments for coastal areas (e.g. FLOODsite: www.floodsite.net; XtremRisK: www.xtremrisk.de; THESEUS: www.theseusproject.eu). A widely used approach for risk analyses is based on the so-called Source-Pathway-Receptor (SPR) concept or Source-Pathway-Receptor-Consequences model, respectively (e.g. Oumeraci, 2004; FLOODsite, 2005). Fig. 1-1 shows that the application of the SPR concept starts with analysing different risk sources, before failure probabilities are calculated and breach models are used to identify the initial conditions for flood propagation behind the coastal defence line. Finally, potential losses in the hinterland are quantified. Direct and indirect losses, which could be classified into tangible (e.g. damages to infrastructure) and intangible (e.g. health impacts, loss of life) losses may be taken into account (e.g. Markau, 2003).

This thesis focuses on estimating the hydrodynamic boundary conditions for risk analyses in coastal areas (i.e. the risk sources shown in Fig. 1-1). All relevant loading parameters for coastal defence structures, i.e. mean sea levels (MSL), storm surges (here extreme still water levels as a combination of tides and wind surges) and wind waves, are analysed.

State of the art methods are applied and new approaches are introduced to explore these parameters separately, before an advanced multivariate statistical approach is presented to jointly examine all relevant loading parameters within risk assessments.
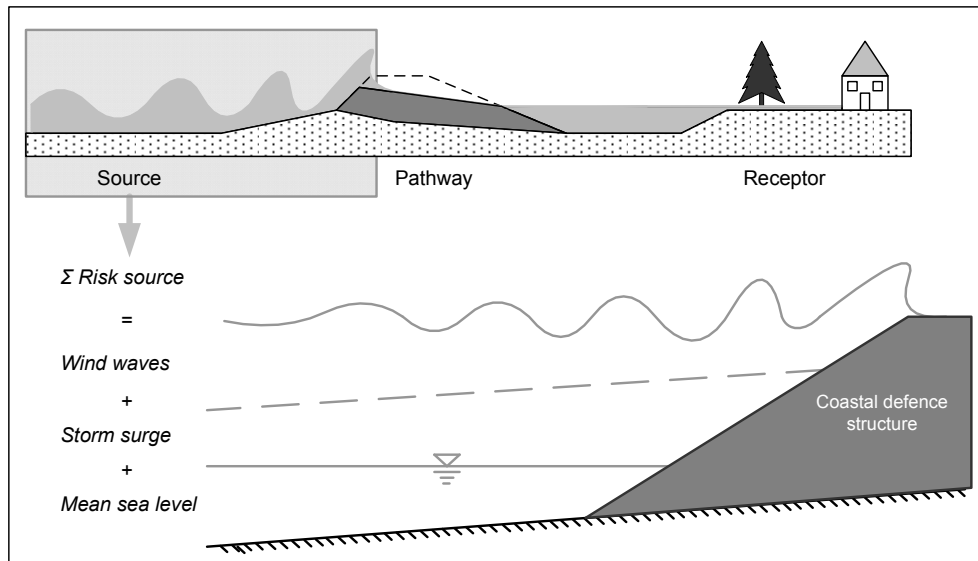
Figure 1-1:   Source-Pathway-Receptor concept and relevant risk sources for coastal areas.

The investigation area of the study is the German Bight, the shallow south-eastern part of the North Sea bounded by the Dutch boarder in the southwest and the Danish border in the northeast. Zeiler et al. (2008) divided the German North Sea into three zones: the offshore waters, the tidal flats of the Wadden Sea, which is one of the United Nations, Scientific and Cultural Organization (UNESCO) Natural World Heritage Sites, and the river estuaries (e.g. Elbe, Weser, Ems, Eider). The maximum depth of the German Bight is 56 m (in the Helgoland Bight), the average depth is 21 m and it covers approximately 18,000 km² (Uhlig and Sahlig, 1990). The tidal regime is semi-diurnal with a mean tidal range from about 2 m to 4 m (meso-tidal to low macro-tidal) (Zeiler et al., 2008). Wind surges (i.e. the difference between observed and predicted still water levels) can reach more than 5 m depending on the tidal phase. The highest surge with a height of 5.64 m occurred on the 9th of February in 1949 during tidal low water at the tide gauge of Husum (Tomczak, 1950). Significant wave heights (i.e. the average of the 33% highest waves observed during a specified time period) can reach up to 10 m or more in the offshore regions. For the area of Helgoland, Gaslikova (2006) estimated a significant wave height of 10 m to have a return period of 50 years, the 99-percentile for the German Bight was found to be 4-5 m from a wave climate hindcast (Weisse and Günther, 2007).

Almost 11,000 km² low lying coastal areas and 2.2 million people are protected from the impact of extreme sea levels (Schüttrumpf, 2008) in the German Bight, first of all by dikes, dunes, flood protection walls, barriers, flood gates and sluices. The dike line along the German North Sea coastline extends to approximately 1,200 km (Schüttrumpf, 2008) and, as an example, the coastal protection system for the city and harbour of Hamburg in the Elbe estuary involves 125 km of storm surge protection walls (Kortenhaus et al., 2008). The latter can also be found along the other major estuaries of the rivers Ems and Weser and on some of the East Frisian Islands. This highlights the need for sustainable coastal management strategies, including reliable risk based design approaches in order to assure high safety standards.

In the following subsections 1.1 to 1.3 the current knowledge about the relevant loading parameters for coastal structures is summarised. The focus is on presenting recent findings on possible future changes due to climate change. Observational records of the different parameters are discussed and considered for the analyses later in the thesis. Section 1.4 provides an introduction to joint probability methods, which have to be applied to derive realistic exceedance probabilities and reliable results from risk assessments. Section 1.5 defines and discusses the objectives of the thesis and then provides a detailed outline to the main sections that follow (i.e. Sects. 2 to 5).

1.1   Mean Sea Level

Sea level change is an important scientific topic as there is currently great concern about rising sea levels. Following a period of relative sea level stability since the end of the last deglaciation approximately 3000 years ago (Lambeck et al., 2010), estimates from archaeological proxy data (i.e. sediment cores collected in salt marshes) and from the few long tide gauge records reveal that there was an increase in the rate of sea level rise (SLR) during the late 19th and early 20th century (e.g. Mitchum et al., 2010; Woodworth et al., 2011). Church et al. (2006) estimated that global sea levels have risen by an average rate of 1.7 mm/a throughout the 20th century and it is predicted that this rise will continue throughout the 21st century at an accelerated rate (Meehl et al., 2007). Hence, mean sea level is considered the main driving factor for future changes in extreme still water levels and ongoing research efforts mainly focus on deriving reliable global and - in recent years also - regional SLR scenarios. Here, a brief summary of the current knowledge on possible

future sea level changes on different spatial scales is provided. This includes results from numerical models (i.e. Coupled Global Climate Models, CGCMs) and from applying probabilistic or semi-empirical approaches. Figure 1-2 shows selected global sea level rise scenarios for the 21st century. These scenarios are comparable, as they all assume a rise of the global mean near-surface temperature of at least 4°C by 2100. At present, global sea level scenarios published in the Intergovernmental Panel on Climate Change's (IPCC) fourth assessment report (AR4; Meehl et al., 2007) are most often considered for coastal planning purposes. The IPCC projected global sea levels to rise by between 0.18 and 0.59 m to the end of this century depending on the amount of future greenhouse gas emissions. The largest uncertainties in these estimates, derived from applying the latest generation of CGCMs, are related to the unknown role of ice sheet dynamics. A scaled-up ice sheet imbalance could add up to 0.20 m SLR depending on the emission scenario (Meehl et al., 2007). Emission scenarios considered by the IPCC are summarised in a Special Report on Emission Scenarios (SRES) (Nakićenović and Swart, 2000).
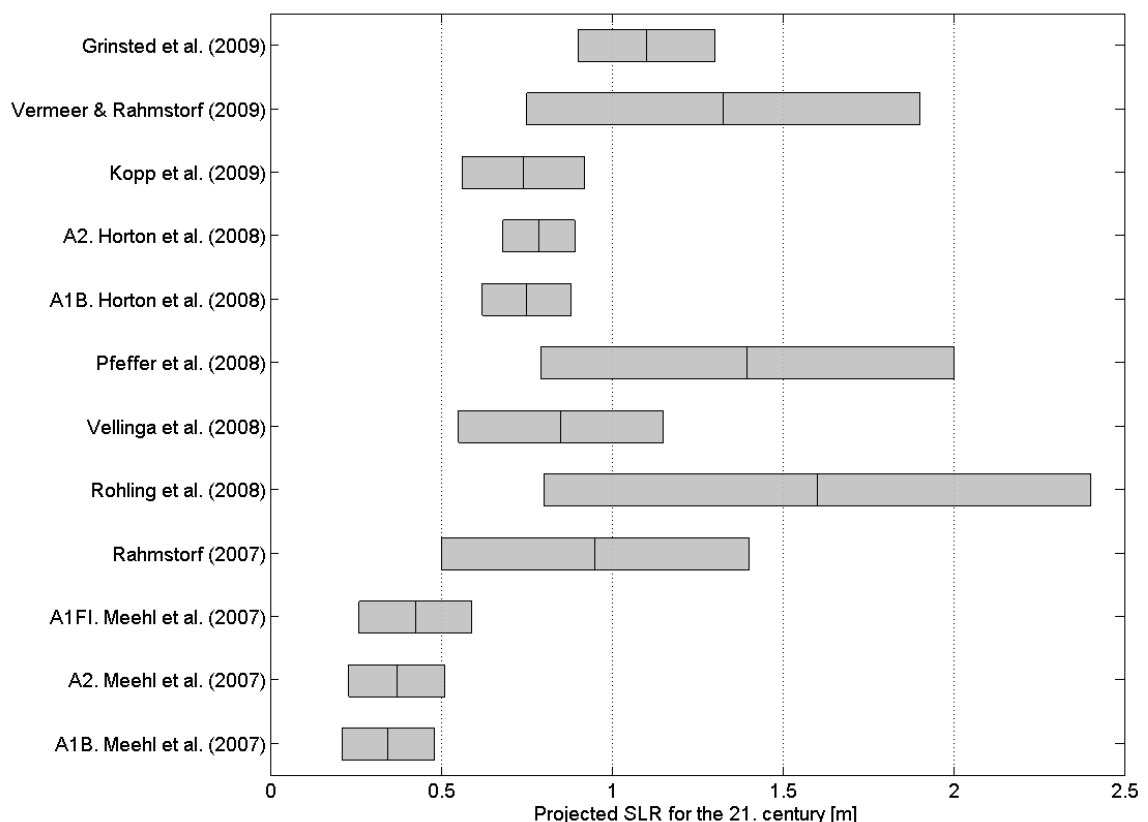
Figure 1-2:   Global sea level rise scenarios for the 21st century assuming at least 4°C temperature change (adapted from Nicholls et al., 2011).

Vellinga et al. (2008) analysed the different contributors to sea level changes. They considered latest observations of flux changes from the Antarctic and Greenland ice sheets and concluded that sea level might rise by 0.55 to 1.10 m until 2100 (and by 1.50 to 3.50 m until 2200). Rahmstorf (2007), Vermeer and Rahmstorf (2009) and Grinsted et al. (2009) used semi-empirical approaches, where historical temperature changes are linked to sea level changes to derive future scenarios. Horton et al. (2008) considered results from CGCMs and historical relationships between temperature and sea level to achieve future SLR estimates for different SRES scenarios. Kopp et al. (2008) used a probabilistic approach by taking into account paleo-climate data from the last interglacial period, serving as a climate analogue. A similar method, based on proxy data, was applied by Rohling et al. (2009) to obtain the scenario shown in Fig. 1-2. Pfeffer et al. (2008) explored the kinematic constraints on ice flow velocities to quantify glacier contributions to 21st century sea level rise. They provide low and high estimates of 0.8 m and 2.0 m SLR, respectively. It is apparent from Fig. 1-2 that the selected post-AR4 publications suggest higher SLR values for the 21st century than the IPCC did in 2007. The scattered results highlight that the uncertainties in projecting future global sea level changes are still considerable large. Further research activities are required to improve the confidence of such projections.

From observational records, it is also evident that regional sea level changes in the past differed significantly from the global average (e.g. Bindhoff et al., 2007). From 15 years of satellite altimetry data (1992 to 2007), the global average rate of SLR was found to be 3 mm/a, while the estimated local rates varied from about -10 to +10 mm/a (e.g. Milne et al., 2009). Possible reasons for these regional differences are discussed in Sects. 2 and 3 of the thesis. Hence, it is expected that future sea level changes will also not be uniformly distributed around the globe. This highlights the need for deriving reliable regional (or local) SLR scenarios to be considered for regional and local planning purposes.

Only few authors estimated possible future sea level changes for regions close to the German Bight. Figure 1-3 shows SLR scenarios, which have recently been published by Lowe et al. (2009) for the United Kingdom (UK) and by Katsman et al. (2008, 2011) for the northeast Atlantic region and the Dutch coastline, respectively. The estimates are based on IPCC projections and take regional oceanographic processes into account (scenarios shown in Fig. 1-3 do not include vertical land movements). Both authors provide 'likely' SLR scenarios (A1FI and A1B scenarios; 0.12 to 0.76 m for the UK and 0.40 to 0.80 m for

the Dutch coastline), as well as high-end scenarios (H++ scenarios in Fig. 1-3; 0.93 to 1.60 m for the UK and 0.40 to 1.05 m for the Dutch coastline). The latter are regarded as very unlikely to occur during the 21st century (probabilities of occurrence cannot be quantified), but are useful for vulnerability testing, as the uncertainties in the projections are currently not fully understood and hence such scenarios cannot be ruled out. The estimated regional changes for the UK and Dutch coastlines are slightly higher than global changes projected by the IPCC (i.e. 0.18 to 0.59 m), when the contribution of scaled-up ice sheet imbalances is not considered.
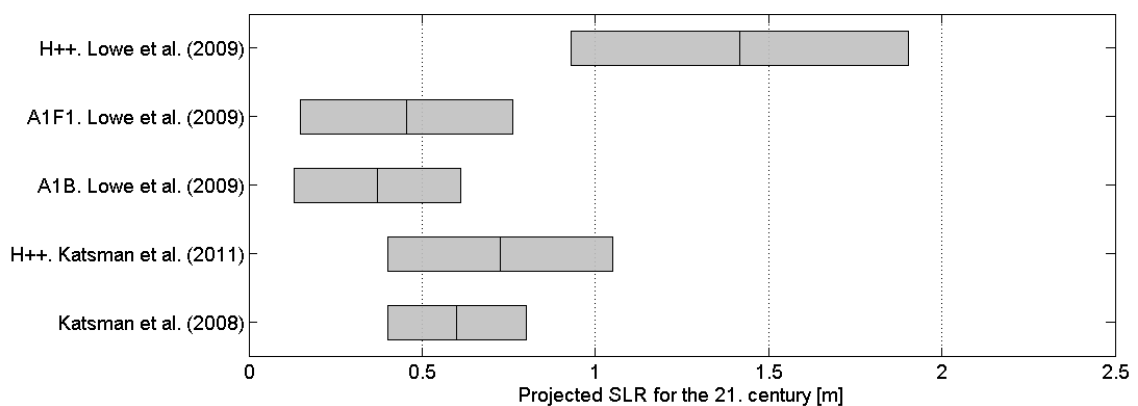
Figure 1-3:   Sea level rise scenarios for the 21st century and for regions close to the German Bight (all scenarios assume at least 4°C temperature rise).

For the German North Sea coastline similar SLR scenarios are not available at present. However, Slangen et al. (2011) used results from an ensemble of CGCMs (which were also used by the IPCC) and additionally analysed the main contributors to relative local sea level changes (i.e. gravitational effects, thermal expansion, ocean dynamics and glacial isostatic adjustment) to derive local SLR scenarios. Vertical land movements were considered in the study by superimposing model results for absolute sea level changes with estimates for global isostatic adjustment; hence the calculated changes are relative changes. For the A1B scenario global sea levels were projected to rise by 0.47 m throughout the the 21st century, while local projections of relative sea level change varied by between -3.91 m and +0.79 m (these are relative changes and negative values could also result from land uplift). Figure 1-4 shows results derived from nine different CGCMs (see labels of the y-axis) for the German Bight area (Slangen, pers. comm.). Local relative SLR scenarios for the 21st century were derived by combining the CGCM results with estimates for the main contributors to local sea level changes. In the figure, global average values are shown, as well as local estimates for grid points nearest to the German Bight (numbers in brackets are

longitude/latitude values of the considered model grid points). All models suggest local sea levels in the German North Sea to rise at higher rates than the global average (about 12 cm, resulting in a total rise of 59 cm by 2100). The differences are mainly caused by glacial isostatic adjustment (GIA), i.e. land subsidence along the German coastline. While some of the considered model grid points are located directly in the German Bight, others are near but not in the investigation area. This highlights that the model resolutions are still very coarse and the results derived from different models vary significantly. Similar findings were reported by Pardaens et al. (2011).
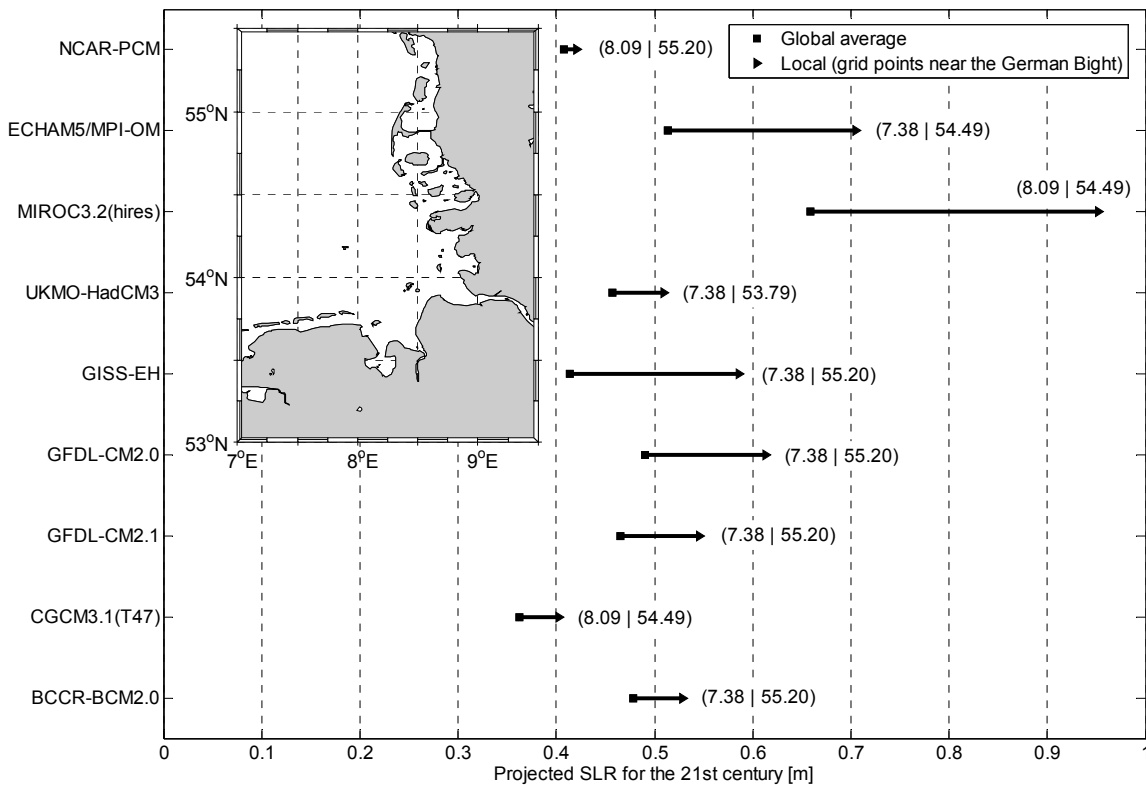
Figure 1-4:   Global and local sea level rise scenarios for the German North Sea and the 21st century derived from nine different CGCMs (data provided by Aimée Slangen, Institute for Marine and Atmospheric research Utrecht).

This brief summary of recent work on regional sea level changes shows that the importance of the subject has been recognised by the scientific community and some major improvements took place. However, much work needs to be done in the future to develop reliable SLR projections (for the German Bight and other areas) and to evaluate sustainable flood risk strategies.

1.2   Storm surges

Storm surges represent the most important loading factor for coastal defence structures in the German Bight. The coastline has always been exposed to extreme sea levels and devastating storm surge events (driven by extra-tropical or mid-latitude storms) occurred at irregular intervals throughout the last millennia. As a reaction, the first dikes were built in the 11th and 12th century to protect people and areas used for agriculture (Meier, 2008; Schüttrumpf, 2008). The chronicles written by Brahms in 1754 and 1757 gave first direction to modern dike forms.

A summary of historical storm surges in the North Sea can be found for example in Petersen and Rohde (1977) and Jensen and Müller-Navarra (2008). Two well known historical events, the Second St. Marcellus Flood (also known as Erste Grote Mandrenke or First Great Man-Drowning) and the Burchadiflood (also known as Zweite Grote Mandrenke or Second Great Man-Drowning), occurred in 1362 and 1634, respectively. In 1362 the island Rungholt and others were completely lost and both events reformed large parts of the coastline (e.g. von Storch et al., 2008a; Meier, 2008). The most disastrous and highest storm surges in the last century occurred on the 16/17 February 1962 and 3 January 1976. In 1962, 340 people died and large parts of the low lying areas along the coastlines and estuaries (first of all the city of Hamburg) were flooded. Most coastal structures were improved and raised as a reaction to this catastrophic event. This is why the damages caused by the 1976 storm surge were comparable small. However this 1976 event led to the highest water levels ever observed at most tide gauges along the German North Sea coastline, to date.

As outlined at the beginning of Sect. 1, modern design approaches involve statistical analyses of extreme sea levels. Nowadays, the Generalized Extreme Value distribution (GEV) or the Generalized Pareto distribution (GPD) are most widely used for extreme value statistics of still water levels and other climate related parameters (e.g. Coles 2001). It has been mentioned that mean sea level changes are expected to be the main driving factor for higher extreme sea levels in the future. Hence, possible future MSL changes need to be considered when performing statistical analyses to design coastal structures with expected lifetimes of up to 100 years or longer.

Figure 1-5 shows the MSL offset method, which is often used to combine SLR scenarios with extreme value statistics. Return periods for future extreme sea levels are examined by

just adding certain projections of MSL to return period curves derived from fitting distribution functions to observed data sets of extreme sea levels (e.g. Araújo and Pugh, 2008; Haigh, 2009).
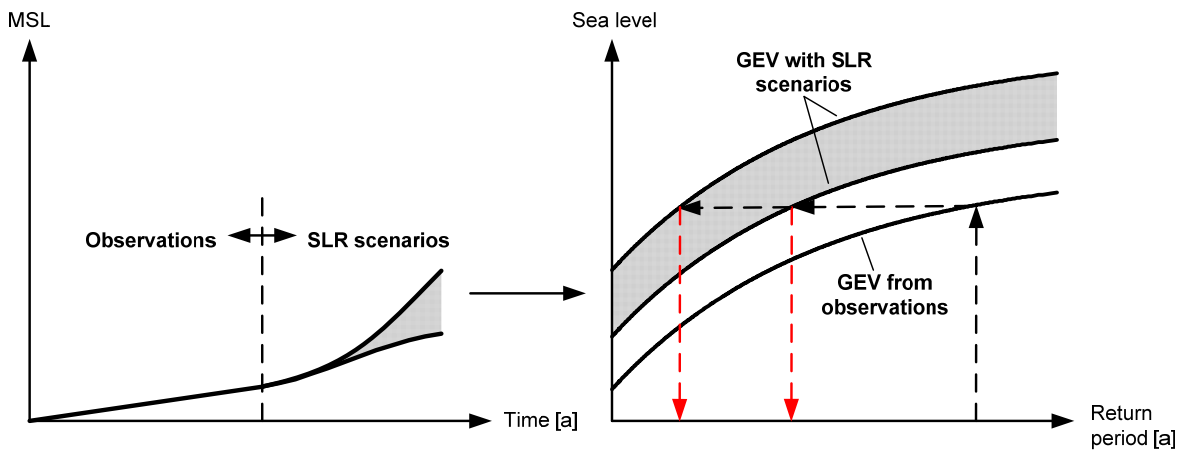
Figure 1-5:   MSL offset method to consider possible future MSL changes in statistical assessments of return periods.

This approach relies on two assumptions: First, it is assumed that future MSL changes fully spread to future changes in storm surge heights. However, altered water depth due to MSL changes may affect the propagation and dissipation of astronomical tide and surge components. This could lead to larger or smaller changes in future storm surge heights compared to MSL changes. Second, it is assumed that changes in extreme sea levels are mainly driven and directly affected by MSL changes and that 'indirect' changes, such as changes in wind and pressure fields or storminess (i.e. changes in storm tracks, frequency and intensity), respectively, have no significant influence (e.g. Haigh, 2009). With the MSL offset method, the return period of a certain water level becomes smaller in proportion to the considered sea level projection (see Fig. 1-5).

From analysing observed changes in extreme sea levels and MSL based on different quasi-global data sets, Woodworth and Blackman (2004), Menendez and Woodworth (2010) and Woodworth et al. (2011) found no significant differences in inter-annual variability and secular trends between both parameters and for most areas. Similar results were reported for example by Zhang et al. (2000) for the US east coast, by Firing and Merrifield (2004) for Hawaii and by Araújo (2005) and Haigh et al. (2010a) for the UK and English Channel. However, from comparing changes in extreme high sea levels (by considering a range of percentile time series) and changes in MSL along the German North Sea coastline, Mudersbach et al. (under review) found significant differences for most of the

considered tide gauges (see also Jensen et al., 1992). They concluded that the differences are mainly caused by changes in the astronomical tides between the 1950s and 1990s. The reasons for these changes are not fully understood at present and need to be explored in further research studies. Prior to the 1950s and from the 1990s on, MSL changes are similar to changes in extreme sea levels, supporting the assumption mentioned above (i.e. mean sea level changes fully spread to changes in extremes).

Different authors also tested the effect of rising sea levels on storm surge heights by running tide-surge models twice, whereas no sea level rise was considered for the first run and a certain SLR scenario was used for the second run (while all the other boundary conditions were kept constant). For the North Sea area various SLR scenarios were used, e.g. 0.1 m by Kauker and Langenberg (2000), 0.5 m by Lowe and Gregory (2005), up to 2 m by Schulte-Rentrop and Rudolph (2011) and Sterl et al. (2009) and 5 m by Howard and Lowe (2010). All authors concluded that changes in storm surge heights were not significantly different from the considered changes in MSL. Thus, in a first approximation mean sea level changes and changes in storm surge heights can be added linearly.

Beside the MSL offset method, two further methods for examining future extreme sea levels are described in the literature, namely the statistical method and the dynamical method. Both are briefly introduced below with the emphasis on available results for the German Bight. A detailed discussion of both methods can be found in Lowe et al. (2010).

In the statistical approach, relationships between storm-related water levels and large-scale driving meteorology are developed from observations (or hindcast model simulations). Future changes in extreme sea levels are then examined by projecting future large-scale meteorology and considering the estimated statistical relationship between the two parameters. Hence, it is assumed that the statistical relationship between the large scale variable and storm surge water levels remains constant under future climate conditions (Lowe et al., 2010). Von Storch and Reichardt (1997) applied the statistical method to the German Bight, by relating extreme sea levels to monthly variations in the mean air pressure field over Europe. They found no significant increase (< 0.1 m) in storm surge heights for a future scenario with doubled atmospheric carbon dioxide concentration. Similar results were reported by Langenberg et al. (1999).

In the dynamical approach, process-based numerical models of shallow water dynamics are used to simulate past/present and future periods. The models are forced by pressure and wind fields (from past/present and for future conditions) to generate a large population of

future extreme sea level events. The latter can be presented and analysed as percentiles or by fitting parametric distribution functions to the data sets (Lowe et al. 2010). The dynamical approach has been used in many different studies (by using many different models) to assess changes in future extreme sea levels in the European shelf region (see Lowe et al. (2010) for a summary). For the German Bight area and the A2 SRES emission scenario, Woth et al. (2006) found significant differences (in the order of 0.2 to 0.3 m) from comparing 99.5%-storm surge percentiles for the 1961 to 1990 period (i.e. the control climate) and the 2071 to 2100 period. Similar changes were reported by Lowe and Gregory (2005) for the south-eastern North Sea, indicating that moderate changes in storminess could affect the heights of future extreme sea levels along the German North Sea coastline (in addition to MSL changes). By using similar analyses techniques, Lowe et al. (2001), Flather and Williams (2000) or Sterl et al. (2009) found much smaller or no changes (Weisse et al., 2011).

To sum up, the presented results indicate that the first assumption accompanied with the MSL offset method (i.e. changes in MSL fully spread to changes in extremes) is applicable to the German Bight. On the other hand, there is some evidence that the second assumption (i.e. no changes in storminess) might not be reliable for the investigation area. When considering the results of Woth et al. (2006) one had to add about 0.4 m (for the A2 emission scenario) to present day extreme sea levels to account for future MSL changes and another 0.2 m to 0.3 m to account for changes in storminess.

However, uncertainties in modelling future extreme sea levels are still large. Gregory and Lowe (2005) split the uncertainties into three components: (1) uncertainties in greenhouse gas emission scenarios, (2) uncertainties in the methods applied to model the response to greenhouse gas emissions and (3) the natural variability. They point out that the sum of uncertainties in future projections is considerable and the magnitude is location dependent. Hence, from our current knowledge the MSL offset method could be used as an approximation when calculating return periods for future extreme sea levels in the German Bight area. Much less information is required and even when applying the MSL offset method the uncertainties related to the MSL projections are large (Woodworth, 2006). Purvis et al. (2008) introduced an approach for estimating future coastal flood risks (with the MSL offset method) by taking the uncertainties in MSL projections into account. Applying non-stationary extreme value analyses (e.g. Menendez and Woodworth, 2010; Mudersbach and Jensen 2010) provides an extension to the simple MSL offset method and

represents a growing research field (especially in recent years). Future changes in storminess (assuming detailed knowledge about the possible changes) may be taken into account by considering time dependent parameters of the extreme value distribution. This means that changes in MSL and storminess are not added separately to the extremes, but directly considered in the statistical analyses. More research on this topic is required.

To this stage the presented results were only related to the storm surge peak water levels. This is not always satisfactory. For risk assessments (i.e. Level IV methods) it is required to analyse storm surge curves, as breach models are applied and initial conditions for flood propagation need to be identified. Many different storm surge curves have to be considered when performing risk analyses (Cai et al., 2007; Purvis et al., 2008). The problem of deriving a sufficient number of scenarios is discussed in Sect. 4 and a stochastic storm surge model is introduced.

1.3   Wind waves

Meteorological conditions during storm surges often cause the emergence of large wind waves. Both parameters are closely linked with the weather conditions and therefore high wind waves often coincide with high water levels. Thus, wave loads on coastal defence structures are an important issue (for some investigation areas) when performing risk analyses. High wind waves may lead to overtopping of sea defences with related failures of structures or coastal erosion (e.g. Pullen et al. 2007; Lowe et al. 2010). In this thesis the main focus is on analysing the two important risk sources mean sea level and storm surges (see Sects. 2 to 4). However, in Sect. 5, combinations of high water levels and high wind waves are investigated and an approach to include wave parameters into the statistical analyses within risk assessments is presented. Therefore, this introductory section to wind waves is less detailed than the previous ones for the other loading parameters. It provides an overview of recent findings from analysing observed and possible future changes of the wave climate in the German Bight.

Results from analysing recent and longer-term changes in the North Atlantic and North Sea wave climate have been published in various papers. Comprehensive reviews of the available literature and summaries of the most important findings were provided for example by Weisse and von Storch (2009), Lowe et al. (2010) and Weisse et al. (2011). For the German Bight area the available observations indicate an increase of extreme wave

heights from the early 1960s to the mid 1990s (e.g. WASA, 1998; Günther et al., 1998; Weisse and Günther, 2007). However, from taking historical records into account, it was found that these changes were not significantly different from those observed earlier in the 20th century (WASA, 1998) and hence were consistent with natural variability.

To project future changes in wave climate, the same methods as for the projection of future changes in extreme sea levels (i.e. the statistical and dynamical method) are applicable. As well as changes in storm surges, future changes in wave climate also strongly depend on corresponding changes in the meteorological driving factors (i.e. changes in atmospheric wind fields) which are very uncertain (Christensen et al., 2007). Grabemann and Weisse (2008) examined future changes in extreme wave heights (i.e. 99-percentiles) along the German North Sea coastline by applying a dynamical wave model driven by wind fields from two different global climate models and by taking two different greenhouse gas emission scenarios into account. They detected a tendency towards an increase of extreme wave heights along the coastline. Similar results were reported by other authors (see Weisse et al. (2011) for an overview), whereas spatial patterns and magnitudes of the estimated changes were highly variable and uncertain. Weisse et al. (2011) inferred that reliable estimates of natural variability are required to allow meaningful interpretations of the signals derived from climate change simulations. Therefore, possible future changes in the wave climate are currently often neglected when performing risk assessments with future scenarios.

1.4   Multivariate statistical analyses

At the beginning of Sect. 1 it has been mentioned, that all relevant loading parameters for coastal defence structures have to be considered for the statistical assessment within a risk analysis. That is joint probabilities of selected storm surge (see Sects. 4 and 5) and wave parameters (see Sect. 5) need to be calculated. Here, a brief introduction to the multivariate extreme value theory is provided (for more information see e.g. Kotz and Nadarajah, 2000; Coles, 2001; Salvadori et al. 2007). A compendium of the historic development of multivariate extreme value statistics can be found in Coles (2001). A discussion of specific aspects of multivariate problems, including a summary of previous studies related to coastal engineering problems can be found in Sect. 5 of this thesis.

In general, dealing with multivariate problems raises two important issues: the dependence of the marginal parameters (i.e. the parameters which are jointly analysed) and the distributions of the marginal parameters. Figure 1-6 shows that the characteristics of the marginal parameters prescribe the procedure, which has to be chosen for calculating joint probabilities. Regarding the problem of dependency, two situations are possible, i.e. the considered parameters are independent or dependent (Salvadori et al., 2007). Chi-squared tests (or other mathematical tests) can be applied to proof independency (e.g. Greenwood and Nikulin, 1996). If the test results support the assumption of independency, joint probabilities can be calculated by simply multiplying the univariate probabilities of the marginal parameters. If the correlation coefficient r between the considered variables is significantly different from zero, the assumption of independency does not apply (conversely, zero correlation does not allow the assumption of independency, as only linear dependency is captured). Various approaches to transform marginal variables in a way that they can be treated as independent are described in literature (e.g. Dixon and Tawn, 1995), but not discussed here. If the considered variables are dependent, one has to choose a multivariate model to calculate joint probabilities. Next, it has to be tested whether the marginal parameters have a (univariate) distribution from the same family (e.g. both parameters are gumbel or normally distributed). In this case, corresponding multivariate statistical models (e.g. bivariate Gumbel or bivariate Normal models) can be used. In literature, methods to transform marginal variables to achieve distributions belonging to the same family are presented (e.g. Hutchinson and Lai, 1991), but also not discussed here.
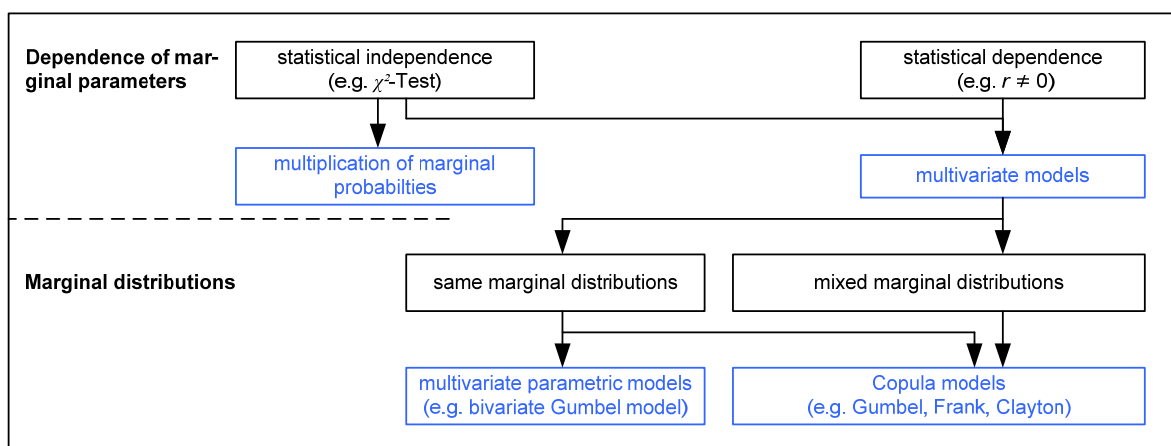
Figure 1-6:   Effects of characteristics of marginal parameters on joint probability analyses.

Copula functions can be applied as an alternative to traditional multivariate parametric models. They allow the joint analysis of dependent variables with mixed marginal

distributions. Hence, Copula models are very flexible and applicable in many cases without the necessity of transforming the available data sets. An introduction to the Copula theory, including a review of relevant literature, is presented in Sect. 5 of the thesis. Bivariate and trivariate Copula models are introduced and applied to jointly analyse all important loading parameters for coastal defence structures (i.e. selected storm surge and wave parameters) to derive realistic exceedance probabilities for risk assessments.

1.5   Objectives and outline of the thesis

As outlined in the previous sections, the thesis aims at analysing all relevant hydrodynamic loading parameters for coastal defence structures, which need to be considered for modern risk based design methods. The important parameters MSL, storm surges and wind waves are investigated separately and jointly (in a statistical sense) for the investigation area German Bight in respect of improving the results from integrated risk analyses (as for example conducted within the German XtremRisK project). The four main objectives are:

1. **To introduce and further develop methods to construct and analyse mean sea level time series**

   Methods to construct and analyse high quality MSL time series for tide gauges in the German Bight from data sets with different temporal resolution are developed. State of the art and some more sophisticated analysis techniques to investigate long-term changes in mean sea level are introduced and validated for time series from selected tide gauge sites.

2. **To analyse the observed mean sea level changes along the entire German North Sea coastline based on a new MSL data set**

   A first-time detailed analysis of observed mean sea level changes along the German North Sea coastline from the mid 19th century to present is performed. This involves the construction of MSL time series for a larger number of tide gauge sites and the application of different analysis techniques (see previous paragraph).

3. **To develop a stochastic storm surge model**

   A stochastic approach to simulate a large number of storm surge scenarios based on observational records is introduced and tested for two selected investigation areas.

The resulting storm surge scenarios can be used as input data for integrated risk analyses and many other applications.

4. **To construct multivariate statistical models based on Copula functions to jointly analyse storm surge and wave parameters**

   Bivariate and trivariate statistical models are constructed from Copula functions. The statistical models are applied to jointly analyse selected storm surge and wave parameters to derive much more realistic and reliable joint exceedance probabilities for risk assessments than before.

The thesis is structured as follows: In Sect. 2, a further developed methodology to generate high quality MSL time series for the German Bight is presented. Various scientifically accepted analysis techniques are applied and a more sophisticated approach to investigate non-linear trends in time series (especially near the ends of the time series) is introduced. The methods are tested and applied to the data sets from the tide gauge sites Cuxhaven and Helgoland.

In Sect. 3, the presented methods are applied to a larger number of MSL time series, derived from tide gauges covering the entire German North Sea coastline. Relative MSL time series of individual stations are analysed, as well as so-called 'virtual station' time series. The results for the German Bight are compared to observed MSL changes on wider regional scales and a first attempt of determining site-specific velocities of vertical land movement is undertaken. The results are expected to contribute to a better understanding of the complex processes leading to regional and local sea level changes and to work out reliable SLR scenarios for the German Bight.

In Sect. 4, a stochastic model to simulate a large number of synthetic and high frequency storm surge curves is presented. Many different storm surge scenarios are required to derive meaningful results from event-based risk assessments. All relevant computational steps of the stochastic simulation are described in detail and results are presented for the tide gauge sites Cuxhaven and Hoernum. The model is validated against available observations and by taking selected results from former numerical model studies into account.

In Sect. 5, for the first time a larger number of important storm surge and wave parameters are considered to calculate joint exceedance probabilties. A bivariate model based on Archimedean Copula functions is used to determine joint probabilities for the important

storm surge parameters 'highest turning point' and 'storm surge intensity'. The model is then extended to the trivariate case and a fully nested Archimedean Copula model is constructed to jointly analyse the two storm surge parameters and significant wave heights.

Sect. 6 contains a summary of the key findings and conclusions are drawn from the analyses and results presented in Sects. 2 to 5. Some recommendations for further research activities to improve the understanding of how to estimate reliable hydrodynamic boundary conditions for risk analyses in coastal areas are given in Sect. 7.

2 Advanced methods to analyse mean sea level rise in the German Bight

2.1 Abstract

In this section, a methodology to analyse observed sea level rise (SLR) in the German Bight, the shallow south-eastern part of the North Sea, is presented. The study focuses on the description of the methods used to generate and analyse mean sea level (MSL) time series. Parametric fitting approaches as well as non-parametric data adaptive filters, such as Singular System Analysis (SSA) are applied. For padding non-stationary sea level time series, an advanced approach named Monte-Carlo autoregressive padding (MCAP) is introduced. This approach allows the specification of uncertainties for the behaviour of smoothed time series near the boundaries. As an example, this section includes the results from analysing the sea level records of the Cuxhaven tide gauge and the Helgoland tide gauge, both located in the south-eastern North Sea. For comparison, the results from analysing a global sea level reconstruction are also presented. The results for the North Sea point to a weak negative acceleration of SLR since 1844 with a strong positive acceleration at the end of the 19th century, to a period of almost no SLR around the 1970s with subsequent positive acceleration and to high recent rates.

2.2 Introduction

Sea level rise (SLR) is one of the major consequences we are facing in times of a warming climate and it is obvious that a higher sea level influences the heights of occurring storm surges and thus results in a higher risk of inundation for the affected coastal areas (see Sect. 1). Therefore, regional and global sea level rise are subjects to many recent scientific publications (e.g. White et al., 2005; Jevrejeva et al., 2006; Wöppelmann et al., 2006; Holgate, 2007; Church et al., 2008; Merrifield et al., 2009; Woodworth et al., 2009a,

2009b). In contrast, mean sea level (MSL) and its variability over the last centuries in the German North Sea area have not been analysed in detail up to now. This is surprising, because many long and continuous sea level records are available (Wahl et al., 2008). Some studies considered time series from a very small number of tide gauges and high resolution data sets have not been used or not been available (e.g. Dietrich, 1954; Jensen and Mudersbach, 2007). Furthermore, various projects dealing with mean tidal conditions, e.g. the mean tidal high waters (MHW) or the mean tidal ranges (MTR) have been conducted so far (e.g. Lüders, 1936; Jensen, 1984 (and literature referenced therein); Führböter and Jensen, 1985; Töppe and Brockmann, 1992; Gönnert et al., 2004). Most of the available sea level records consist of high and low water heights and times (from here on referred to as high and low waters), which are not directly applicable for MSL analyses. The simple averaging of high and low waters leads to the mean tide level (MTL) and not to the MSL. The latter can be estimated by averaging high frequency sea level data consisting of at least hourly measurements. The difference between MSL and MTL is small in most areas (e.g., Pugh, 2004; Wöppelmann et al., 2006), but up to more than 20 cm along the German North Sea coastline due to shallow water effects (Lassen, 1989). This has to be taken into account when generating and analysing mean sea level time series. In addition, some differences between observations and model results, often referred to as 'negative sea level budget' (e.g., Church et al., 2008), have not been completely understood up to now. All the more important is the proper analysis of available data sets from tide gauges and in the recent past also from satellites.

The present study has three main objectives. The first one is to introduce an enhanced approach to combine MSL and MTL data. The second objective consists in introducing an advanced method for padding or extrapolating time series before applying any smoothing technique to identify the optimal fit. The third objective is to analyse, as an example, the available sea level records from two tide gauges in the German North Sea.

To address the first objective, a modification of the so called *k*-factor method is introduced in Sect. 2.3 (Lassen, 1989; Lentz, 1879; Wahl et al., 2008). This modification allows the consideration of non-stationarities in *k*-factor time series, where the *k*-factor is subsequently used to convert MTL to MSL. Based upon the resulting MSL time series, long-term trend analyses are possible and smoothing techniques can be applied without leading to gaps. The latter usually occurs, if time series consisting of MSL and MTL data are analysed without applying any methods to combine both variables. In addition, a shift

of up to more than 20 centimetres somewhere in the time series (as it may happen in the German Bight) certainly leads to significant errors and misinterpretations when performing long-term trend estimations. Sea level time series from the German North Sea area show high variability due to the influences of stochastic meteorological processes (Müller-Navarra and Giese, 1999). Therefore, it is not always possible to detect shifts of 10 to 20 centimetres by just looking at the time series.

As mentioned above, the second objective of the study is to introduce an advanced method for padding time series before applying any smoothing technique. Whenever smoothing a time series, one has two opportunities. The first one is to start and stop the smoothing at a specified time (depending on the chosen window length) before reaching the ends of the original time series. For example a moving average with a window length of 19 years usually starts 9 years later than the original time series and ends 9 years earlier. The second opportunity, which is increasingly considered when analysing climate time series, is to find some meaningful extrapolation from a physical point of view, before applying any smoothing technique. This enables the smoothed time series to cover the same period as the original time series. The method presented in this study, namely Monte-Carlo autoregressive padding (MCAP), results in a very data adaptive smooth and allows the specification of uncertainties near the ends of the time series due to the padding. Especially the latter is not the case with any other common techniques (e.g., Ghil et al., 2002; Mann, 2004; Jevrejeva et al., 2006; Jansen et al., 2007; Trenberth et al., 2007; Mann, 2008). However, to understand recent SLR and to derive projections for the near future, especially the behaviour of the time series in recent years (i.e. near the posterior boundary) is important.

The third objective is addressed by presenting the results from analysing the available sea level records from two important tide gauges in the German North Sea. The Cuxhaven tide gauge provides the longest record with data since 1844 (data from 1843 is available but was not properly processed at the time of the analyses). The Helgoland tide gauge provides high quality data due to its offshore location on an island. In a next step, the results from analysing the abovementioned sea level time series are compared to global patterns of SLR derived from analysing a global sea level reconstruction. The results may contribute to the validation of regional climate models and provide indications of SLR for regional and local planning purposes. This seems to be of special importance. First, the most recent SLR scenarios published by the Intergovernmental Panel on Climate Change (IPCC) (Meehl et

al., 2007) are subject to an extensive scientific discussion. Some authors find hints from observations or semi-empirical models that the scenarios might underestimate future SLR (Rahmstorf, 2007; Rahmstorf et al., 2007; Jevrejeva et al., 2008; Grinsted et al., 2009). Especially the results from semi-empirical models, using empirical relationships between temperature and SLR to estimate future projections, are also lively discussed by the scientific community (e.g. Holgate et al., 2007; von Storch et al., 2008b). Second, and even more important, it has to be tested whether a significant correlation exists between SLR in the German North Sea region and global SLR.

2.3　Data and Methods

Figure 2-1 shows the locations of the Cuxhaven and the Helgoland tide gauges in the south-eastern North Sea. The Cuxhaven station is located at the Elbe estuary and provides permanent sea level data from 1844 to 2008.
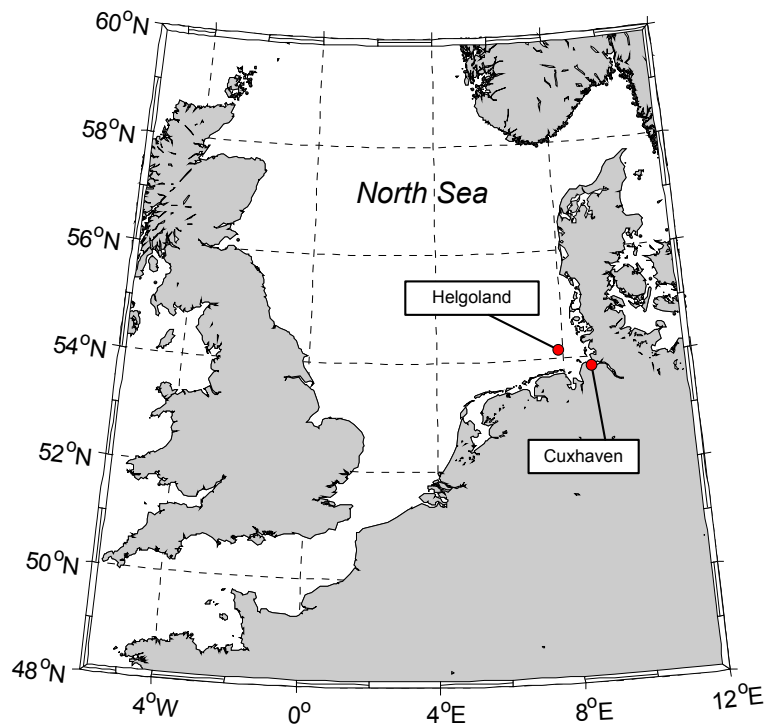
Figure 2-1:　Locations of the tide gauges Cuxhaven and Helgoland in the south-eastern North Sea.

From the beginning of the record until 1918 only high and low waters are available and afterwards high frequency data with at least hourly values. The Helgoland station is installed in the harbour of the island of Helgoland (Rohde, 1990), which is located about 62 kilometres north-westerly of the Elbe Estuary. Due to its exposed location in the deep

water, the tide gauge provides almost unaffected sea level measurements and the tide curves are less deformed. High frequency data are available since 1953, with a period from 1990 to 1999 where only high and low waters exist.

All data sets were corrected for local datum shifts and for glacial isostatic adjustment (GIA; first of all to allow for a meaningful comparison with the global reconstruction in Sect. 2.4) by considering a rate of land subsidence of 0.34 mm/a for the Cuxhaven data and of 0.51 mm/a for the Helgoland data (Peltier, 2004). GIA is a global process in response to large scale changes in the surface mass load resulting from the last deglaciation. The effect of GIA (rebound or subsidence) is usually assumed to be linear, at least over the last couple of hundred years. Other geological effects may also contribute to land subsidence or uplift (e.g. tectonics, volcanic activity, withdrawal of natural resources etc.), but GIA is the only one assessable through numerical models. The sum of all the other effects can be measured via continuous global positioning systems (CGPS), whereas the CGPS antenna need to be located near the tide gauges. Such measurements are expected to contribute to a reduction of the uncertainties in further studies (Schöne et al., 2009) (see also Sect. 2.5).

To combine MSL time series calculated from the high frequency data and MTL time series calculated from the low frequency data (i.e. high and low waters), monthly *k*-factor time series *k(t)* are determined. The dimensionless *k*-factor is a reference value for the difference between MSL and MTL and is calculated with Eq. (2-1) for the time periods where high frequency data sets are available (Lassen, 1989):

$$k(t) = \frac{\big(MHW(t) - MSL(t)\big)}{MTR(t)} \qquad\qquad (2\text{-}1)$$

where *MHW(t)* is the monthly mean high water, *MSL(t)* is the monthly mean sea level and *MTR(t)* is the monthly mean tidal range. For the German North Sea coastline, *k*-factors are found to vary by between 0.43 and 0.49 [-]. A *k*-factor of 0.5 [-] means that the tide curve has a perfect sinusoidal form and that MSL equals MTL.

Before combining MSL and MTL time series, it has to be tested whether the *k*-factor is a stationary parameter for the investigated site or whether it shows non-stationary behaviour. Therefore, two tests on stationarity are applied to the monthly *k*-factor time series. The first one is a sliding-window test with a window length of one year to eliminate potential seasonal effects (Mudersbach and Jensen, 2008; van Gelder, 2008). The second test is a

two dimensional non-parametric Kolmogorov-Smirnov test as described by Chen and Rao (2002) and Mudersbach and Jensen (2008). If the k-factor is found to be stationary, a monthly MSL time series can be derived with Eq. (2-2):

$$MSL(t) = MTR(t) \cdot (0.5 - k) + MTL(t) \qquad\qquad (2\text{-}2)$$

where $MSL(t)$ is the monthly mean sea level, $MTR(t)$ is the monthly mean tidal range, k is the mean k-factor calculated for the time period providing high frequency data and $MTL(t)$ is the monthly mean tide level. If the k-factor shows non-stationary behaviour, a first or higher order polynomial function has to be fitted to the data and extrapolated backwards before correcting MTL values. Equation (2-3) considers a time dependent k-factor:

$$MSL(t) = MTR(t) \cdot (0.5 - k(t)) + MTL(t) \qquad\qquad (2\text{-}3)$$

where the variables are the same as in Eq. (2-2) and $k(t)$ is the time dependent k-factor.

Once a consistent MSL time series has been constructed, different methods can be used to analyse long-term and recent linear and non-linear changes. Parametric approaches provide the advantage of allowing extrapolation into the future, whereas data adaptive non-linear methods are valuable to detect inflection points and periods of remarkably high or low rates of SLR.

Here, the following computational steps are conducted to analyse MSL time series: (1) A first order polynomial function, a second order polynomial function and an exponential function are fitted to the time series. The fit providing the smallest mean-squared error (MSE) is selected and its 95% confidence bounds are specified. (2) Overlapping decadal linear trends are estimated with 95% confidence levels. (3) To analyse the non-linear behaviour of the time series, a moving average (MA) and Singular System Analysis (SSA) (Golyandina et al., 2001) are applied. The window length of the MA and the embedding dimension D of the SSA are set equal (hereinafter embedding dimension D is used to describe both). Here, the default value is $N/5$, as suggested by Golyandina et al. (2001), where N is the number of observations.

For padding the time series a new approach named Monte-Carlo autoregressive padding (MCAP) is introduced. MCAP leads to a data adaptive smooth and additionally provides

uncertainties for the behaviour of the smoothed time series towards the ends. The first step of MCAP includes de-trending of the original time series (see Fig. 2-2a) using a first order polynomial fit of the form:

$$y(t) = \alpha \cdot t + \beta \qquad (2\text{-}4)$$

where α represents the linear trend of the time series. In a second step a specified number (default value is 10,000) of surrogate data sets is generated (see Fig. 2-2b) with a first order auto-regressive (AR1) model of the form:

$$z_t = \theta \cdot z_{t-1} + \varepsilon_t \qquad (2\text{-}5)$$

where θ is the autocorrelation parameter and ε_t is a white noise process (Box and Jenkins, 1976). The surrogate data sets are two times the chosen embedding dimension longer than the original time series. If the embedding dimension is chosen to be $D = 15$ years, the surrogates have 30 values more than the original time series. Next, the first and the last parts (one time the chosen embedding dimension) of the surrogate data sets are used for padding the de-trended original time series as shown in Fig. 2-2c.
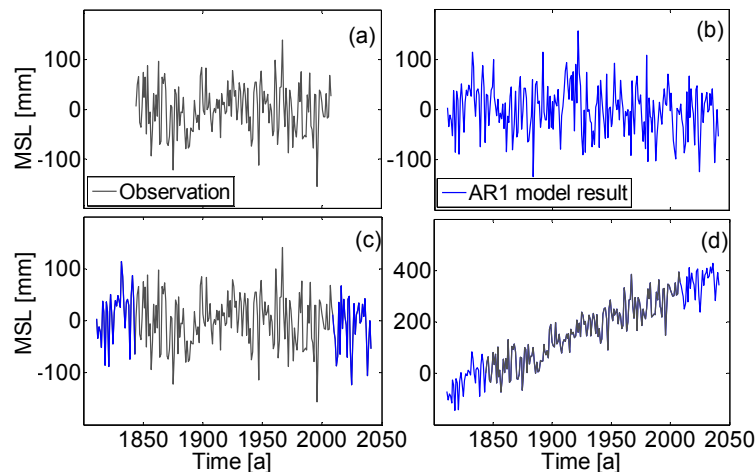
Figure 2-2:   Steps of MCAP: (a) de-trended annual Cuxhaven MSL time series, (b) result of the AR1 Model, two times the chosen embedding dimension longer than the observed time series, (c) padded de-trended annual Cuxhaven MSL time series, using the ends of the result of the AR1 model, (d) padded annual Cuxhaven MSL time series with long term-trend of the observed time series re-included. Steps (b) to (d) are repeated 10,000 times through Monte-Carlo simulations.

The ends of the surrogates (which are used for padding the original time series) display more or less strong positive or negative trends. In the last step, the long-term linear trend of the observed time series (see Eq. 2-4) is re-included as shown in Fig. 2-2d. By following this approach, the trend of the padded time series differs slightly from the trend of the original time series. This implies that the long-term trend of the investigated sea level time series will not change dramatically within the next few decades. Figure 2-2 shows the results of the different steps of MCAP for the Cuxhaven time series. The steps shown in Figs. 2-2b to 2-2d are repeated 10,000 times. As a result one yields a set of 10,000 surrogates, which are all two times the chosen embedding dimension (or as default: two times $N/5$) longer than the original time series and show varying long-term trends due to the padding.

For the SSA reconstruction, those empirical orthogonal functions (EOFs) providing trend information have to be identified. Here, a Mann-Kendall-Test (Mann, 1945) is applied in addition to the two tests on stationarity that have been mentioned above (i.e. a sliding-window test and a Kolmogorov-Smirnov test). Once the EOFs providing trend information are isolated, they are used for the reconstruction (resulting in a smoothed time series). The MSE is used here again, to measure the misfit of the 10,000 SSA reconstructions (from the 10,000 surrogates) compared to the original time series. The SSA reconstruction, which provides the smallest error, is highlighted in the resulting plot (see Sect. 2.4). The remaining reconstructions are represented by a shaded band and indicate the uncertainty range for the smoothed time series near the boundaries due to the padding. This information is important, because the a priori assumption that future sea level will provide a small MSE is weak. The 'true' smooth near the posterior boundary can be estimated in the future, when longer data sets are available. For example, using SSA with an embedding dimension of $D = 33$ years means that the 'true' smooth for the period from 1844 to 2008 can be estimated at first in 2040.

The tide gauge records from Cuxhaven and Helgoland are used here to represent patterns of SLR in the German North Sea area. This seems to be justified, because both stations play an important role for sea level observation in the German North Sea and different authors proved that a very small number of long and high-quality tide gauge records may capture the variability found from a considerably larger number of stations (e.g., Holgate, 2007). To compare the estimated patterns of SLR for the North Sea area to global patterns of SLR, a global sea level reconstruction published by Church and White (2006) is

analysed using the presented methods. A recently updated version of the reconstruction, providing data from 1870 to 2007, is available on the website of the Permanent Service for Mean Sea Level (PSMSL, www.psmsl.org).

2.4 Results

Before presenting the results from analysing the selected sea level time series from the North Sea and the global sea level reconstruction in detail, the efficiency of the MCAP approach is demonstrated. Figure 2-3 shows the results for truncated intervals of the Cuxhaven annual MSL time series. The estimated smooth providing the smallest MSE, the results from 10,000 MCAP simulations and the 'true' smooth are calculated and compared in the figure. In addition, two simpler approaches for padding climate time series introduced by Mann (2004), namely the 'minimum slope' and the 'mean padding' approach, are included for comparison purposes. The 'minimum slope' approach was used in the most recent IPCC assessment report (Trenberth et al., 2007) and is included in Figs. 2-3a and 2-3b. The 'mean padding' approach was also used in the IPCC's Fourth Assessment Report (Jansen et al., 2007) and is included in Figs. 2-3c and 2-3d for comparison purposes. Mann (2008) argued that both approaches tend to artificially suppress the trends towards the ends of the time series.

The results show that there is always a difference between the estimated and the 'true' smoothes. Especially for the 1844 to 1920 interval the 'true' smooth clearly suggests a stronger SLR compared to the estimated smoothes. A positive acceleration of SLR is indicated by the 'true' smooth as well as by the MCAP results, while the results from using the 'mean padding' approach indicate a negative acceleration. In all test cases, the SSA reconstructions using MCAP show better agreement with the 'true' smooth than the reconstructions from using the padding approaches applied in the most recent IPCC assessment report. Solely the reconstruction from using the 'minimum slope' approach for the 1844 to 1980 interval slightly exceeds the shaded band resulting from 10,000 MCAP simulations. All the other reconstructions and the 'true' smoothes proceed inside the uncertainty bands, which indicates the benefit of the approach. It should be noted, that the application of other methods for padding time series (e.g. Jevrejeva et al., 2006; Rahmstorf et al., 2007, Mann, 2008) lead to better results than the two methods used here for comparison purposes. Especially the 'adaptive' approach introduced by Mann (2008)

results in a very data adaptive smooth (as the name indicates). But neither this one, nor any of the other methods allows the specification of uncertainties near the ends of the time series due to the padding.
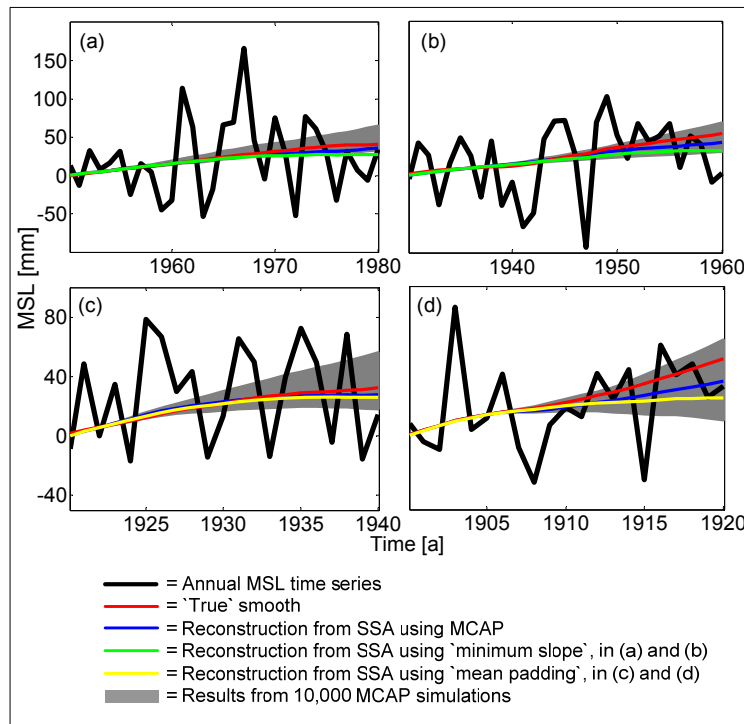
Figure 2-3:   Comparison of different methods for padding time series. Results are shown for the posterior boundary of truncated intervals of the annual MSL time series of the Cuxhaven gauge station: (a) the 1844 to 1980 interval, (b) the 1844 to 1960 interval, (c) the 1844 to 1940 interval and (d) the 1844 to 1920 interval.

In the following, the results from analysing the available data sets of the Cuxhaven and Helgoland tide gauges are presented. Figure 2-4 shows the results of the sliding-window test on stationarity, which is applied to the monthly k-factor time series. The latter are calculated for the time periods providing high frequency data as described in Sect. 2.3. From 20,000 Monte-Carlo simulations it was found that exceedance rates of the 95% confidence bounds of up to 60% are possible with stationary time series. Thus, both time series are found to be stationary from the sliding-window test as well as from the Kolmogorov-Smirnov test. The k-factor time series of the Cuxhaven station (Fig. 2-4b) shows some irregularities at the end of the 1930s and in the 1940s (month numbers 250 to 400), which most probably result from interrupted measures (first of all dredging) in the Elbe estuary during and after the Second World War. As the k-factors are found to be stationary for both stations (with the sliding-window test as well as with the Kolmogorov-

Smirnov test), the means are calculated for the periods from 2000 to 2008 for the Helgoland station and from 1998 to 2008 for the Cuxhaven station, respectively. Those periods provide sea level data with a resolution in time of one minute and former studies suggest that the accuracy of the *k*-factor improves in proportion to the resolution in time (Wahl et al., 2008). The estimated mean is $k = 0.4783$ [-] for the Helgoland station. This equals a difference between MSL and MTL of about 5 cm. The mean *k*-factor for the Cuxhaven station is found to be $k = 0.4685$ [-], which equals a difference between MSL and MTL of about 9 cm. The lower *k*-factor for the Cuxhaven station clearly illustrates that the tide curve is subject to stronger deformations near the coastline due to shallow water effects.
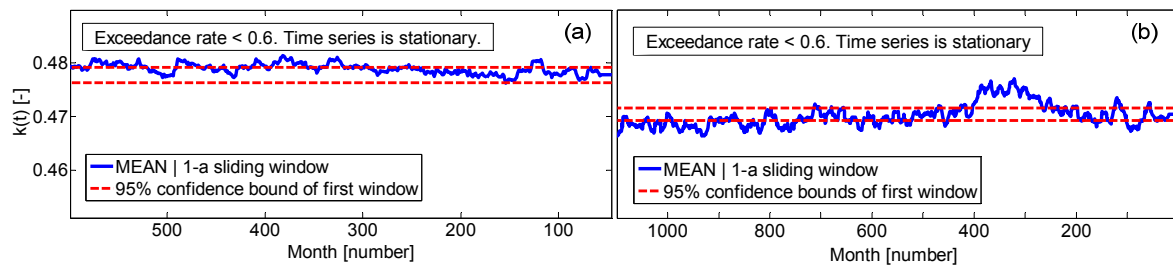
Figure 2-4:   Results of the sliding-window test on stationarity applied to the monthly *k*-factor time series of the Helgoland (a) and Cuxhaven (b) tide gauges.

The mean *k*-factors are considered to combine the available MTL data from 1990 to 1999 for the Helgoland station and from 1844 to 1917 for the Cuxhaven station with the shorter MSL time series (see Eq. (2-2)). Figure 2-5 shows the resulting monthly and annual MSL time series and fitted second order polynomial functions. The latter lead to the smallest MSEs of the considered parametric approaches described in Sect. 2.3 (i.e. polynomial and exponential functions).

The Helgoland station shows a significant positive acceleration of 0.18 ± 0.05 mm/a² (two times the quadratic coefficient of the second order polynomial fit), a linear long-term trend of 1.85 ± 0.42 mm/a for the entire period and a linear trend of 8.50 ± 2.32 mm/a for the reduced period since 1993 (i.e. the satellite period; all quoted errors are 1-σ standard errors). The Cuxhaven MSL time series shows a weak negative acceleration from the mid 19th century, which is consistent with the results reported by Woodworth et al. (2009a) for most of the European gauges providing records back to the 19th century. The estimated linear trend is 2.03 ± 0.08 mm/a for the entire period (i.e. 1844 to 2008), 1.75 ± 0.17 mm/a

for the twentieth century, 1.81 ± 0.44 mm/a for the period from 1953 to 2008 and 6.44 ± 3.05 mm/a for the reduced period from 1993 to 2008.
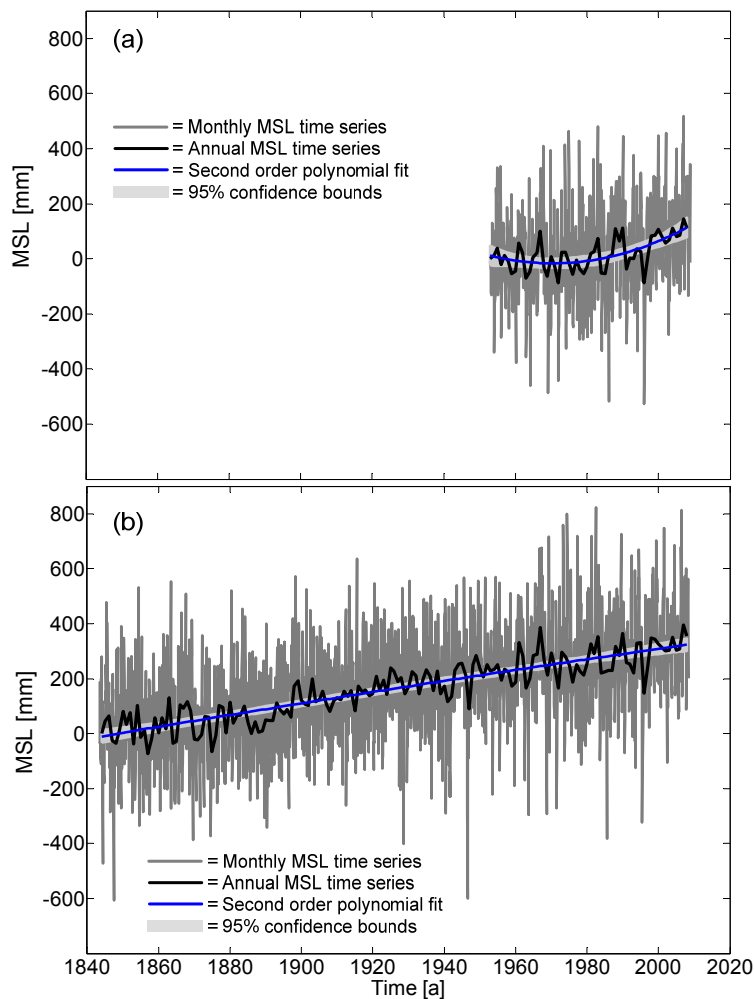
Figure 2-5:   Monthly and annual MSL time series for the Helgoland tide gauge (a) and the Cuxhaven tide gauge (b) and results from parametric fitting.

The linear trends for the period covered by both tide gauges (i.e. 1953 to 2008) are almost equal, which indicates a high quality of the data. Furthermore, remarkable high or low annual MSL values in general occur at both gauges at the same time. For example the low value for the year 1996, due to offshore winds and very little precipitation and runoff, or the high value for the year 1967, a year with many storm surges. The trend found for the twentieth century from the Cuxhaven time series differs slightly from that found by Woodworth et al. (2009b). They derived a linear trend of 1.4 ± 0.2 mm/a from investigating a large number of tide gauges around the UK. The trends estimated for the short period from 1993 to 2008 are more than twice as high as the trend found from global altimetry data for almost the same time period (Beckley et al., 2007). This is an interesting

fact, whereas 16 years of data are a very short period for analysing high variability sea level time series as found in the German North Sea region.

The results from non-linear data adaptive smoothing using SSA with an embedding dimension of $D = 11$ years for the Helgoland time series and of $D = 33$ years for the Cuxhaven time series and the resulting annual rates of SLR are shown in Fig. 2-6.
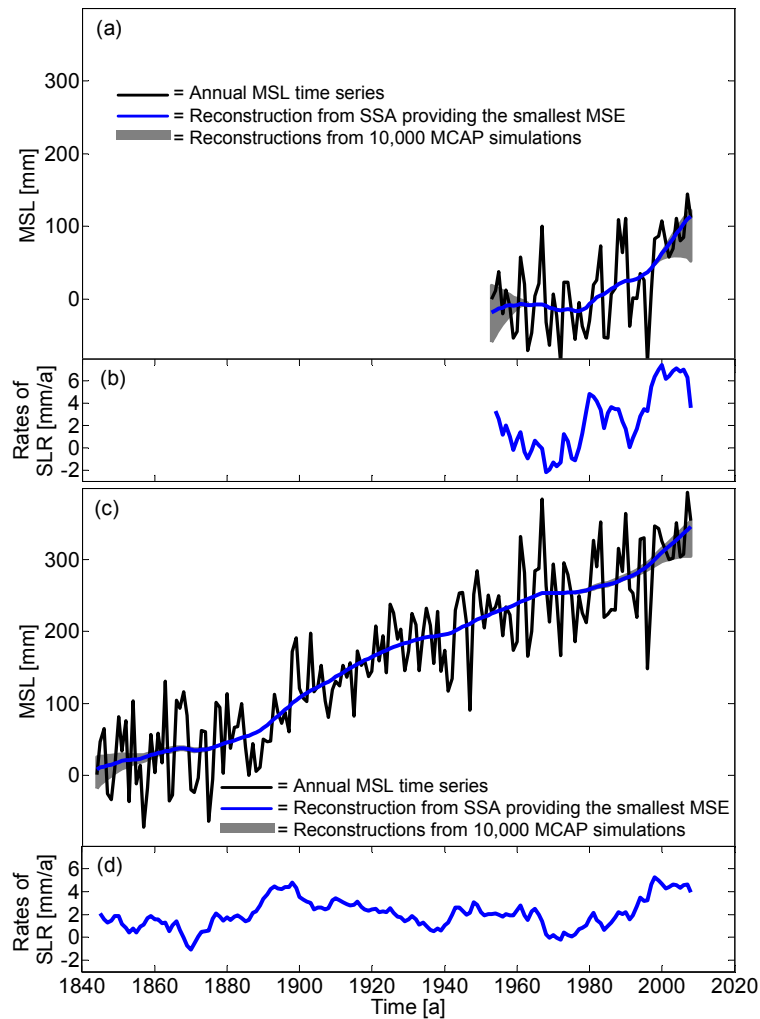
Figure 2-6:   Results from non-linear smoothing using SSA in combination with MCAP and annual rates of SLR estimated as the first deviation of the reconstruction providing the smallest MSE for the Helgoland MSL time series ((a) and (b)) and the Cuxhaven MSL time series ((c) and (d)).

The results for the Cuxhaven tide gauge (Figs. 2-6c and 2-6d) point to a period of strong positive acceleration of SLR at the end of the 19th century, to a negative acceleration in subsequent years and to a period of almost no SLR around the 1970s with subsequent positive acceleration. High rates are observed for the period around 1900 and the highest rates, in the order of 5 mm/a, around the year 2000. The inflection point at the end of the 19th century is remarkably close to observed inflection points around 1880 at the Liverpool

tide gauge (Woodworth, 1999) and around 1890 at the Brest tide gauge (Wöppelmann et al., 2006).

The post 1970 acceleration is approved by the results from analysing the shorter MSL time series from the Helgoland tide gauge (Figs. 2-6a and 2-6b). The observed rates around 2000 from the Helgoland sea level time series are even higher than those found from the Cuxhaven time series, but clearly decrease in recent years. However, the annual rates were estimated from the SSA reconstruction providing the smallest MSE and the uncertainties increase near the boundaries.

Results from analysing a recently updated global sea level reconstruction (Church and White, 2006) are shown in Figure 2-7. The time series was downloaded from the PSMSL website and provides data from 1870 to 2007. Thus, an embedding dimension of $D = 28$ years has been chosen for the SSA analysis. The smoothed time series shows remarkably different patterns of SLR than the sea level time series from the German Bight. A positive acceleration occurred at the end of the 1930s, leading to high rates of SLR around 1940. A subsequent negative acceleration led to small rates of SLR for the period after 1960 and rates are increasing again in recent years.
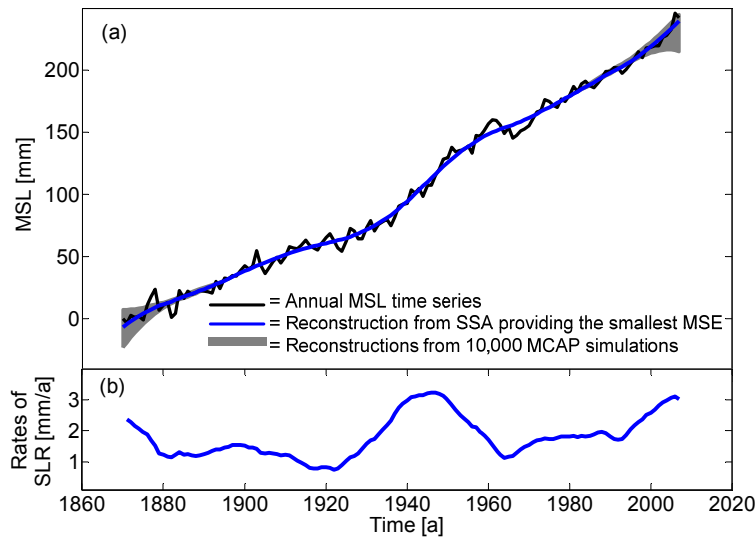
Figure 2-7:   Results from non-linear smoothing using SSA in combination with MCAP and annual rates of SLR estimated as the first deviation of the reconstruction providing the smallest MSE for a worldwide sea level reconstruction from 1870 to 2007.

Figure 2-8 clearly approves the existence of different patterns of SLR. It shows the difference Δ between the estimated annual rates of SLR for the Cuxhaven station (Fig. 2-6d) and the annual rates of SLR estimated from the global reconstruction

(Fig. 2-7b). The resulting time series highlights a stronger SLR in the German North Sea area for a period covering some decades at the end of the 19th century and at the beginning of the 20th century and for another period covering the last ten to fifteen years. For both periods the annual rates of SLR in the German North Sea area are found to be up to 3 mm/a higher than those estimated from the global sea level reconstruction. For other periods (e.g. around 1940) the rates of SLR found from the global reconstruction are more than 2 mm/a higher than those found from the Cuxhaven tide gauge.
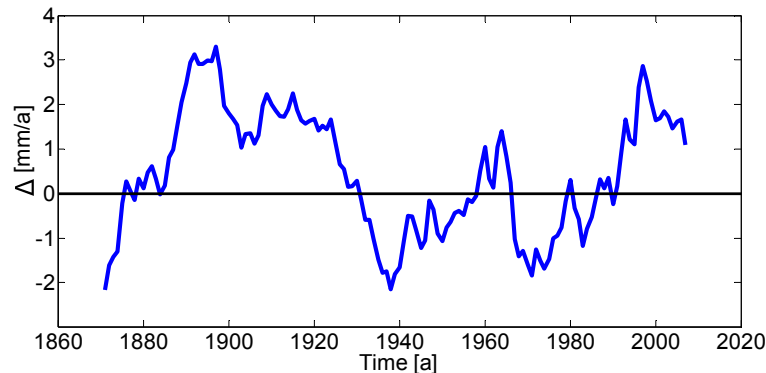
Figure 2-8:   Difference Δ for the period of 1870 to 2007 between the annual rates of SLR estimated from the Cuxhaven MSL time series and the annual rates of SLR estimated from a global sea level reconstruction.

The correlation coefficient between the annual rates of SLR from the Cuxhaven station and the Helgoland station is $r = 0.71$ [-] for the overlapping period (i.e. 1953 to 2008). The correlation between the annual rates of SLR from the Cuxhaven station and the annual rates estimated from the global sea level reconstruction is comparably weak. The correlation coefficient for the overlapping period from 1870 to 2007 is found to be $r = 0.33$ [-]. However, one has to consider that only one single time series from the German Bight is compared to a global reconstruction which is based on a much larger number of tide gauge records (more than 300 for some time periods).

2.5   Conclusions and Outline

In this section, advanced methods to construct and analyse mean sea level time series have been introduced. The presented modification of the *k*-factor method and the MCAP approach for padding non-stationary sea level time series including uncertainty assessment contribute to overcome an existing lack of knowledge when analysing mean sea level time series, especially in shallow seas. The results from analysing the available data sets from

two relevant tide gauges in the German North Sea highlight a post 1970 acceleration of SLR, which has not been reported before and which has obviously declined in recent years. The comparison between the Cuxhaven time series (representing the German Bight) and a global sea level reconstruction clearly reveals the existence of different patterns of SLR. Higher rates of SLR are detected in the German North Sea for a period covering some decades starting at the end of the 19th century and for another period covering the last ten to fifteen years. However, coastal structures along the German North Sea coastline are well-conditioned and to some extend prepared for an expected SLR. In addition, the sea level is part of a complex system undergoing natural variability and there are still considerable uncertainties in the results.

Nevertheless, the study also indicates the need for further research in this field. Uncertainties might be reduced by taking into account the results from CGPS measurements to improve the rates of vertical land movements considered for sea level analyses (e.g. Wöppelmann et al., 2007 and 2009). Furthermore, a reduction of variability of the time series will result in an error reduction. This might be done by considering more high quality MSL time series from German North Sea tide gauges or by quantifying the impacts of stochastic meteorological processes such as wind setup or air pressure. Most of these research activities are currently addressed in Germany. More and more tide gauges are equipped with CGPS by the Federal Agency of Hydrology (BfG, Koblenz). A time consuming digitisation exercise is prepared and partially fulfilled at the University of Siegen. This is to allow for the consideration of more high quality MSL time series to improve the results presented here, e.g. by estimating a synthetic time series for the entire German North Sea area based on a larger number of individual time series (see Sect. 3). The comparison of such a 'virtual station' time series with a global reconstruction is expected to lead to more reliable results. The impacts of wind set up and air pressure are planned to be quantified in close cooperation with oceanographers from the Federal Maritime and Hydrographic Agency (BSH, Hamburg).

Finally, the presented results highlight the need for further studies to improve regional climate models or regional sea level projections, respectively. It is shown that there is at least some doubt that regional patterns of SLR in the German North Sea area are consistent with global patterns of SLR. Thus, the use of global SLR scenarios (as for example published by the IPCC) for regional planning purposes should be an interim solution as long as no reliable regional SLR projections are available for the German Bight area. The

results presented here and those expected after finishing the digitisation exercise and from including data sets from further tide gauges (see Sect. 3) may contribute to the validation of regional climate models for the German North Sea area.

3 Mean sea level changes in the German Bight from the mid 19th century to present

3.1 Abstract

In this section, mean sea level changes in the German Bight, the south-eastern part of the North Sea, are analysed. Records from 13 tide gauges covering the entire German North Sea coastline and the period from 1843 to 2008 are used to derive high quality relative mean sea level time series. Changes in mean sea level are assessed using non-linear smoothing techniques and linear trend estimations for different time spans. Time series from individual tide gauges are analysed and then 'virtual station' time series are constructed (by combining the individual records) which are representative of the German Bight and the southern and eastern regions of the Bight. An accelerated sea level rise is detected for a period at the end of the nineteenth century and for another one covering the last decades. The results show that there are regional differences in sea level changes along the coastline. Higher rates of relative sea level rise are detected for the eastern part of the German Bight in comparison to the southern part. This is most likely due to different rates of vertical land movement. In addition, different temporal behaviour of sea level change is found in the German Bight compared to wider regional and global changes, highlighting the urgent need to derive reliable regional sea level projections for coastal planning strategies.

3.2 Introduction

Changing sea levels are one of the major concerns we have to deal with in times of a warming climate. Many authors have recently studied observed global and regional sea level changes based on tide gauge or altimetry datasets (e.g. Church and White, 2006; Cazenave et al., 2008; Church et al., 2008; Domingues et al., 2008; Haigh et al., 2009;

Woodworth et al., 2009a and 2009b; Wöppelmann et al., 2008 and 2009; Mitchum et al., 2010; Houston and Dean, 2011; Watson, 2011) and possible future global sea level changes have been assessed using climate models (summarised in Meehl et al., 2007) or semi-empirical models (Rahmstorf, 2007; Grinsted et al., 2009; Vermeer and Rahmstorf, 2009; Jevrejeva et al., 2010). As it has been outlined in Sect. 1.1, the results from these studies, which analysed sea level changes on different spatial scales with different methods, clearly point to the existence of considerable regional variability in the rates of sea level change (e.g. Church et al., 2004 and 2008; Mitrovica et al., 2001 and 2009). This arises due to an uneven distribution of meltwater from ice sheets and glaciers, gravitational effects, non-uniform thermal expansion and salinity changes. As Miller and Douglas (2007) and Woodworth et al. (2010) reported, gyre-scale atmospheric pressure variations may also contribute to different regional behaviour of sea level changes.

As there has been considerable spatial variation in sea level changes in the past, it is likely that future changes in sea level will also exhibit strong spatial variability. Currently, global sea level projections from the Intergovernmental Panel on Climate Change's (IPCC) Fourth Assessment Report (Meehl et al., 2007) are used for most coastal planning purposes, and regional differences from the global mean changes are ignored. To overcome this inadequacy, reliable regional sea level projections are urgently needed. Thus, studies of regional sea level have become all the more important in recent years.

In Sect. 2 sophisticated techniques to analyse sea level rise were described and as an example applied at two stations (Cuxhaven and Helgoland) in the German Bight. The overall aim of this present section is to apply these analyses techniques to a much larger tide gauge dataset (13 sites) in the same region. The main objectives are to: (1) determine more accurately than before rates of relative mean sea level (RMSL) changes at single tide gauge sites in the German Bight, (2) examine whether there are differences in RMSL changes along the German coastline, (3) compare the changes in sea level observed in the German Bight with those observed on a wider regional and global scale, and finally (4) to provide simple estimates of rates of vertical land movement based on the RMSL time series. It is hoped that the results from this study (and others) will contribute to the validation of regional models used for the estimation of future sea level rise projections.

The structure of the section is as follows: In Sect. 3.3, the tide gauge datasets and the investigation area are described. The methodology used to generate and analyse the high quality RMSL time series is also briefly discussed (see Sect. 2 for more detailed

information). The results are described in Sects. 3.4. The key findings are summarised and discussed in Sect. 3.5 and the conclusions and an outline are given in Sect. 3.6.

3.3   Data and Methods

Figure 3-1 shows the investigation area in the south-eastern North Sea. Originally 18 tide gauges were selected for the study, each with records of at least 50 years in duration. Fifty years has been identified as a sufficient length for long-term trend analyses (Douglas 1991; Pugh 2004), although the underlying variability still has to be taken into account. The effect of the length on the resulting long-term trend and the related standard error has recently been assessed by Haigh et al. (2009) for the UK. Of the initial 18 sites, five were not considered further due to impacts from: inland drainage (tide gauges of Schluettsiel and Bensersiel), barrages (tide gauge of Toenning), significant coastal engineering measures (tide gauge of Buesum), and suspicious data (tide gauge of Borkum). The final 13 sites chosen for the analyses are shown in Fig. 3-1 and are almost evenly distributed along the German North Sea coastline.

Figure 3-2 shows the lengths of data available at each of the study sites and distinguishes between two different sources of data. The older data mainly consists of time series of high and low waters, which can be averaged over a year to give an estimate of mean tide level (MTL). The second source of data is high frequency (at least hourly values) sea level measurements, which can be averaged over a year to give an estimate of mean sea level (MSL). High frequency datasets are available since the late 1990s for most of the considered tide gauges. Longer high frequency datasets are available for Helgoland, Cuxhaven and Wilhelmshaven. To partially resolve the shortcoming of missing high frequency data from the past, selected data from the tide gauges of Hoernum (1951, 1965, 1976, 1987) and Wyk (1951, 1952) have recently been digitised by the Agency of Roads, Bridges and Waters in Hamburg (LSBG) and the Government-Owned Company for Coastal Protection, National Parks and Ocean Protection (LKN). Most tide gauges provide data from 1936/1937 onwards. The Cuxhaven tide gauge provides the longest record (starting in 1843, which is one year more than used in Sect. 2), followed by Norderney (starting in 1901) and Lt. Alte Weser (starting in 1903). All considered data sets were checked for errors and corrected for local datum shifts, as reported in IKÜS (2008) and Jensen et al. (2010). No inverse barometer correction was applied.
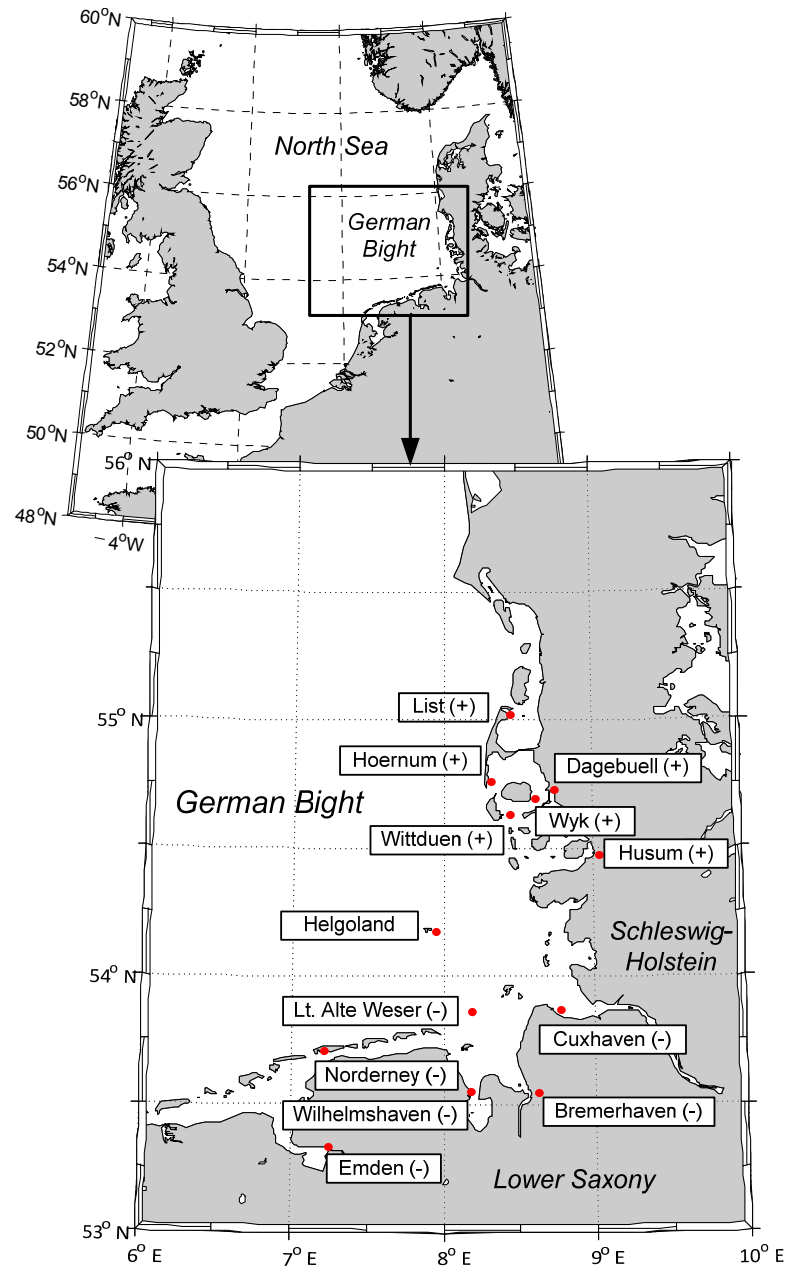
Figure 3-1:   Investigation area and locations of the considered tide gauges along the German North Sea coastline. Gauges marked with (+) are used to construct a virtual station time series for the eastern part of the German Bight and gauges marked with (-) are used to construct a virtual station for the southern part.

In regions such as the southern North Sea, strong shallow water effects deform the tide resulting in large (> 20 cm) differences between MTL and MSL. Hence, this has to be considered when generating and analysing mean sea level time series. Not accounting for the difference between MTL and MSL would lead to erroneous trend estimates. The *k*-factor method, as described in detail in Sect. 2, is used to transfer MTL to MSL. *k*-factors

are reference values for the observed differences between MTL and MSL, and have been calculated for all tide gauges following Eq. (2-1).
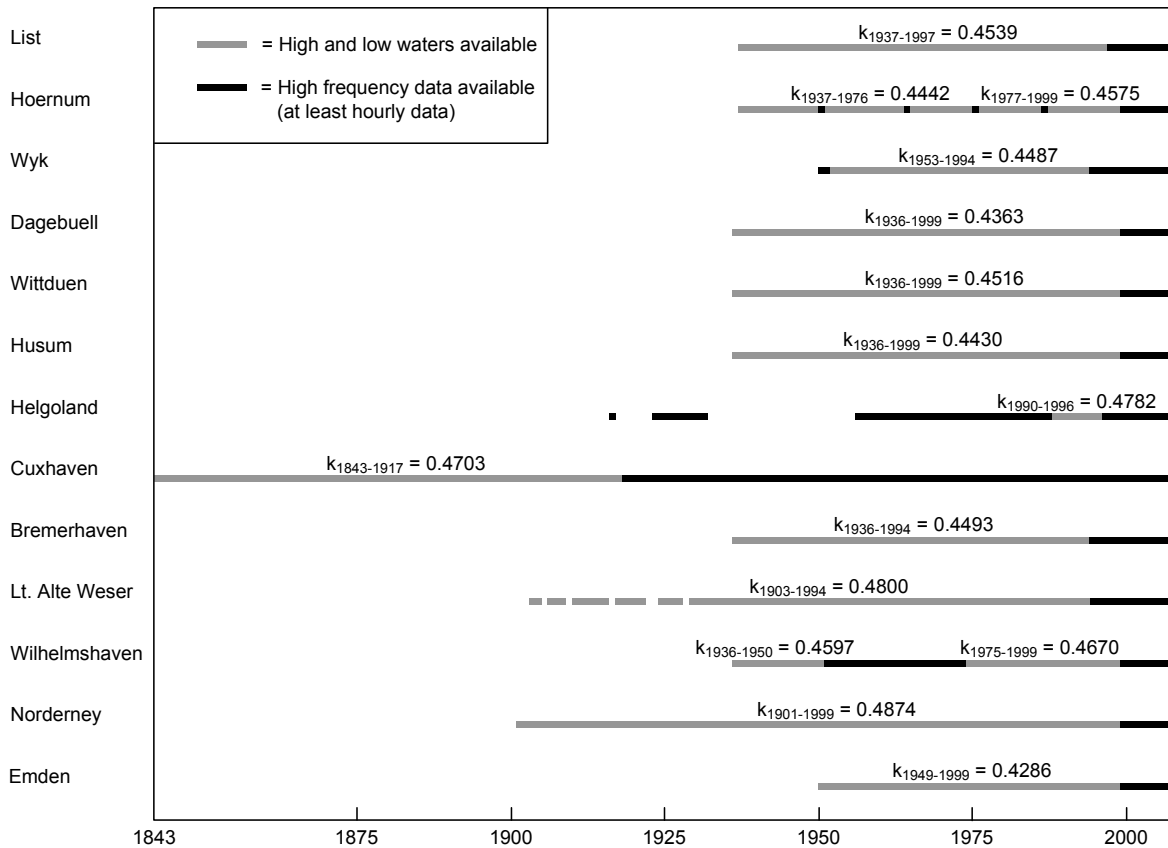
Figure 3-2:   Duration of the sea level data sets and the *k*-factors calculated for different time periods. These were used to transfer the MTL data, derived from tidal high and low waters, to MSL data.

A symmetric tide has a *k*-factor of 0.5. The smaller the calculated *k*-factor, the stronger the asymmetry of the tide and the larger the deviation between MTL and MSL. Before the mean *k*-factors can be used to combine the long MTL time series with the (for most gauges) shorter MSL time series they have to be tested for stationarity (i.e. the time series have to be free of trends, shifts and periodicity) (e.g. Mudersbach and Jensen, 2010). In Sect. 2, three different tests on stationarity have been introduced (i.e. sliding-window test, Kolmogorov-Smirnov test and Mann-Kendall test) and are considered here to search for significant trends or shifts in the monthly *k*-factor time series. Figure 3-2 shows the calculated mean *k*-factors for the considered tide gauges. For some gauges (i.e. Wilhelmshaven and Hoernum), non-stationary behaviour of the *k*-factors has been detected and different *k*-factors for different time periods have been considered. The tide gauge of Emden shows the lowest mean *k*-factor of $k = 0.4286$ [-], which, considering a mean tidal range of MTR = 323 cm at this site, equates to a difference between MTL and MSL of

about 23 cm. The highest *k*-factor of *k* = 0.4874 [-] is derived for the tide gauge of Norderney and equates to a difference between MTL and MSL of only 3 cm (considering a mean tidal range of MTR = 244 cm at this site).

The *k*-factor-corrected RMSL time series, for each of the 13 study sites, are the dataset analysed in the remainder of the section. The methods used to analyse these time series are the same as those described in detail in Sect. 2 and hence are only briefly described below.

To detect non-linear changes in sea level a non-linear smoothing technique (here, Singular System Analysis (SSA) with an embedding dimension of *D* = 15 years) is applied to the RMSL time series at each site. This is done in combination with Monte-Carlo autoregressive padding (MCAP), an advanced approach to assess the uncertainties when continuing the smoothing towards the ends of the available time series. Identifying the SSA reconstruction that gives the smallest mean squared error (MSE) against the observations, results in a very data adaptive smooth of the available time series. The rates of sea level rise (SLR) are estimated as the first differences of the SSA reconstructions providing the best fit. These methods allow for the detection of inflection points and periods of high or low (or even negative) rates of SLR. To analyse the longer-term changes, linear trends from single time series are estimated for a range of different periods. These periods were chosen based on the length of the available time series and the results from the non-linear smoothing.

After analysing individual sites, so-called 'virtual stations' are constructed by averaging observed rates of SLR per year (i.e. the first differences of the annual MSL time series) from a specified number of tide gauges. The resulting time series are integrated backwards by adding up the previously calculated averaged rates of SLR. These time series are also assessed using the non-linear smoothing and linear trend methods described above and in Sect. 2. The derived virtual station for the entire German Bight is contrasted to a northeast Atlantic and a global sea level reconstruction (Jevrejeva et al., 2006). Rates of SLR calculated from each of the three time series are compared and correlation coefficients are calculated for running 20-year periods. The northeast Atlantic reconstruction was obtained from Svetlana Jevrejeva and the global reconstruction was downloaded from the PSMSL website. The global reconstruction by Jevrejeva et al. (2006) goes back to the year 1700 and thus provides a longer overlapping time period with the German Bight reconstruction compared to the global reconstruction by Church and White (2006) that has been used in

Sect. 2. Wahl et al. (2011) show that both of the global reconstructions do not differ substantially for the overlapping time period.

Finally, a simple method (following the approach of Haigh et al., 2009) is used to provide an estimate of rates of vertical land movement at the 13 study sites. Woodworth et al. (2009b) found that the rate of SLR solely from oceanographic processes (i.e. no vertical land movements) around the UK was 1.4 mm/a for the period from 1901 to 2006. Given the regional connection between the two study areas (UK and German Bight), it is assumed that similar long-term sea level changes took place over the last century in the German Bight (based on the results presented in the following, this appears appropriate, but the simplicity of the approach is recognised). Thus, the linear trends derived for stations providing data for the period from 1901 to 2006 are subtracted from 1.4 mm/a to give an estimate of vertical land movement at these sites. The tide gauges providing long records are then used as 'reference stations' to give estimates of vertical land movement for the other tide gauges considered in the present study. In addition, estimates of vertical land movement from a glacial isostatic adjustment (GIA) model and from geological studies are also presented for comparison purposes.

3.4   Results

3.4.1 RMSL changes along the German North Sea coastline

Figure 3-3 shows the results from the non-linear smoothing of the considered tide gauge records. The uncertainties increase towards the ends of the time series due to the padding (i.e. extrapolating the time series before smoothing, see Sect. 2). The shaded bands represent the results from a large number of SSA reconstructions from which the one providing the best fit (i.e. the smallest MSE) compared to the observations is highlighted in the plot. The underlying annual MSL time series are in good agreement, showing noticeable high or low values for the same years, which indicates high data quality and regional coherence. Most of the smoothed time series point to an accelerated SLR over the last few decades, with a starting point in the 1970s. For most of the shorter records, the estimated recent rates of SLR are the highest ones observed. However, longer records (i.e. Cuxhaven and Norderney) show similar rates in the past, indicating that the recent high rates of rise are not as yet particularly unusual.
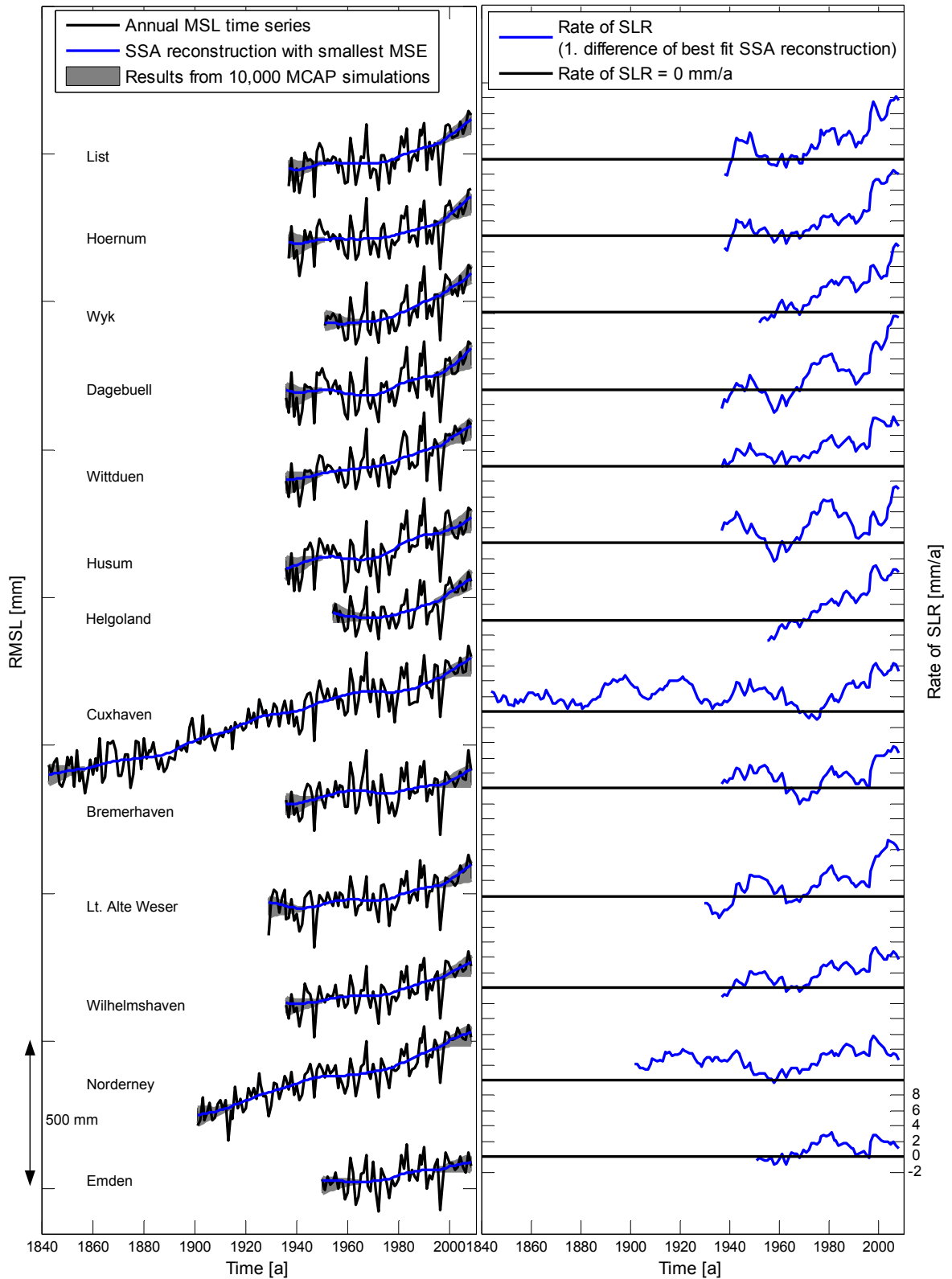
Figure 3-3:   Mean sea level time series for the considered tide gauges and results from non-linear smoothing applying SSA with an embedding dimension of $D = 15$ years in combination with 10,000 MCAP simulations (left) and rates of SLR estimated as the first differences from the SSA reconstruction providing the best fit (right); time series have been plotted with arbitrary offsets for presentation purposes.

The findings are confirmed by calculating linear trends for different common time periods, as shown in Tab. 3-1. All stated errors are 1-σ standard errors (equivalent to 68% confidence levels).

Table 3-1:   Linear trends with 1-σ standard errors and correlation coefficients (values in parentheses) for common time periods for individual time series and virtual station time series.

Tide gauge	Linear trends of RMSL for different time spans ± 1-σ standard errors [mm/a] (correlation with 'virtual station' of the German Bight)				
	1843-2008	1901-2008	1937-2008	1951-2008	1971-2008
List (+)	-	-	2.0 ± 0.3 (0.98)	2.4 ± 0.4 (0.98)	4.2 ± 0.8 (0.98)
Hoernum (+)	-	-	1.8 ± 0.3 (0.98)	2.1 ± 0.4 (0.98)	3.7 ± 0.8 (0.98)
Wyk (+)	-	-	-	2.8 ± 0.5 (0.98)	4.6 ± 0.8 (0.97)
Dagebuell (+)	-	-	1.7 ± 0.4 (0.95)	2.2 ± 0.5 (0.96)	3.7 ± 0.9 (0.97)
Wittduen (+)	-	-	2.4 ± 0.3 (0.97)	2.6 ± 0.4 (0.97)	3.9 ± 0.8 (0.97)
Husum (+)	-	-	2.2 ± 0.3 (0.96)	2.5 ± 0.5 (0.96)	3.6 ± 0.9 (0.97)
Helgoland		-	-	2.1 ± 0.4 (0.96) *	3.5 ± 0.7 (0.96)
Cuxhaven (-)	2.3 ± 0.1 (0.99)	2.2 ± 0.2 (0.96)	2.1 ± 0.3 (0.95)	2.0 ± 0.4 (0.94)	3.6 ± 0.8 (0.94)
Bremerhaven (-)	-	-	1.2 ± 0.3 (0.92)	1.0 ± 0.5 (0.90)	2.5 ± 0.8 (0.94)
LT Alte Weser (-)	-	1.9 ± 0.2 (0.88) *	1.7 ± 0.3 (0.95)	1.7 ± 0.4 (0.95)	3.1 ± 0.8 (0.96)
Wilhelmshaven (-)	-	-	1.9 ± 0.3 (0.98)	2.0 ± 0.4 (0.99)	3.4 ± 0.7 (0.99)
Norderney (-)	-	2.4 ± 0.1 (0.95)	2.4 ± 0.3 (0.96)	2.8 ± 0.4 (0.95)	4.2 ± 0.6 (0.96)
Emden (-)	-	-	-	1.3 ± 0.4 (0.94)	2.1 ± 0.7 (0.94)
'virtual Station' (eastern German Bight)	-	-	2.2 ± 0.3 (0.99)	2.5 ± 0.4 (0.99)	4.1 ± 0.8 (1.00)
'virtual Station' (southern German Bight)	2.0 ± 0.1 (1.00)	1.7 ± 0.1 (0.99)	1.8 ± 0.3 (0.99)	1.8 ± 0.4 (0.99)	3.2 ± 0.7 (0.99)
'virtual Station' (German Bight)	2.0 ± 0.1	1.7 ± 0.1	2.0 ± 0.3	2.1 ± 0.4	3.6 ± 0.7

* Some years of the considered time period are missing, but at least 93% are available (see also Fig. 3-2)

Higher trends (3.6 mm/a on average) are estimated for the time period from 1971 to 2008, compared to the periods from 1951 to 2008 and 1937 to 2008 (2.0 and 2.1 mm/a on average). However, standard errors for the shortest time period are relatively large (in the order of 0.8 mm/a). The long records show slightly higher rates again, when longer time periods (1901 to 2008, 1843 to 2008) are considered. For the period from 1951 to 2008, for which data are available from all gauges, the trends vary between 1.0 mm/a (Bremerhaven) and 2.8 mm/a (Norderney). Standard errors are in the order of 0.4 mm/a.

The tide gauge of Norderney is most influenced by the local datum corrections reported in IKÜS (2008). In previous studies, these datum corrections were not accounted for (e.g. Jensen and Mudersbach, 2007). Thus, the trends presented here for Norderney might differ from those reported in earlier studies. The estimated long-term trend (1843 to 2008) for the Cuxhaven station is 2.3 mm/a. Trends found for the period starting in 1971, which has been identified as the starting point of the recent SLR acceleration, are mostly greater than 3.5 mm/a.

It has been recognised that standard errors can be reduced by applying 'master station' methods (e.g. Woodworth et al., 2009; Haigh et al., 2009), lowering the variability (e.g. by subtracting a sea level index describing the coherent part of sea level variability of the considered time series). This approach has been tested with the datasets from the German Bight using the de-trended virtual station for the entire German Bight (see Sect. 3.3) as 'master station'. This leads to an error reduction of up to 75% for the period from 1937 to 2008. However, the estimated trends do not change significantly.

In general, higher RMSL trends are observed for tide gauges in the eastern part of the German Bight (federal state of Schleswig-Holstein) compared to those located in the southern part (federal state of Lower Saxony). Significant differences (at 95% confidence level) between the two groups of gauges (in Tab. 3-1: List to Husum, marked with (+); Cuxhaven to Emden, marked with (-)) are found for the periods from 1951 to 2008 and 1971 to 2008.

3.4.2 Temporal changes of RMSL from virtual stations

In this section, virtual stations for the entire German Bight and southern and eastern parts of it are analysed. As outlined in Sect. 3.3, virtual stations are constructed by first differentiating the individual time series, before averaging the resulting rates of sea level change between adjacent years. Figure 3-4 (top) shows the results of this computational step (all 13 RMSL time series are considered). The resulting time series highlights the strong short-term variability in sea level changes along the German North Sea coastline. The absolute maximum difference between two adjacent years of observations is of the order of 150 mm and is about 50 mm on average. The absolute maximum first difference found from the monthly RMSL time series (not shown here, but in Fig. 2-5 for selected tide gauges) is in the order of 770 mm and is about 140 mm on average. Church et al.

(2004) and Church and White (2006) assumed that differences of more than 250 mm between adjacent monthly values were related to local datum shifts and the time series were broken into separate sections. Defining such limits is necessary when performing global studies considering a large number of records from tide gauges along different coastlines. However, the presented results indicate importantly that changes in the order of 250 mm (first of all due to meteorological forcing) between two adjacent months are not unusual for MSL time series from the German North Sea area. This high variability of course also complicates the estimation of long-term changes from short time series (e.g. < 30 years).

Figure 3-4 (middle) shows the standard deviations for the particular years above the average. As the Cuxhaven station is the only one providing data for the 19th century, the virtual station is the same as the Cuxhaven time series for this period and the standard deviation is zero. Some outliers occur at the beginning of the 20th century. This is because the Norderney time series shows different changes compared to the Cuxhaven and the Lt. Alte Weser records. As stated in Sect. 3.4.1, the Norderney record has been corrected for a number of datum shifts reported in IKÜS (2008), which occurred after 1937. The different behaviour in comparison to Cuxhaven and Lt. Alte Weser at the beginning of the twentieth century might indicate that other datum shifts occurred before 1937, but no detailed information on datum changes is available before 1937. This warrants further investigation and a more detailed data archaeology exercise. The standard deviations remain constant, in the order of about 20 mm, from the end of the 1930s onwards, indicating higher data quality for this period. Since the 1930s, the maintenance of the tide gauge equipment has improved and more precise levelling has been undertaken. Figure 3-4 (bottom) shows the number of records averaged to construct the 'virtual station' time series. Only the Cuxhaven tide gauge provides data for the period before 1900 (and two to four gauges from then on until the mid 1930s), which increases the uncertainties for this time period(s). Other methods of determining virtual stations (e.g. empirical orthogonal function (EOF) analyses) are not discussed here, but were examined in a related study by Albrecht et al. (2011).

The time series shown in Fig. 3-4 (top) is integrated backwards to achieve a time series representative of RMSL changes for the entire German Bight (Fig. 3-5, top). The influence of vertical land movement has not been removed before constructing the virtual station

time series. Hence, it is affected by the spatial differences in vertical land motions and therefore should be seen as representing the average RMSL changes in the German Bight.

The values in parentheses in Tab. 3-1 are correlation coefficients for different time spans, calculated for the individual time series and the virtual station for the entire German Bight. The considered time series are highly correlated, with coefficients mostly greater than $r = 0.95$ [-]. Tide gauges covering the eastern part show slightly better correlation with the virtual station than those covering the southern part. The latter is confirmed by EOF analyses conducted by Albrecht et al. (2011).
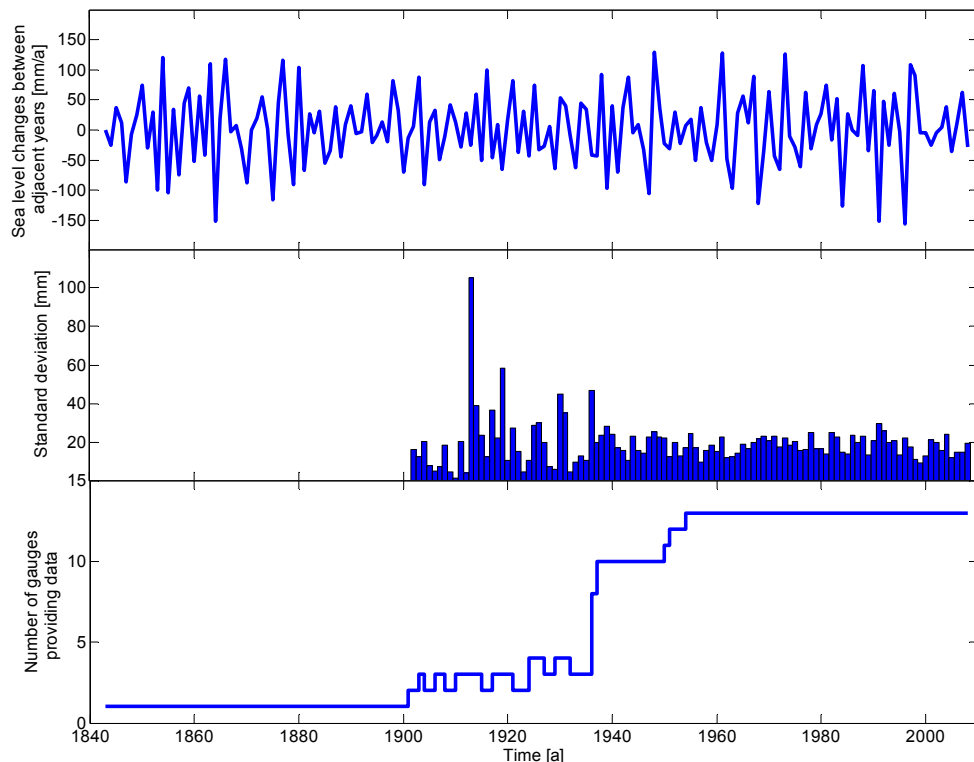
Figure 3-4:   Averaged rates of SLR between adjacent years (top), standard deviation about the average (middle) and number of tide gauges providing data for any given year (bottom).

The non-linear smoothing techniques have been applied to the virtual station time series and the results are shown in Fig. 3-5. In consistency with the results from analysing the individual stations, an acceleration of SLR took place at the end of the nineteenth century, followed by a deceleration. SLR started to accelerate again around the 1970s with a post-1990 intensification, leading to high recent rates in the order of 4 to 5 mm/a. These findings are similar to those reported in Sect. 2, based on the results from analysing only two tide gauges (Cuxhaven and Helgoland).

Linear trends calculated using the virtual station for the entire German Bight are presented in Tab. 3-1 and are in the order of 2 mm/a for the majority of the considered time spans. The trend estimated for the period from 1971 to 2008 is 3.6 ± 0.7 mm/a and increases to 7.3 ± 2.7 mm/a for the shorter period from 1993 to 2008. In comparison, the global trend estimated using altimetry data for the latter period is 3.5 ± 0.4 mm/a (Mitchum et al., 2010). Although the estimated trend for the German Bight is reduced when vertical land movements in the order of 0.5 to 1.0 mm/a are accounted for (see Sect. 3.4.4), the results indicate a more rapid SLR over the last one and a half decades in the German Bight area compared to the observed global changes.
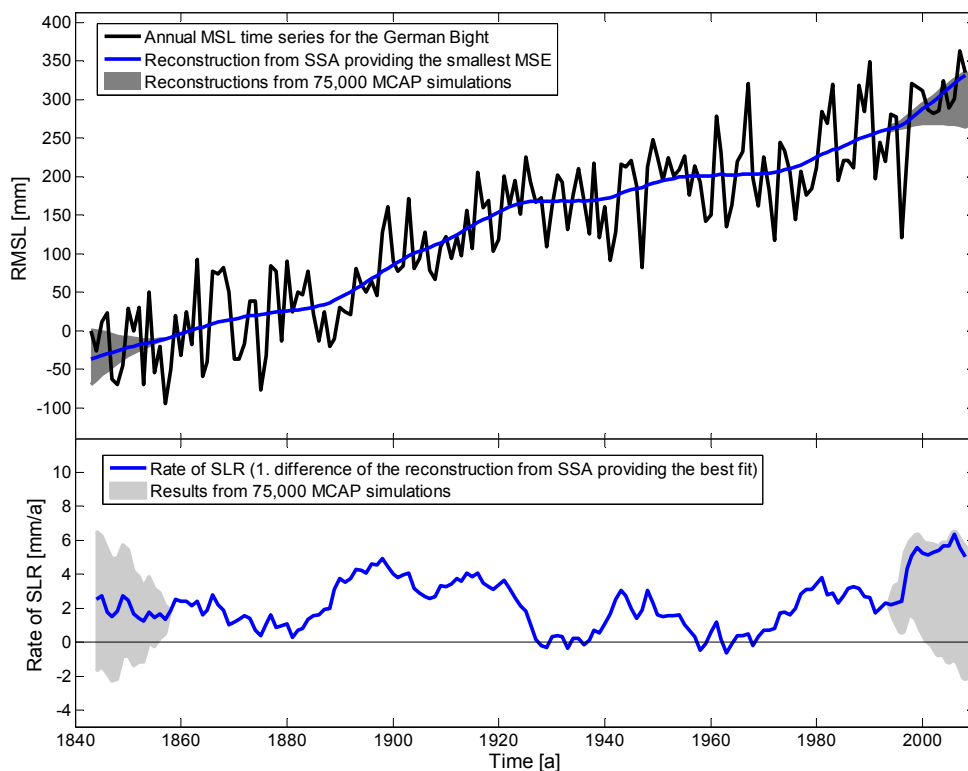
Figure 3-5: Virtual station time series for the entire German Bight and results from non-linear smoothing applying SSA in combination with MCAP.

Figure 3-6 shows linear trends calculated for different time spans from the virtual station for the entire German Bight. Trends are calculated for all overlapping 20-, 30-, 40- and 50-year periods and 1-σ standard errors are displayed. The trend values are plotted at the final year of the time window considered for the trend calculation. A window length of 20 years appears to be too short to meaningful assess the underlying high variability present in the RMSL time series. The results for 30-, 40- and 50-year time spans confirm the existence of two periods of SLR acceleration (end of the 19th century and recent decades). Similar

inflections at the end of the nineteenth century can be observed from other long European sea level records (e.g. Liverpool and Brest). Miller and Douglas (2007) and Woodworth et al. (2010) argue that these are related to gyre-scale atmospheric pressure variations.
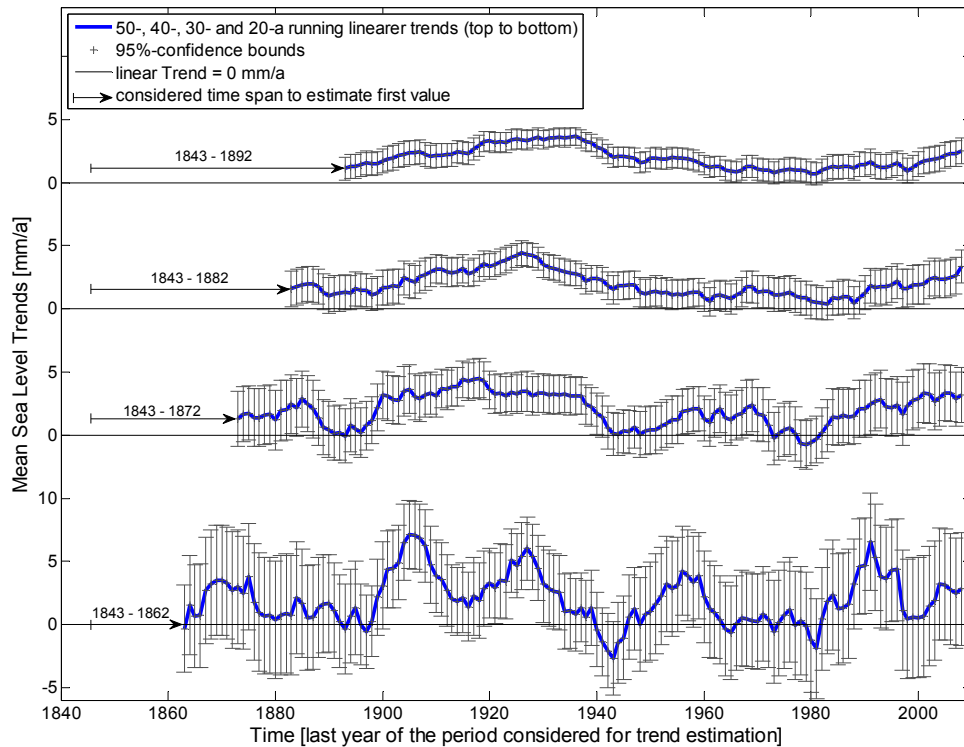
Figure 3-6:   Running linear trends of the virtual station of the entire German Bight for different time spans (50-, 40-, 30- and 20 years, from top to bottom).

As higher rates of SLR are found for the tide gauges covering the eastern part of the German Bight compared with those covering the southern part, two further virtual stations are constructed. A virtual station is determined for the eastern German Bight based on the time series from the tide gauges of List, Hoernum, Wyk, Dagebuell, Wittduen and Husum (marked with (+) in Fig. 3-1 and Tab. 3-1) and a virtual station for the southern German Bight is created from the tide gauges of Cuxhaven, Bremerhaven, Lt. Alte Weser, Wilhelmshaven, Norderney and Emden (marked with (-) in Fig. 3-1 and Tab. 3-1). The offshore tide gauge of Helgoland is omitted at this stage. Again, non-linear smoothing is applied to these time series and linear trends are calculated.

The non-linear smoothing of the two virtual stations is shown in Fig. 3-7. The estimated linear trends for different time periods and the related correlation coefficients with the virtual station for the entire German Bight are listed in Tab. 3-1. As found from analysing the time series of individual gauges, the virtual station for the eastern German Bight shows

higher rates of relative SLR than the virtual station for the southern German Bight. The post-1970 acceleration with an intensification from the 1990s onwards is confirmed by both time series and the recent rates found from non-linear smoothing are in the order of 4 to 6 mm/a for the southern part of the German Bight and 7 to 8 mm/a for the eastern part.
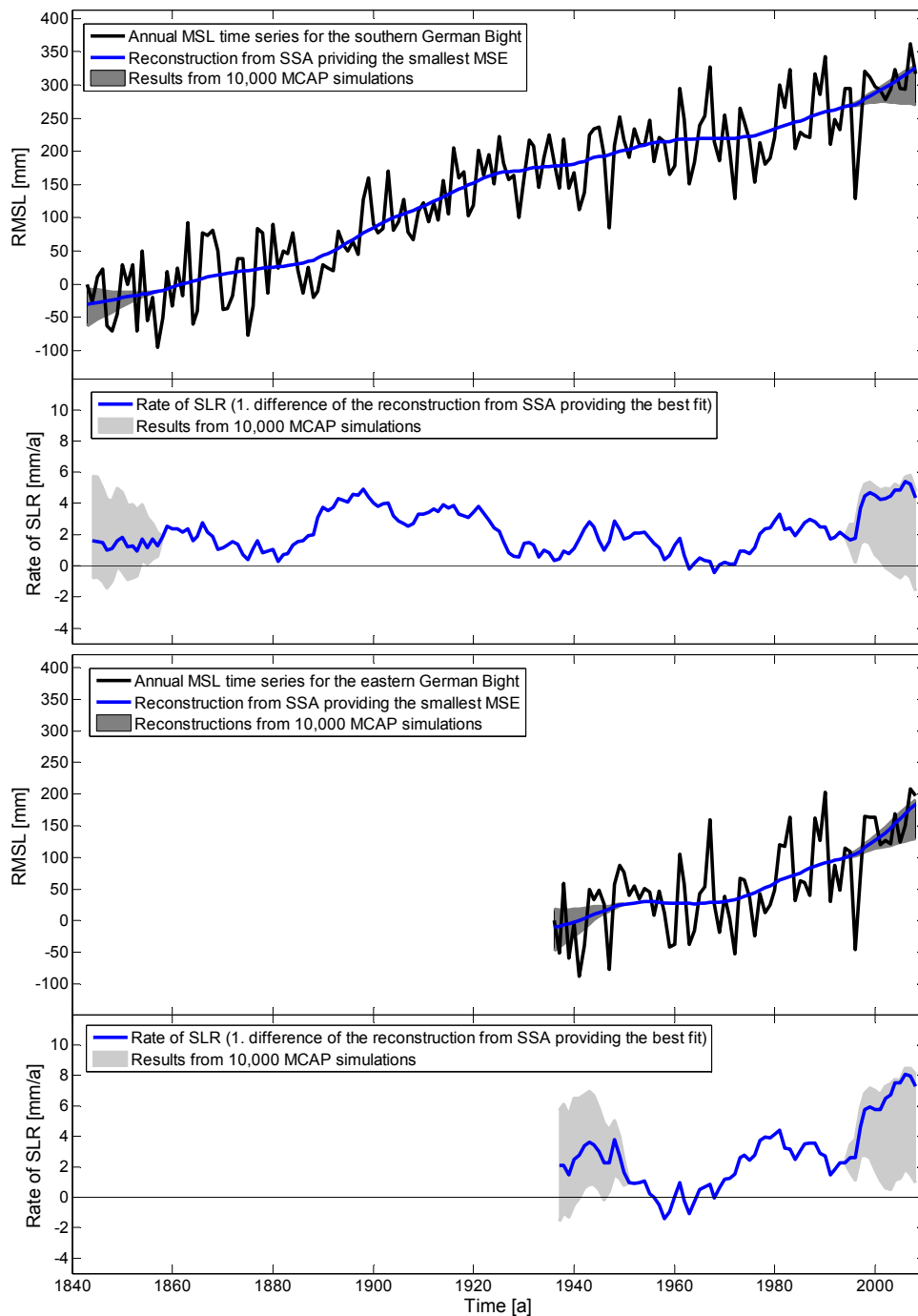
Figure 3-7:   Virtual station time series for the southern German Bight (top) and the eastern German Bight (bottom) and the non-linear smoothing applying SSA in combination with MCAP.

3.4.3 Sea level changes on regional, trans-regional and global scales

In this section, the coherent temporal changes evident in sea level in the German Bight are compared to those observed over a wider regional and global scale. Figure 3-8 (top) shows the estimated rates of SLR for the German Bight virtual station and global and northeast Atlantic reconstructions.
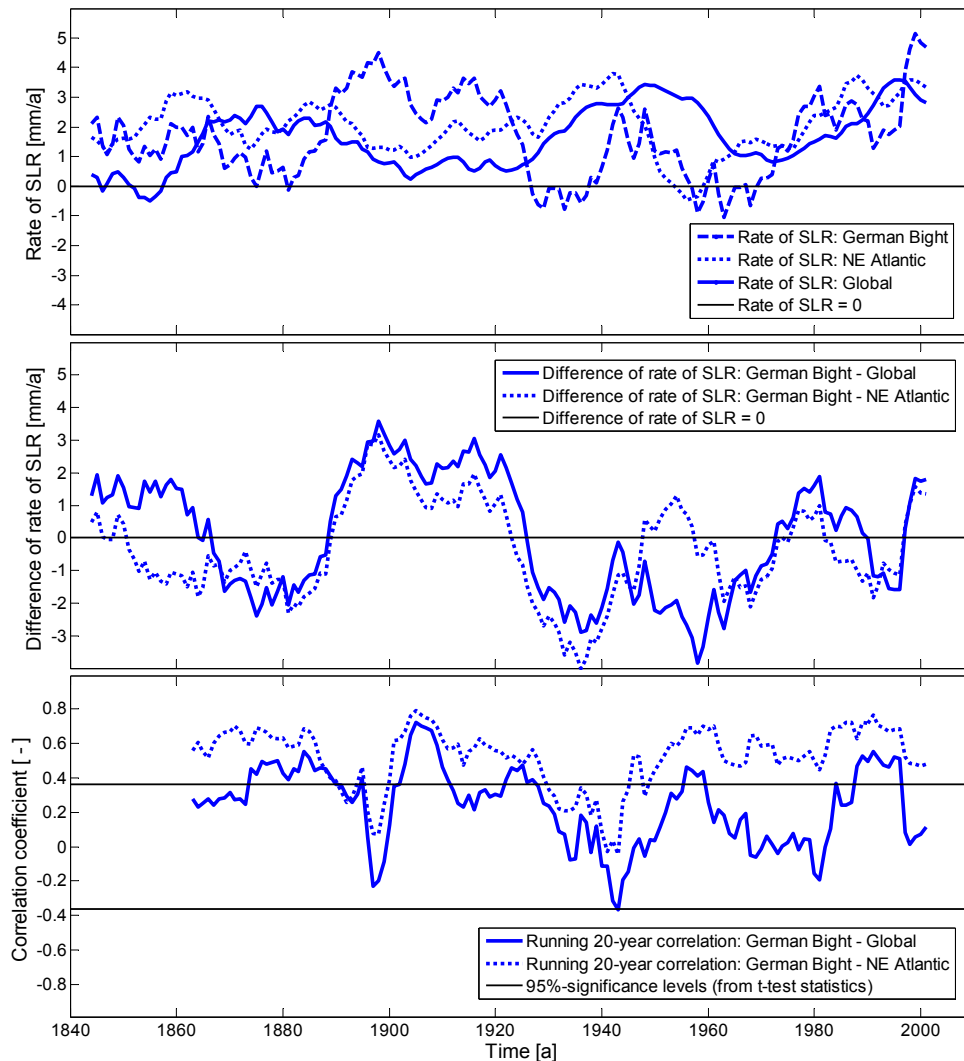
Figure 3-8:   Rates of SLR estimated for the German Bight virtual station, the global reconstruction and the northeast Atlantic reconstruction (top); Differences of rates of SLR between the pairs German Bight-Global and German Bight-northeast Atlantic (middle); 20-year running correlation coefficients between the annual MSL time series for the pairs German Bight-Global and German Bight-northeast Atlantic (bottom) (each correlation coefficient is displayed for the last year of the considered 20-year period).

For consistency, in this part of the analysis, the time series of the tide gauges from the German Bight were corrected for GIA (Peltier, 2004), as has been done by Jevrejeva et al. (2006). The time period from 1843 to 2001 is considered, as this is the period covered by

the reconstructions. Figure 3-8 (middle) shows the estimated rates of SLR by calculating the differences between the pairs: German Bight–Global and German Bight–northeast Atlantic. The results from the comparison with the global reconstruction are similar to those presented in Sect. 2 where only the Cuxhaven station was used for comparison. Considerably higher rates of SLR are found from the reconstruction for the German Bight for the period covering several decades around 1900 and from the global reconstruction for a period around the 1940s. The reconstruction for the northeast Atlantic agrees slightly better with the reconstruction for the German Bight, especially for a period around the 1950s.

Figure 3-8 (bottom) shows running 20-year correlation coefficients between the annual MSL time series for the pairs: German Bight–Global, and German Bight–northeast Atlantic. The 95% significance levels (from t-test statistics) are also displayed and highlight that most of the estimated correlation coefficients for the pair German Bight–Global are insignificant (66% percent of the estimated coefficients for 20-year periods). In contrast, 83% of the 20-year correlation coefficients estimated for the pair German Bight–northeast Atlantic are found to be significant.

3.4.4 Vertical land movements

Up to this point, it was mostly dealt with relative mean sea level changes, which unquestionably is the most important parameter to be considered for coastal planning purposes. However, for a better understanding of the underlying processes, a separation of the isostatic and the eustatic components is important. Vertical land movements can arise from a range of processes (see e.g. Woodworth, 2006). Regional land movements can be caused by GIA, a rebound effect resulting from the deglaciation after the last ice age as already described in Sect. 2 (e.g. Shennan and Horton, 2002; Teferle et al., 2006). Locally, other effects such as sediment compaction, extraction of ground water and other natural resources, collision of tectonic plates, sediment loading or subsurface faulting (e.g. McKee Smith et al., 2009) may also contribute to land subsidence or uplift.

As stated in Sect. 3.3, the current best estimate for twentieth century SLR around the UK solely from oceanographic processes (vertical land movements removed by considering results from geological and geodetic studies) is 1.4 ± 0.2 mm/a, derived by Woodworth et al. (2009b) from analysing tide gauge data from 1901 to 2006 (with most of the long

records coming from tide gauges located along the UK east coast). Considering both, the results presented above (which show similar sea level characteristics between the German Bight and the northeast Atlantic (Sect. 3.4.3)) and the close regional connection between the investigation areas, it is assumed that similar long-term sea level changes took place over the last century in the German Bight and around the UK. Other effects like atmospheric pressure variations and winds in the North Sea area are not taken into account, as there is no indication in literature that they led to significant differences between the long-term sea level trends (> 100 years) in the two nearby investigation areas. Thus, the estimated RMSL trends of the tide gauges Cuxhaven, Lt. Alte Weser and Norderney (calculated for the period from 1901 to 2006) are subtracted from 1.4 mm/a. This, initially, gives estimates of rates of vertical land movement for the three tide gauges providing the longest records (-0.7 ± 0.2 mm/a for Cuxhaven, -0.5 ± 0.1 mm/a for Lt. Alte Weser and -0.9 ± 0.2 mm/a for Norderney; negative values denote land subsidence). For error estimation, the uncertainty of 0.2 mm/a stated by Woodworth et al. (2009) for the oceanographic component is ignored, following Haigh et al. (2009). Hence, this assumes that all the uncertainty in the estimated RMSL trends is associated with vertical land movements. Therefore, the stated errors are 1-σ standard errors from estimating the linear trends for the considered time span (1901 to 2006). The estimated rate for Cuxhaven is comparable with the rate of -0.68 ± 0.08 mm/a found by Shennan (1987) from geological studies, which suggests our simple method of estimating vertical land movements is appropriate (see also Führböter and Jensen, 1985). Augath (1993) estimated a vertical velocity of -0.5 mm/a to -0.7 mm/a for the Langeoog area (located about 75 km westerly of Cuxhaven; see also Bungenstock and Schäfer, 2009), which is again consistent with our simple estimate.

For the following calculations, it is proceeded on the assumption that vertical trends describe ongoing long-term processes (e.g. Schöne et al., 2009; Woodworth et al., 2009b). Hence, all RMSL trends of the three long records reported in Tab. 3-1 can be corrected for vertical land movements considering the rates estimated above. Afterwards, the tide gauges Cuxhaven, Lt. Alte Weser and Norderney serve as 'reference stations' to derive estimates of vertical land movement for other stations. Therefore, the averaged corrected trends (influence of vertical land movements removed) from the 'reference stations' for a particular time period are compared to the RMSL trends of other stations for the same period.

As an example, the corrected trends for the period from 1937 to 2008 are 1.4 ± 0.3 mm/a for Cuxhaven, 1.3 ± 0.3 mm/a for Lt. Alte Weser and 1.4 ± 0.3 mm/a for Norderney (for the considered period 1937 to 2008 the trends are the same or similar to the 1.4 mm/a reported by Woodworth et al. (2009) for the period 1900 to 2006; this is not the case for other periods considered in the study, e.g. 1951 to 2008). The average value is 1.4 mm/a (standard error is already included in the estimated rates of vertical land movement for the 'reference stations', see below). To achieve an estimate of vertical land movement for the tide gauge of List, the RMSL trend of 2.0 ± 0.3 mm/a for the period 1937 to 2008 reported in Tab. 3-1 is subtracted from the average value of 1.4 mm/a. Thus, the rate of vertical land movement for List is estimated to be -0.6 ± 0.5 mm/a. Following this approach, the standard errors from calculating different linear trends accumulate. The quoted error of 0.5 mm/a for the tide gauge of List is derived by adding the mean standard error of 0.2 mm/a resulting from calculating the vertical land movement rates for the 'reference stations' to the standard error of 0.3 mm/a stated in Tab. 3-1 for the tide gauge of List for the period 1937 to 2008.

The results for all tide gauges are shown in Fig. 3-9, indicating higher rates of subsidence for the eastern part of the German Bight, as expected considering the results described in Sects. 3.4.1 and 3.4.2, where higher trends in RMSL have been detected for this area. Based on the results, uplift appears to be occurring at the gauges of Bremerhaven and Emden. In the case of Emden this is surprising, as it was expected that land subsidence would be evident at this site due to the withdrawal of gas in the vicinity of the area (IKÜS, 2008).

Rates of vertical land movement from the GIA model of Peltier (2004; downloaded from the PSMSL website) are also included in Fig. 3-9 for comparison (no error estimates are available for the GIA values). Discrepancies between the rates derived from GIA modelling and from tide gauges vary from site-to-site. This illustrates that correcting sea level records for GIA is only a good approximation for some gauges, but a very poor one for other gauges (i.e. those where local effects lead to additional subsidence or uplift).
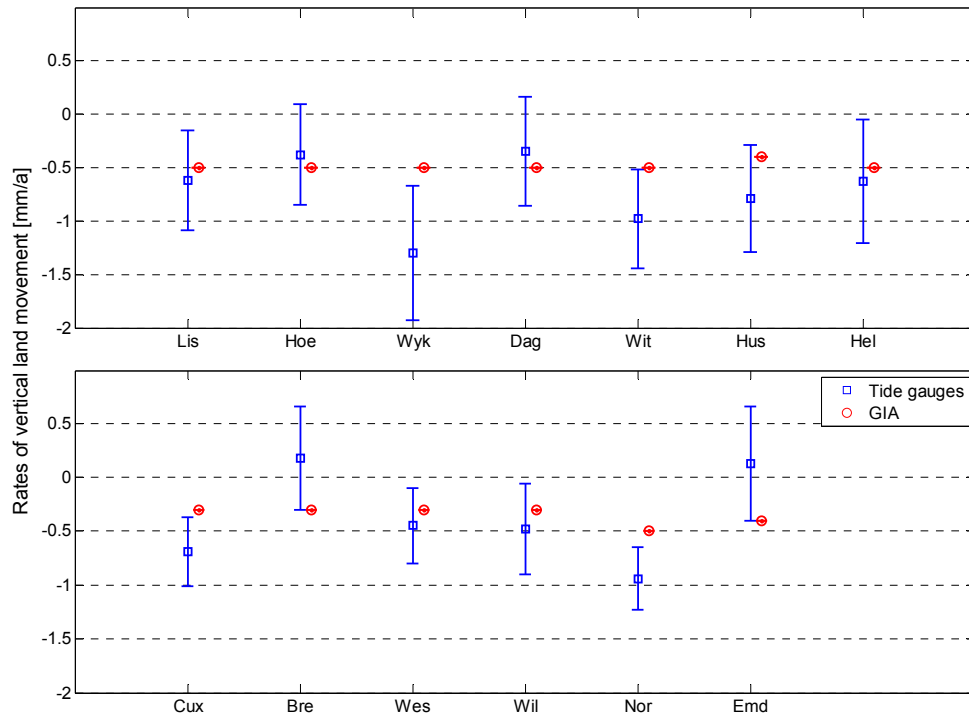
Figure 3-9:   Rates of vertical land movement for the considered tide gauges from estimates based on the RMSL time series (blue) and from a GIA model (red).

3.5   Discussion

The results of this study indicate that the available sea level records from the German Bight area are of good quality. Long records (> 75 years) are available for most of the considered tide gauges. However, no observations are available prior to 1936 for the eastern part of the German Bight (see Fig. 3-2). Most of the tide gauges in this area were installed before 1936, but the data prior to 1936 has not yet been digitised (i.e. it exists in the form of analogue tidal charts or paper lists of tidal high and low waters). Further digitisation exercises are necessary, making the analogue data available for sea level analyses, such as the ones presented here. Due to the high correlation between the individual time series and the virtual station (see Tab. 3-1), it is recommended that the focus be on significantly extending one or two records, rather than partially extending the records for several gauges. EOF analyses may help to identify specific gauges, or combinations of gauges, which provide most reliable information about the decadal sea level variability in the region (Albrecht et al., 2011). The estimated correlation coefficients in Tab. 3-1 indicate that the tide gauges of List or Hoernum (showing correlation coefficients of $r = 0.98$ [-] for all considered time spans) might be most appropriate/ representative to provide useful information about the average sea level changes along the

coastline of Schleswig-Holstein from the end of the 19th or beginning of the 20th century. The tide gauges of Husum and Dagebuell may provide even longer data sets, as they have been installed in 1867 and 1873, respectively.

The analysis of the individual station time series, as well as the assessment of the virtual stations, reveals two periods of accelerated SLR (commencing at the end of the 19th century and from the 1970s on with a post-1990 intensification). Woodworth et al. (2009b) searched for sea level accelerations in selected sea level records around the world and different regional and global sea level reconstructions. They found evidence for a positive acceleration in 1920/1930 and a negative acceleration (or deceleration) in 1960. They also report that these findings are not consistent for all regions (i.e. the 1920/1930 acceleration is absent for most of the considered European records, whereas the 1960 deceleration is evident). This is partly consistent with the findings reported in the present study. As the comparison in Fig. 3-8 (top) shows, the 1920/1930 acceleration is not evident in the German Bight virtual station, whereas the post 1960 deceleration is present to some extent. The recent acceleration (which started in the 1970s) evident in the German Bight is not reported by Woodworth et al. (2009b) for the European tide gauges.

Woodworth et al. (2009b) argued that the temporal behaviour in sea level records is consistent with the behaviour of other climate-related parameters (temperature, volcanic eruptions etc.), but that it is not possible yet to reliably capture such features by numerical modelling. This emphasises the need to extend the available sea level data sets (spatial distribution and length). Updating the analyses undertaken in this study at regular intervals (i.e. every 5 to 10 years) will be necessary to examine whether another deceleration will take place in the near future or whether the recent acceleration denotes the beginning of an anthropogenically influenced SLR in the German Bight area.

The differences found from comparing the virtual station time series for the German Bight with a global sea level reconstruction (Jevrejeva et al., 2006) raises the question whether global sea level rise projections (as published by the IPCC) are appropriate for regional coastal management assessments. This and the better agreement between the virtual stations for the German Bight and the northeast Atlantic region highlight the necessity to derive reliable regional SLR scenarios. Further analyses, to compare the sea level reconstruction for the German Bight with some global, trans-regional or other regional sea level reconstructions in detail, are likely to be useful. Furthermore, the consideration of additional climate related parameters may improve our understanding of the underlying

processes which contribute to temporal and spatial changes in sea level around the German Bight. The influence of atmospheric pressure variations and wind forcing is not considered in the present study, but may contribute to a reduction of the variability of the RMSL time series. Woodworth et al. (2009b) found that the 'inverse barometer' accounts for one third of the variability observed from UK mean sea level time series, whereas larger-scale atmospheric or ocean processes (such as gyre-scale circulation) are also important. Investigating the correlation between the virtual station of the German Bight and the North Atlantic oscillation (e.g. Hurrel, 1995) can explain the observed behaviour to some degree as outlined by Dangendorf et al. (2012). A comparison with variations in surface temperature, salinity or river runoff would also be useful.

Higher RMSL trends are observed for the tide gauges in the eastern part of the German Bight (federal state of Schleswig-Holstein) compared to those located in the southern part (federal state of Lower Saxony). This information is essential for coastal planners, as long-term relative sea level changes are an important factor when defining future design water levels for coastal protection measures. The regional differences are most likely due to different rates of vertical land movement, although other effects, such as atmospheric pressure variations or local winds may also contribute.

A simple method is used to provide an estimate of rates of vertical land movement at the 13 study sites. Increasingly, direct measurements of vertical land movement are being made at tide gauge sites around the world using the Continuous Global Position System (CGPS; e.g. Wöppelmann et al., 2007 and 2009; Schöne et al., 2009). Currently, no reliable estimates of vertical land movement from CGPS are available for the German North sea coastline. This is because most of the CGPS sensors have been installed over the last few years and do not yet provide long enough time series to determine rates to an appropriate level of accuracy. However, more reliable information will be available in the near future, as the record lengths increase.

3.6 Conclusions and outline

This section examines changes in relative mean sea level in the German Bight over the last 166 years. Time series from 13 tide gauges covering the entire German North Sea coastline are analysed. Non-linear smoothing techniques are applied to identify the underlying decadal and longer-term variability, which includes the identification of periods with high

or low rates of sea level rise. It was found that an acceleration of sea level rise commenced at the end of the 19th century followed by a deceleration. Another period of acceleration with its starting point in the 1970s and intensification from the 1990s has been identified, but the high rates of sea level rise during this period are comparable with rates at other times during the last 166 years. Higher rates of sea level rise are detected for tide gauges covering the eastern part of the German Bight than for those covering the southern part, which is an important finding for coastal planning purposes. The comparison of a virtual station time series for the German Bight with a global sea level reconstruction reveals different temporal behaviour of sea level changes, but reasonable agreement is found between the German Bight virtual station and the northeast Atlantic reconstruction.

Rates of vertical land movement are estimated from the sea level records using a simple approach and are compared with geological data and GIA model outputs. Higher rates of vertical land movement are found for the eastern part of the German Bight. This is to some extent supported by the GIA model results. The comparison between the rates estimated from the sea level records and those predicted by the GIA model, illustrate that the single consideration of GIA to correct tide gauge data for vertical land movements can only serve as an approximation. In the future, precise vertical land movement rates are expected to be derived from longer CGPS time series allowing more reliable trend estimates.

To conclude, the presented results indicate the importance of regional sea level studies based on long and high quality sea level observations and it is recommended that further digitisation and data archaeology exercises are undertaken. Increasing the length of sea level records that are currently available will allow for more thorough analyses of the underlying physical processes and lead to more reliable results. The latter is essential to improve the accuracy of regional sea level rise projections (as discussed in Sect. 1.1) to be considered in coastal management strategies and for integrated risk analyses.

4 A stochastic storm surge model

4.1 Abstract

In this section a methodology to stochastically simulate a large number of storm surge scenarios (here: 10 million) is described. The applied model is very cheap in computation time and will contribute to improve the overall results from integrated risk analyses in coastal areas. Initially, the observed storm surge events from the tide gauges of Cuxhaven (located in the Elbe estuary, see Fig. 3-1) and Hoernum (located in the southeast of Sylt Island, see Fig. 3-1) are parameterised by taking into account 25 parameters (19 sea level parameters and 6 time parameters). Throughout this section (as in the rest of the thesis) total water levels are considered. The astronomical tides are semidiurnal in the investigation area with a tidal range > 2 m. The second step of the stochastic simulation consists in fitting parametric distribution functions to the data sets resulting from the parameterisation. The distribution functions are then used for Monte-Carlo simulations. Based on the simulation results, a large number of storm surge scenarios are reconstructed. Parameter interdependencies are considered and different filter functions are applied to avoid inconsistencies. Storm surge scenarios, which are of interest for risk analyses, can easily be extracted from the results.

4.2 Introduction

Performing integrated risk analyses is a crucial task for coastal managers and engineers and becomes even more important in times of a warming climate, which potentially leads to changes of mean sea level heights, storminess or the wave climate. At the same time, the concentration of people living and assets located in coastal areas is rapidly growing and is expected to continue to grow dramatically in the future (McGranahan et al., 2007; Nicholls

et al., 2011). Today millions of people and billions of assets are threatened by inundation caused by mean sea level changes and first of all by storm surge impacts.

The European Union (EU) has recently passed a directive 'on the assessment and management of flood risks (2007/60/EC)' (EU, 2007). The directive requires the EU member states to investigate flood risks for potentially affected areas (inland and coastlines). For coastal areas, different storm surge scenarios have to be considered to map the flood extent. At least three different scenarios (with low, medium and high probabilities of occurrence) should be taken into account for the analyses. The preparation of flood risk maps includes the estimation of the adverse consequences (number of affected inhabitants, types of economic activities in the affected areas, pollution etc.). Based on this information, flood risk management plans have to be established. The quantification of potential losses in the hinterland as well as the estimation of failure probabilities of existing flood defence structures is not provided. However, this is what has to be done when applying risk based design methods or performing integrated risk analyses, respectively, which have gained more importance in river and coastal engineering in recent years (e.g. FLOODsite, 2009; Schumann, 2011). In Germany, the joint research project XtremRisK (www.xtremrisk.de) was launched in 2008 to perform pilot studies (i.e. integrated risk analyses) for two investigation areas in the German Bight (Sylt Island and Hamburg) (Oumeraci et al., 2009; Burzel et al., 2010).

A widely used approach to conduct integrated risk analyses is based on the Source-Pathway-Receptor concept (SPR concept; e.g. Oumeraci, 2004) as discussed in Sect. 1 and shown in Fig. 1-1. First, the risk sources are analysed before failure probabilities of the flood defence structures are calculated. Breach models (for dykes or dunes) are applied to identify the initial conditions for flood propagation and finally, potential losses in the hinterland are quantified. This section focuses on the first part, i.e. the investigation of the risk sources (here: first of all, storm surges). In Sect. 1 it has been outlined that different risk sources have to be taken into account for flood risk analyses in coastal areas. Mean sea level represents a quasi-static loading factor for coastal defence structures, as possible changes occur comparably slow and adaptation strategies can be planned. Results from analysing observed mean sea level changes in the German Bight are presented in Sects. 2 and 3 of the thesis. Storm surges and wind waves, which may coincide due to meteorological forcing, represent dynamic loading factors leading to high water levels for shorter time periods. Throughout this thesis, the term 'storm surges' describes extreme still

water levels (i.e. waves not included) that arise from the combination of astronomical tides and a meteorologically induced surge component. Investigations on long-term changes of storm surges in the German Bight have recently been undertaken by Mudersbach et al. (under review).

It is necessary to consider a large number of storm surge scenarios for a scenario-based risk analysis, as outlined by Fig. 4-1. Initially, a risk curve (as shown in Fig. 4-1, left) has to be estimated before its integration leads to the overall flood risk. The approximation of a risk curve requires a larger number of events to be used as sampling points (Fig. 4-1 contains only four events for presenting purposes). Figure 4-1 (right) highlights that storm surge scenarios with extremely high water levels are not relevant for an integrated risk analysis because the exceedance probabilities P_e of such storm surge events and thus the related probabilities of flooding P_{flood} are approximately zero. At the same time, storm surge scenarios with low water levels can also be neglected, as the potential losses D caused by such events are approximately zero.
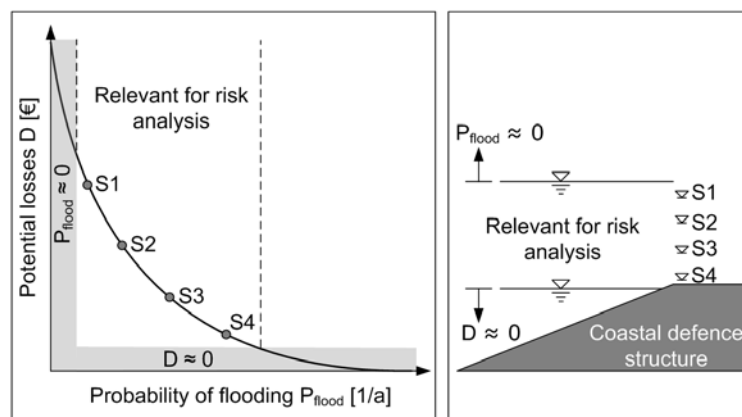
Figure 4-1:   Risk curve (left) and relevance of different storm surge scenarios with different water level heights for risk analyses in coastal areas (right).

For deriving a sufficient number of relevant storm surge scenarios as input data for risk analyses, different methods are available and have been considered in former studies. Numerical hydrodynamic models can be used (e.g. Jensen et al., 2006; Mudersbach and Jensen, 2009) as well as empirical approaches (e.g. Gönnert et al., 2010). Both methods are very time consuming and therefore restrict the number of scenarios which can be generated. Furthermore, it is important to take storm surges with different characteristics into account. This does not only include the storm surge water level height, but also the temporal evolution of the storm surge water levels (i.e. the time-dependent behaviour of the water levels) or the duration of the storm surge events (see Sect. 5 and e.g. Cai et al.,

2008). In this section, an approach to stochastically simulate a large number of storm surge scenarios (here: 10 million) is presented. Selected storm surge scenarios from the simulated results, which are relevant because of their characteristics, can directly be considered for risk analyses. Uncertainties are reduced by considering a larger number of scenarios. Further, the required computation time is comparable small. At the same time, the simulated storm surge events can be used as input data for statistical assessments (in addition to the observations), which also play an important role when performing integrated risk analyses. A multivariate statistical model based on Copula functions to jointly analyse selected storm surge and wave parameters is presented in Sect. 5. In this following section, the results presented here (i.e. stochastically simulated storm surge events) are considered as the data basis and joint exceedance probabilities are calculated (with and without information on the wave conditions included).

Risk-based design methods and probability concepts in which stochastically simulated input variables are used have already been established in different fields (e.g. structural and mechanical engineering, hydrology etc.) (Ang and Tang, 2007; Reeve, 2010). Especially for designing dams or reservoirs, similar approaches to the one presented here for coastal areas are widely used. The methodology considered, for example, by Klein (2009) or Bender and Jensen (2011) to stochastically simulate flood hydrographs, consists of similar computational steps. However, significant enhancements were necessary to account for the different systematic situations in coastal regions. This section provides detailed information about all relevant computational steps of stochastic storm surge simulation; the applicability of the model to different investigation areas (i.e. an island and an estuary) is tested and a validation section is included.

The section is organised as follows: in Sect. 4.3 the considered data sets are introduced. The applied methodology is described in detail in Sect. 4.4. The key results are presented and discussed in Sect. 4.5 and conclusions are summarised in Sect. 4.6.

4.3   Data

The following analyses are based on the available sea level observations from the tide gauges of Hoernum and Cuxhaven. Hoernum is located in the southeast of Sylt Island (see Fig. 3-1) in the northeastern part of the German Bight. Cuxhaven is located in the Elbe estuary in the southeastern part of the German Bight (see Fig. 3-1). The tidal regime is

semi-diurnal and the mean tidal ranges for Cuxhaven and Hoernum are 297 cm and 205 cm, respectively (estimated for the 19-yr period from 1990 to 2008). The tide gauges have been chosen as they provide long records and they are located in areas of special interest. Sylt Island is the biggest German North Sea island and a popular tourist destination. The island hosts valuable monetary and ecological assets and is very vulnerable to extreme storm surge events. In December 1990, a storm surge evoked by the low pressure system 'Anatol' caused extensive erosion along major parts of the island's coastline. The tide gauge of Cuxhaven provides the longest record of all German gauges and is used as the reference station to assess the flood risk for the city of Hamburg, the only German megacity located in an estuary. The most devastating storm surge event along the German North Sea coastline over the last century occurred in February 1962. 340 people died (315 in Hamburg) and major parts of the city of Hamburg were flooded.

In order to take the temporal behaviour of storm surge water levels into account, it is necessary to analyse high frequency observations (at least hourly data). The tide gauge of Hoernum provides data from 1936 onwards (digital high frequency data since 1999, digital high and low waters and analogue tidal charts before 1999). Cuxhaven provides continuous data from 1900 onwards (digital high frequency data since 1918, digital high and low waters and analogue tidal charts before 1918; data sets from the 19th century consist of only one tidal high/tidal low water per day and are therefore not usable).

To identify storm surge events from the available tidal high water (HW) time series, a peak over threshold (POT) method is applied. When forecasting storm surges along the German North Sea coastline, the Federal Maritime and Hydrographic Agency (BSH) uses a threshold of 150 cm above mean tidal high water level (MHW) to separate storm surges from mean conditions (e.g. Wieland, 1990; www.bsh.de). Under present conditions, this equals a total water level of about 305 cmNN for Cuxhaven and of about 253 cmNN for Hoernum (where cmNN stands for cm above Normal Null, which is the German ordnance datum).

To select appropriate thresholds for extreme value analyses, Coles (2001) proposed two different methods, namely the Stability Method (STM) and Mean Residual Life (MRL) plots. Both methods have been used here. In the STM, parameters of a Generalized Pareto distribution (GPD) are fitted to the available (and de-trended) data sets by considering different thresholds u. Figure 4-2 (top) shows the results for the shape parameter of the GPD (left: Cuxhaven, right: Hoernum) with 95 %-confidence bounds included (confidence

bounds for Hoernum cannot be reliably calculated for large values of u). An appropriate threshold is assumed where the shape parameter is approximately constant. As it can be seen, an objective interpretation of the results is difficult. For Cuxhaven, the value of 150 cm above MHW appears to be a suitable choice, whereas the results for Hoernum suggest choosing a slightly smaller value. To create MLR plots, the values exceeding different thresholds u are averaged (see Coles, 2001 for more information). Figure 4-2 (bottom) shows the results for Cuxhaven (left) and Hoernum (right). An appropriate threshold is assumed where the function starts to become approximately linear. Again, the results are not clear and the interpretation is even more complicated compared to the STM. Thus, thresholds of u = 150 cm above MHW for Cuxhaven (equals a total water level of 305 cmNN under current conditions) and of u = 145 cm above MHW for Hoernum (equals a total water level of 248 cmNN) are chosen for the present study. Further methods to identify appropriate threshold values are described and discussed by Lang et al. (1999).
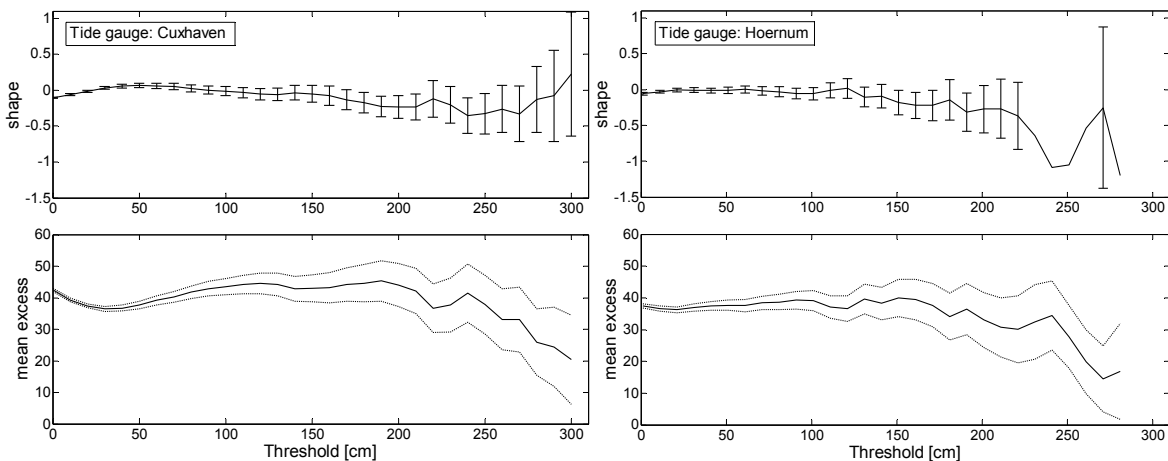
Figure 4-2:   Results of the Stability Method (top) and Mean Residual Life plots (bottom) with 95%-confidence bounds to identify appropriate thresholds for the selected tide gauges Cuxhaven (left) and Hoernum (right).

Figure 4-3 shows the available HW time series for Cuxhaven from 1900 to 2008 (left) and for Hoernum from 1936 to 2008 (right) and the estimated threshold time series. MHW is defined here as the 10-yr running mean of the observed HW to take long-term sea level changes into account. The number of threshold exceedances for Cuxhaven is 388 and 232 for Hoernum, due to the shorter time period that is involved.
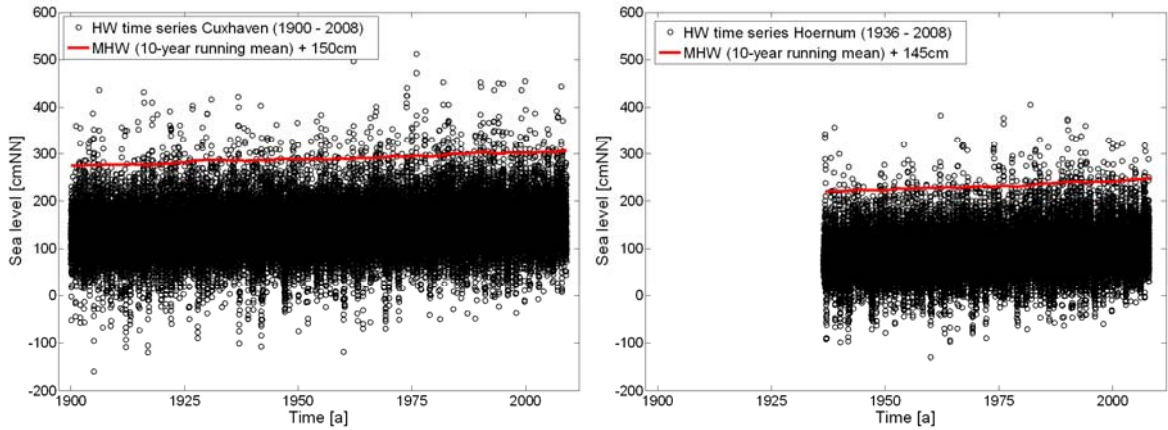
Figure 4-3: Tidal high water time series for Cuxhaven (left) and Hoernum (right) with the estimated threshold time series.

As mentioned previously, it is necessary to take into account the temporal evolution of water levels during storm surge events in addition to the maximum storm surge water levels. Therefore, it is required to define storm surge scenarios not only in height but also in length or duration. The numbers of successive high tides exceeding the selected thresholds are shown in Fig. 4-4.
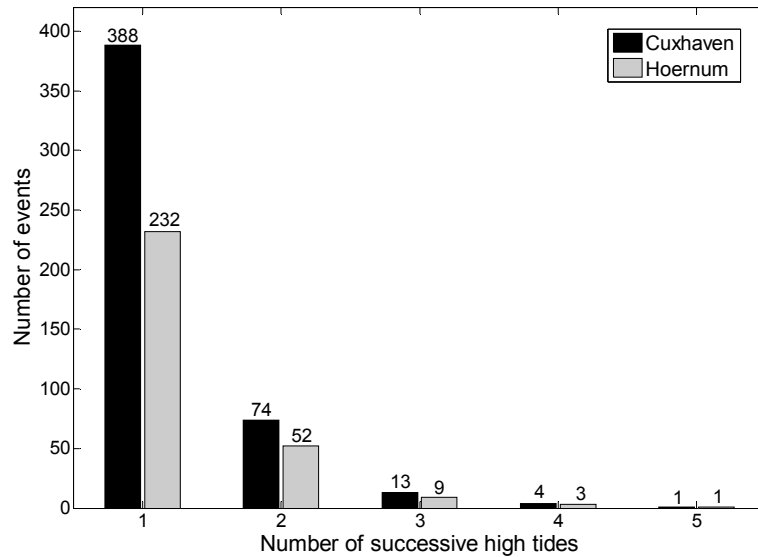
Figure 4-4: Number of successive high tides exceeding the selected threshold values.

In the majority of cases, the events last one or two tidal cycles. Four or five high tides in a row have rarely been observed in the past. Thus, three tides of the observed storm surge events (initial tide, main tide, follow-up tide; i.e. 1.5 days) are considered in the following. To assure independency, two storm surge events have to be at least 30 hours apart from each other (referring to the time when the maximum water levels occur). This reduces the number of relevant events to 314 for Cuxhaven and 175 for Hoernum. Prior to 1918 for

Cuxhaven and 1999 for Hoernum, the events were digitized from the available analogue tidal charts for the present study.

4.4   Method

The method used to stochastically simulate synthetic storm surge scenarios consists of three computational steps, which are described in the following.

4.4.1 Parameterisation of observed storm surge events

Initially, the observed storm surge events are parameterised. As outlined in Sect. 4.2, the total water levels (arising from the combination of tides and surges) are taken into account instead of removing the deterministic tidal component before parameterising the residual surge component. This procedure is justified for the following reasons: (1) parameterisation of the surge residuals is much more complex and increases the uncertainties compared to parameterising the total water level time series as described below, (2) the re-combination of randomly simulated surge curves with the deterministic tide requires either independency between the two components or a detailed understanding of the existing non-linear tide-surge interaction in the investigation area. Both are not the case for the German Bight. Therefore, the total water levels are considered throughout this study, as these are also relevant for coastal managers.

From sensitivity studies, it was found that a total number of 25 parameters is sufficient to capture the main characteristics of a storm surge event consisting of three tides. Figure 4-5 shows the 25 parameters, which are (1) the tidal high and low waters of the three tides comprising a storm surge event, (2) the water levels one hour before and one hour after the high and low waters and (3) the time periods between two adjacent high and low waters. Parameters 1 to 19 represent sea level heights whereas parameters 20 to 25 are time parameters. The height parameters can all be expressed relative to parameter 10 (i.e. the maximum water level observed during the storm surge event). This means that parameters 1, 4, 7, 13, 16 and 19 (tidal high and low waters) refer to parameter 10. Parameter 7, for example, is calculated by subtracting the observed tidal low water level (i.e. the absolute water level of parameter 7) from the maximum water level observed during the storm surge event (i.e. parameter 10). The parameters surrounding the tidal high and low waters refer to

the particular peak water levels. Parameter 3, for example, is calculated by subtracting the water level which has been observed one hour before the high water (i.e. the absolute water level of parameter 3) from the tidal high water level (i.e. the absolute water level of parameter 4).
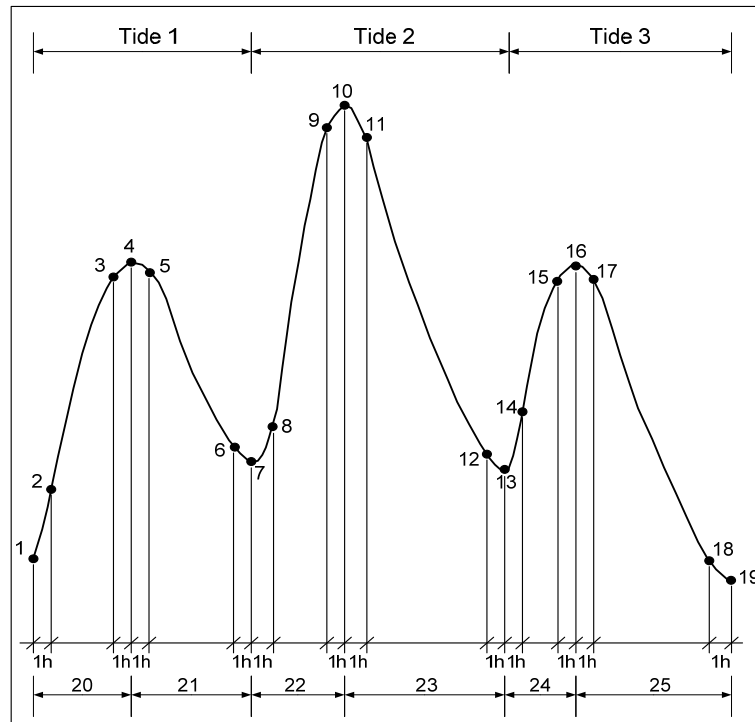
Figure 4-5: Parameters, which are considered to parameterise observed storm surge events consisting of three tides.

For the reconstruction of a storm surge curve based on the 25 parameters, three different methods are tested, namely linear interpolation, cubic spline interpolation, and piecewise cubic hermite interpolation. Figure 4-6 shows, as an example, the results from parameterising and reconstructing a selected storm surge event at the Hoernum tide gauge. The storm surge was induced by the extra-tropical cyclone 'Tilo' that occurred in November 2007. The quality of the reconstruction results, considering the different interpolation methods, is evaluated by calculating root mean squared errors (RMSE). As it can be seen in Fig. 4-6, the estimated RMSEs are similar and all three methods lead to good results for the selected storm surge event. The smallest RMSE is achieved with the piecewise cubic hermite interpolation (also known as cspline; e.g. Kahaner et al., 1988). This was confirmed from parameterising and reconstructing all of the other observed storm surge events (i.e. 314 events for Cuxhaven and 175 events for Hoernum) using the three different interpolation methods.
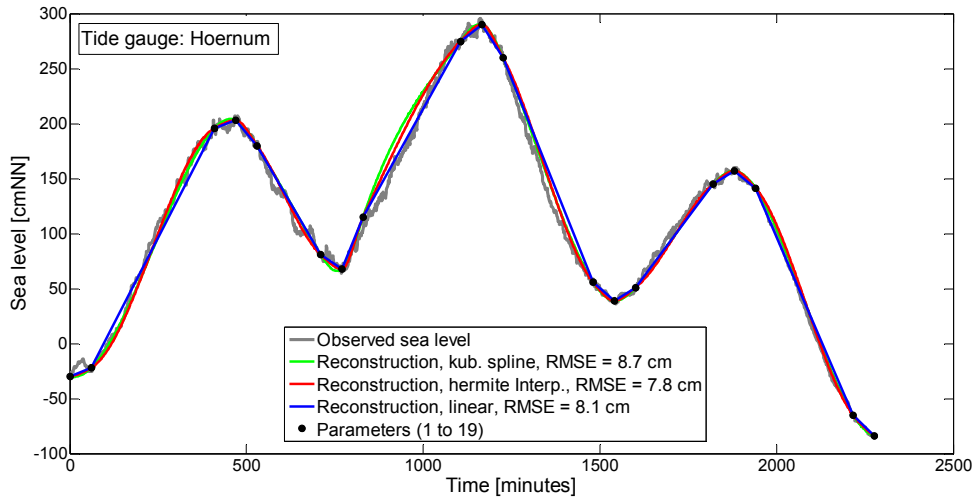
Figure 4-6:   Results from parameterising and reconstructing a selected storm surge event by applying different interpolation methods to reconstruct the observed storm surge curve.

Figure 4-7 shows the results of the parameterisation and reconstruction by applying piecewise cubic hermite interpolation for further storm surge events, four for Cuxhaven (left) and four for Hoernum (right). The applied methodology leads to good results for all of the selected events. The maximum storm surge water levels are usually higher in Cuxhaven compared to Hoernum. From visual inspection, it was found that similar results have been achieved for the rest of the observed storm surge events considered for the present study. As a result of the parameterisation of all observed storm surge events, 25 parameter time series are available for the two selected tide gauges. Each of the 25 time series consists of 314 realisations for the tide gauge of Cuxhaven and 175 realisations for the tide gauge of Hoernum.
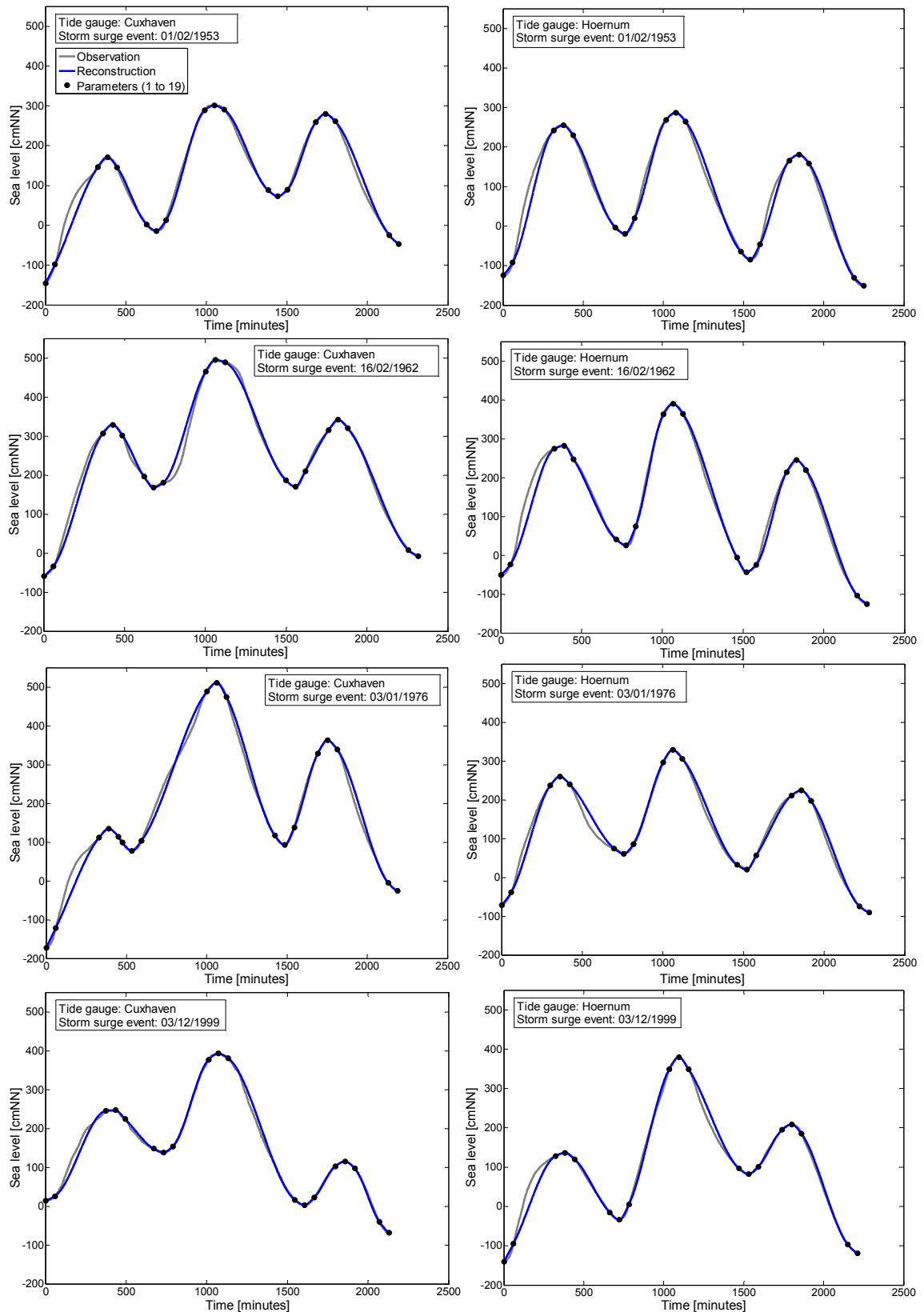
Figure 4-7: Results from parameterising and reconstructing selected storm surge events observed at the tide gauges of Cuxhaven (left) and Hoernum (right).

4.4.2 Monte-Carlo simulations

The next step of the stochastic storm surge simulation procedure consists of fitting parametric distribution functions to the data sets resulting from the parameterisation. The distribution functions are subsequently used as a basis to run a large number of Monte-Carlo simulations. Table 4-1 contains an overview of the considered distribution functions, widely used in hydrology. In the equations, parameter a denotes the location parameter (i.e. the threshold parameter for the GPD), b the scale parameter and k the shape parameter. The maximum likelihood approach is applied to estimate the parameters (see e.g. Rao and Hamed, 2000).

Table 4-1: Distribution functions considered in the present study to be fitted to the time series resulting from the parameterisation of the observed storm surge events.

Distribution	Equation
Generalized Pareto	for $k \neq 0$ $$GP(x) = 1 - \left(1 + \frac{k(x-a)}{b}\right)^{\frac{-1}{k}}$$ for $k = 0$ $$GP(x) = 1 - e^{\left(-\frac{x-a}{b}\right)}$$
LogNormal	$$LogN(x) = \frac{1}{b\sqrt{2\pi}} \int_0^x \frac{1}{t} e^{-\frac{(\ln t - a)^2}{2b^2}} \, dt$$
Normal	$$N(x) = \frac{1}{b\sqrt{2\pi}} \int_{-\infty}^x e^{\frac{-(t-a)^2}{2b^2}} \, dt$$
Weibull	$$WBL(x) = 1 - e^{-\left(\frac{x}{b}\right)^k}$$

All of the four functions are fitted to the 25 parameter time series, which are available for the two selected tide gauges as a result of the parameterisation. The distributions fitting best to the underlying data sets are identified by calculating the RMSEs of the theoretical non-exceedance probabilities compared to the empirical non-exceedance probabilities (i.e. the plotting positions). The latter are determined following the approach proposed by Gringorten (1963) (Eq. 4-1), which has also been used by Jensen et al. (2006) for storm surge analyses in the German Bight:

$$PLP_{Gringorten} = \frac{i - 0.44}{N + 0.12}$$
(4-1)

where $PLP_{Gringorten}$ is the probability that a given value is less than the i-th smallest observation in the data set consisting of N observations, and i is the i-th smallest value in the data set arranged in ascending order. An overview of alternative methods to calculate plotting positions is given by Chow (1964) and Jensen (1985). Most of the methods lead to similar results when large sample sizes are available.

Figure 4-8 shows the results from fitting distribution functions to the time series of selected parameters (1, 10, 14 and 23) for the tide gauges of Cuxhaven (left) and Hoernum (right). The figure shows the estimated plotting positions and the theoretical distribution functions (with 95%-confidence levels) leading to the smallest RMSEs. The LogNormal distribution, for example, is most qualified to describe the available data set for parameter 1 for the tide gauge of Cuxhaven (top, left), while the Normal distribution leads to a smaller RMSE for the tide gauge of Hoernum (top, right). For parameter 1 (i.e. the difference between the maximum storm surge water level and the water level of the first tidal low water, see Fig. 4-5), the observed values range from 200 to 500 cm for Hoernum and 350 to 700 cm for Cuxhaven. For the important parameter 10, which is the maximum storm surge water level (or the highest turning point), the GPD fits best to the available data sets for both gauges. For Cuxhaven, a highest turning point of about 515 cmNN represents a 100-yr storm surge event, while a 100-yr event for Hoernum has a water level of about 420 cmNN. Figure 4-8 shows that at least one of the considered distribution functions leads to good results for the selected parameter time series. The same is true for the other 21 parameters for both gauges.

An overview of the overall results is provided by Fig. 4-9, where the calculated RMSEs are shown for all parameters and the tide gauges of Cuxhaven (left) and Hoernum (right). Only the results for the distribution functions leading to the smallest RMSEs are shown and the marker types denote which type of distribution was identified to fit best to the available data sets. The RMSE values vary between 0.01 and 0.065 cm for Cuxhaven and 0.01 and 0.04 cm for Hoernum. No outliers are evident for both of the gauges. The slightly higher values for Cuxhaven may result from the differences in the mean tide curve compared to Hoernum or from the fact that more historical events are considered for Cuxhaven. The uncertainties in these historical events are larger.
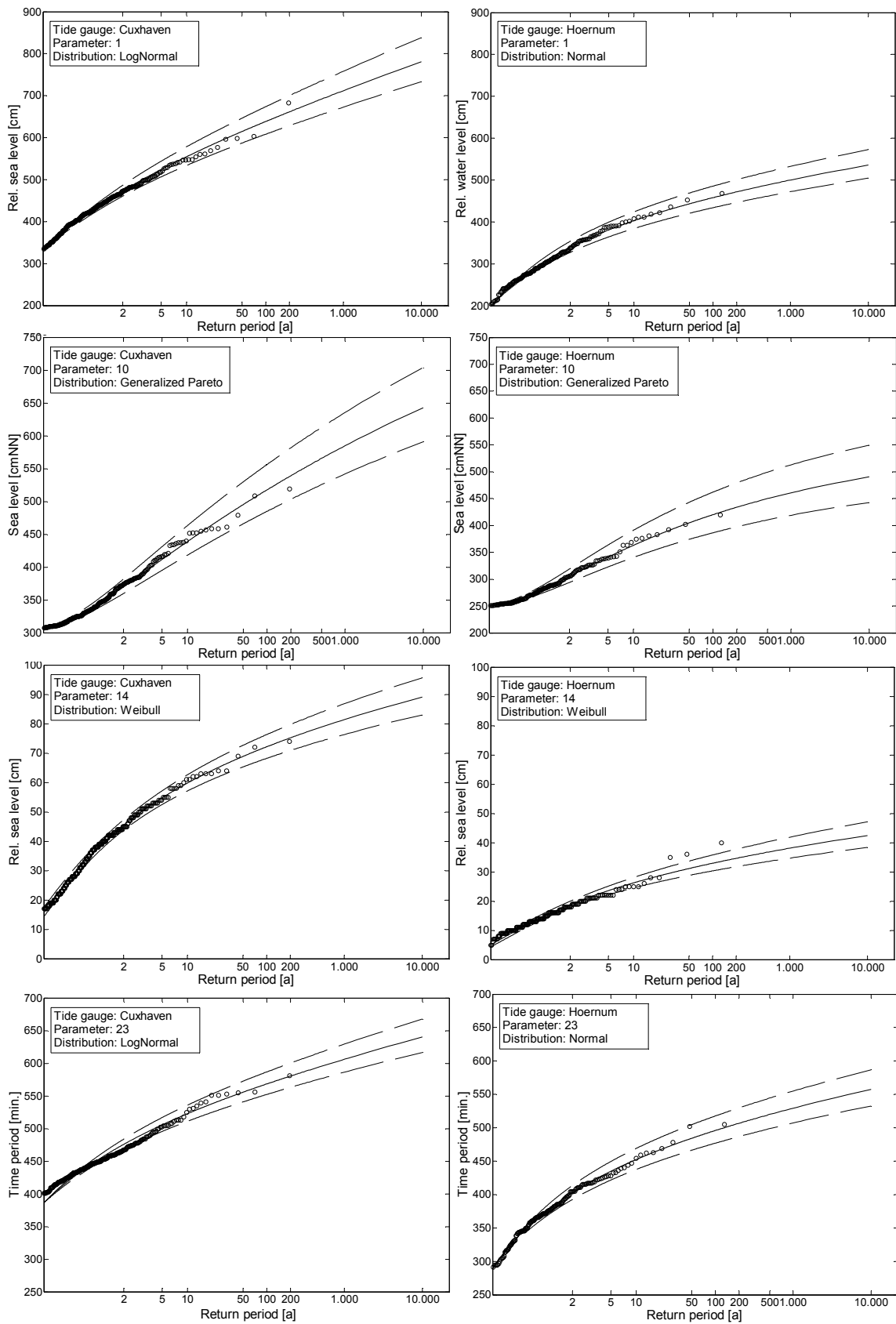
Figure 4-8:   Results from fitting distribution functions to selected parameter time series for the tide gauges
               Cuxhaven (left) and Hoernum (right).
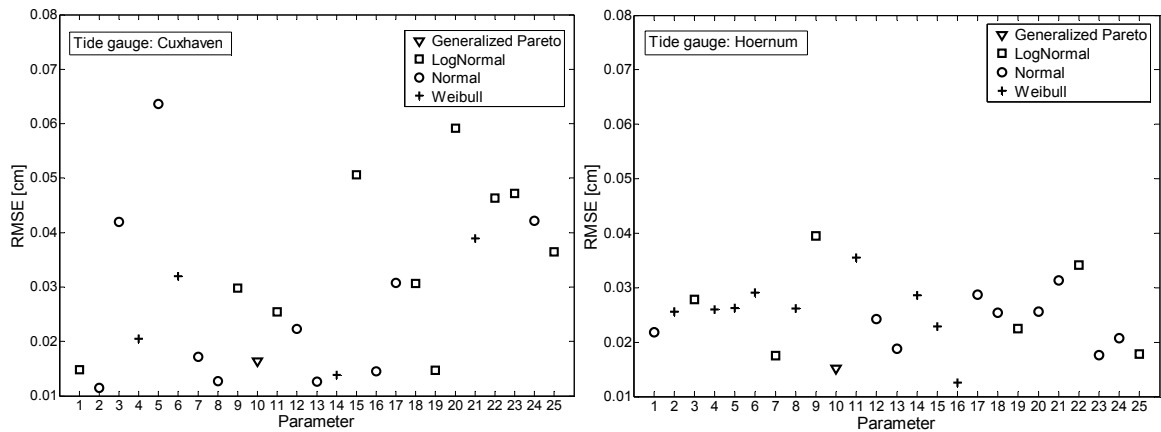
Figure 4-9:   RMSE values calculated after fitting distribution functions to the 25 parameter time series of the tide gauges Cuxhaven (left) and Hoernum (right) (only the values for the distribution functions with the smallest RMSEs are shown).

The fitted theoretical distributions are then used with Monte-Carlo simulations to estimate a large number of values for each parameter. As a result, each of the parameter data sets no longer consists of 314 or 175 realisations, respectively, but of a much larger number (here 10 million to assure stability for the statistical assessment performed in Sect. 5). Existent interdependencies between the parameters are considered by first modelling the observed interdependencies between the relative sea level parameters (which are directly or indirectly related to parameter 10) and parameter 10. Linear regression functions are applied to model the existing dependencies which are evident from the observed storm surge events. The slopes of the regression functions are then used to adjust the simulated results for the relative sea level parameters.

4.4.3 Filter functions and model validation

Before the model is validated, some filter functions are applied to the simulation results. Although the interdependencies between the sea level parameters are considered within the Monte-Carlo simulations and good results have been achieved from fitting distribution functions to the parameter time series, some inconsistencies (e.g. strongly deformed storm surge curves) occur in the results. A list of the applied filter functions with a short description and the considered threshold values is provided in Tab. 4-2. Most of these filters contribute to avoiding strong and implausible deformations of the storm surge curves and most threshold values are empirically calculated based on the observations. The filter 'peak-flatness', for example, removes simulated storm surge events where flat lines

occur around the peak water levels (i.e. the water level is constant for at least one hour, which usually does not happen in the German Bight area due to the prevailing tidal regime). Most of the filter functions listed in Tab. 4-2 do not affect the statistics of the simulation results. The filter function 'max. water level' provides the only exception, as it removes simulated events where parameter 10 (i.e. the highest turning point) is extraordinary high and is physically implausible under current climate conditions. This may happen within the Monte-Carlo simulations when the asymptote of the distribution function fitted to parameter 10 is very large. To identify the threshold values for this filter function (651 cmNN for Cuxhaven and 513 cmNN for Hoernum; see Tab. 4-2), the highest values derived in former studies based on numerical model runs or empirical analyses for the selected investigation areas have been examined. For Cuxhaven, Jensen et al. (2006) simulated a storm surge event with a maximum water level of 651 cmNN, based on a hydrodynamic model, and denoted this as the highest storm surge being physically possible under current climate conditions and based on the available data sets. The estimated uncertainty range is 603 cmNN to 672 cmNN. Gönnert et al. (2010) derived a maximum value of 610 cmNN for the same tide gauge from empirical studies (within the XtremRisK project). They superimposed the different storm surge components (i.e. the astronomical tide, the surge and the external surge, which is generated in the Atlantic and enters the North Sea) by considering the highest values that have been observed in the past, also taking into account the non-linear interactions between the different components. For the present study, the higher value of 651 cmNN is used. The maximum value for the tide gauge of Hoernum derived by Jensen et al. (2006) was 489 cmNN (I. Bork, pers. comm., 2010), while Gönnert et al. (pers. comm., 2011) estimated a maximum value of 513 cmNN with the empirical approach (with an uncertainty range from 444 cmNN to 537 cmNN). Again, the higher value of 513 cmNN is considered for the present study. In summary, simulated storm surge events exceeding a water level of 651 cmNN at the tide gauge of Cuxhaven are removed, as well as simulated storm surge events exceeding a water level of 513 cmNN at the tide gauge of Hoernum. All of the other filter functions shown in Tab. 4-2 can be denoted as 'form filters', as they contribute to avoiding strong deformations of the storm surge curves, but they do not affect the statistics. The latter is important, as stochastically simulated storm surge events are also used as a basis for statistical analyses as presented in Sect. 5.

Table 4-2:   Filter functions considered for the present study to avoid inconsistencies in the simulation results.

Abbreviation	Description	Threshold
max. water level	exceedance of the maximum storm surge water level currently considered physically possible	Cuxhaven: 651 cmNN Hoernum: 513 cmNN
surrounding peaks	first and third tide are higher than second tide	Cuxhaven: 0 cm Hoernum: 0 cm
peak-flatness	difference of the water level one hour before/after a peak (high or low water) and the peak water level itself is very small (i.e. almost a flat line)	Cuxhaven: 1 cm Hoernum: 1 cm
peak-steepness	difference of the water level one hour before/after a peak (high or low water) and the peak water level itself is very large	Cuxhaven: 112 cm* Hoernum: 59 cm*
peak-skewness	water level one hour before a peak shows a much larger/smaller difference compared to the peak water level than the water level one hour after the peak	Cuxhaven: 98 cm* Hoernum: 44 cm*
tidal range	tidal range is very small	Cuxhaven: 8 cm* Hoernum: 25 cm*
low water evolution	second low water is smaller than the first low water or third low water is smaller than fourth low water	Cuxhaven: 0 cm Hoernum: 0 cm

*Threshold values were empirically calculated based on the available observations

Before the overall simulation results are presented and discussed in the following Sect. 4.5, the model is validated. This is done first by comparing observed and simulated dependence structures (i.e. rank correlation coefficients) between the considered 19 sea level parameters. Figure 4-10 shows the results for the tide gauges of Cuxhaven (top) and Hoernum (bottom). In the upper left triangles of the matrices, the observed interdependencies are displayed. Kendall's rank correlation τ, a well known non-parametric measure of dependence, is calculated for all parameter pairs following Eq. (4-2) (e.g. Kendall, 1938; Karmakar and Simonovic, 2009):

$$\tau = \binom{N}{2}^{-1} \sum_{i<j} sign\left[(x_i - x_j)(y_i - y_j)\right] \qquad (4-2)$$

with $sign = 1$ if $\left[(x_i - x_j)(y_i - y_j)\right] > 0$, $sign = -1$ if $\left[(x_i - x_j)(y_i - y_j)\right] < 0$ and $i,j = 1,2,...,N$. For the pairs with values for τ larger or equal 0.3 [-], the actual calculated values for τ are shown in the upper left triangles of the matrices displayed in Fig. 4-10. For the parameter

pairs where the values of τ are smaller than 0.3 [-], it is assumed that no significant correlation exists (e.g. Degen and Lohrscheid, 2002) and it is not expected that the model captures such weak interdependencies. For the parameter pairs for which significant correlation is evident from the observations, the values for τ are calculated based on the simulation results and displayed in the lower right triangles of the matrices shown in Fig. 4-10.
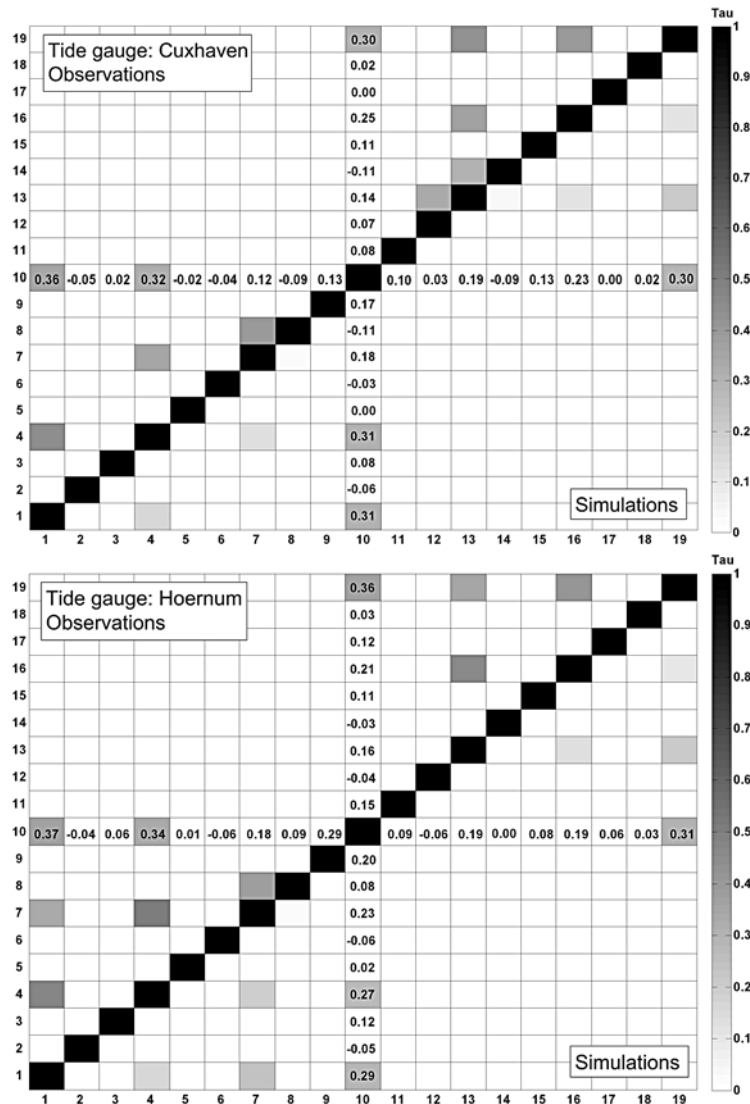
Figure 4-10: Rank correlation matrices for the 19 sea level parameters from the observations (upper left triangles) and the simulation results (lower right triangles) for the tide gauges of Cuxhaven (top) and Hoernum (bottom). The values for τ between parameter 10 and all other parameters are written as numbers, as these relationships are considered to account for interdependencies as described in the text.

The relationship between parameter 10 and the other sea level parameters has been used to correct the simulation results as described in Sect. 4.4.2. Hence, all values for τ calculated

between parameter 10 and the other sea level parameters are written in the matrices. For both gauges, no significant interdependencies are evident from the observations for most of the parameter pairs. For those pairs where large values of τ (i.e. $\tau \geq 0.3$ [–]; only significant positive correlation is evident in the data sets) are calculated based on the observations similar values for τ are also derived from the simulation results. Only very few parameter pairs show significant correlation in the observed data sets, while almost no correlation is evident from the simulation results (e.g. the pair (12|13) for Cuxhaven or the pair (7|8) for Hoernum). These small differences in the rank correlation matrices do not affect the overall simulation results.

A second stage of validation was undertaken. This involved comparing selected storm surge events from the stochastic simulation with 'reference storm surges'. These reference events are the outcome of former studies focussing on the same investigation areas, whereas hydrodynamic models and empirical approaches were used to derive extreme storm surge events. Figure 4-11 shows the results for Cuxhaven (left) and Hoernum (right). The reference storm surges shown in the figure have previously been considered for the filter function 'max. water level' (see Tab. 4-2). These storm surges are compared to 10 selected storm surge events from the simulation results. The reference storm surge that has been chosen for Cuxhaven (Fig. 4-11, left) is the outcome of a three year research project aimed at determining the highest storm surge water levels that are physically plausible and may occur along the German North Sea coastline under current climate conditions (see Jensen et al., 2006). A range of extreme (but physically consistent) weather conditions were considered to force a hydrodynamic model. The storm surge event, which is used here as a reference event, was the highest one derived. From Fig. 4-11 (left), it is obvious that the selected stochastically simulated storm surge curves are very similar to the reference event. Only the peak water levels of the initial tides are slightly smaller in the simulations compared to the reference storm surge. This is due to the fact that the second tidal low water (i.e. the absolute water level of parameter 7) is very high compared to the first high water (i.e. the absolute water level of parameter 4) in the reference storm surge. This is not typical for storm surges in Cuxhaven and thus only a few events showing this phenomenon are available from the simulation results. Furthermore, the selected reference storm surges (for Cuxhaven, as well as for Hoernum) are very extreme events and hence, only few storm surges with similar highest turning points (i.e. parameter 10) are simulated. The reference event for Hoernum is the result of extensive empirical analyses recently

conducted by Gönnert et al. (2010 and pers. comm.). Different surge components were analysed separately and superimposed (by considering the non-linear interaction) to construct extreme storm surge events. Figure 4-11 (right) shows that the character of the reference storm surge event is fully resolved by the 10 stochastically simulated storm surges. Overall, the findings from the model validation presented in Figs. 4-10 and 4-11 highlight that the applied methodology to stochastically simulate storm surge scenarios leads to reasonable and reliable results compared to other methods (e.g. hydrodynamic modelling or empirical studies) that can be used to derive storm surge scenarios.
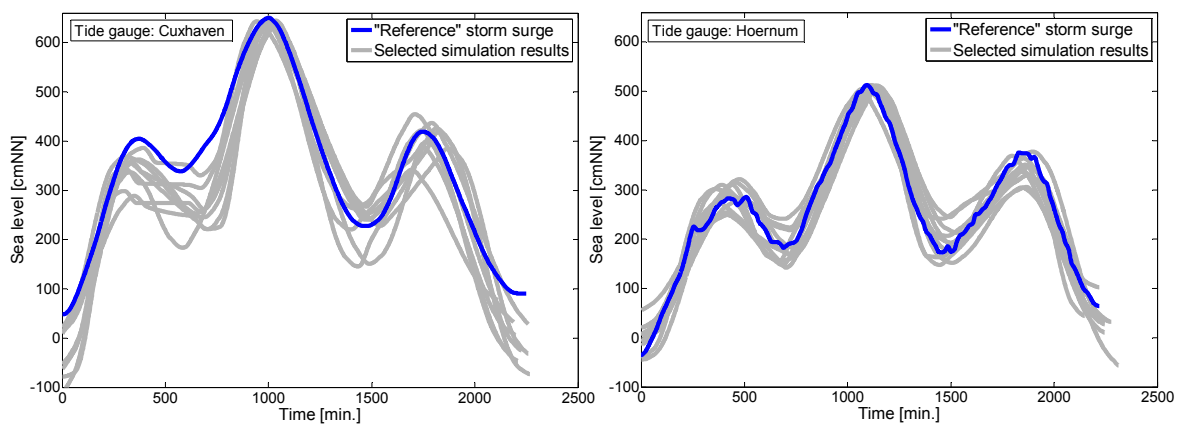
Figure 4-11:   Comparison of selected simulated storm surges with 'reference' storm surges from former studies (left: Cuxhaven; right: Hoernum).

4.5   Results and discussion

To present the overall results from the stochastic storm surge simulation (i.e. 10 mio. synthetic and high frequency storm surge scenarios), the two important storm surge parameters 'highest turning point' (S) and 'intensity' (F) are taken into account. The parameter 'highest turning point' represents the maximum water level during a storm surge event. As described in Sect. 4.2, taking only this parameter into account is not sufficient for risk analyses where the complete storm surge curve has to be considered for e.g. breach modelling or calculation of potential losses in the hinterland. Therefore, the additional parameter 'intensity' is introduced in Fig. 4-12 (in Germany this parameter is also known as 'fullness'). The intensity of a storm surge represents the area between the observed storm surge water level and a given threshold (here: the German ordnance datum NN, which nowadays is approximately 15 cm above mean sea level height). Therefore, it serves as a proxy for the energy input into the existing coastal defence structures during storm surge events. The combined analysis of the two storm surge parameters S and F firstly

allows for presenting the overall simulation results and secondly, the characteristic of a storm surge curve is well represented by these two parameters. Thus, a multivariate statistical approach to consider these two parameters also for the statistical assessment of storm surge events within risk analyses is presented in Sect. 5.
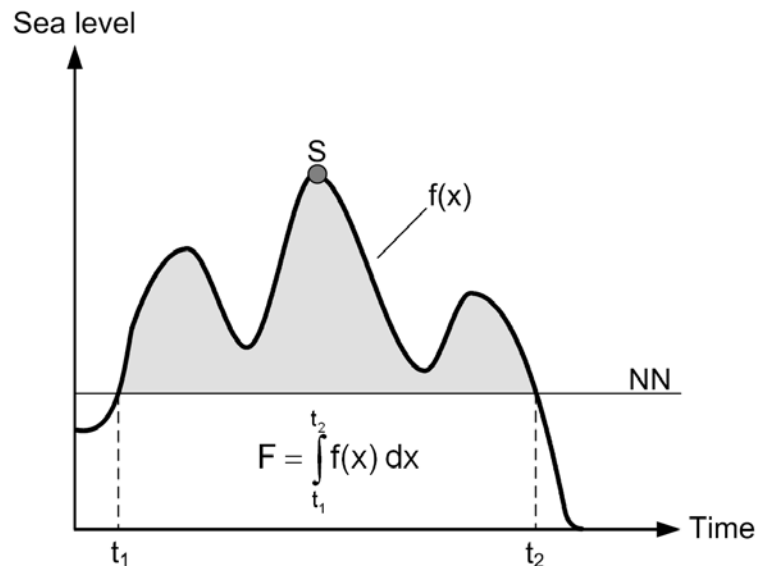
Figure 4-12: Definition of the storm surge intensity as considered for the present study.

The stochastic simulation results are shown in Fig. 4-13 for Cuxhaven (top) and Hoernum (bottom) (the unit of the intensity was divided by 1000 for plotting purposes). In both subplots, the observed storm surge events, represented by the parameters S and F and shown as black dots, are enclosed by the simulation results shown as grey dots. Both data sets (i.e. observed and simulated) show a similar structure of dependence. One million of the simulated events are shown in the figure for presenting purposes. Envelopes from all 10 million simulated events are also displayed. For both gauges, none of the observed events exceeds the estimated envelopes and the rank correlation (Kendall's τ) is found to be $\tau = 0.43$ [−] for the observations (for both gauges) and $\tau = 0.44$ [−] and $\tau = 0.45$ [−] for the simulation results for Cuxhaven and Hoernum, respectively. This highlights that the stochastic storm surge model leads to reasonable results.

The generated data sets may be used for various future applications, as for example, as a basis for statistical assessments as presented in Sect. 5. Selected storm surge scenarios, as shown in Fig. 4-13 (right), can directly be considered as input data for integrated risk analyses, contributing to a reliable approximation of a risk curve as shown in Fig. 4-1 (left). The simulated storm surge scenarios displayed in Fig. 4-13 (right) all have the same

'highest turning points' for the particular tide gauges, while having significantly different 'intensities'. This also affects the potential damages along the coastal defence line and in the hinterland; it could be expected that the estimated losses caused by the selected storm surge events are considerably different.
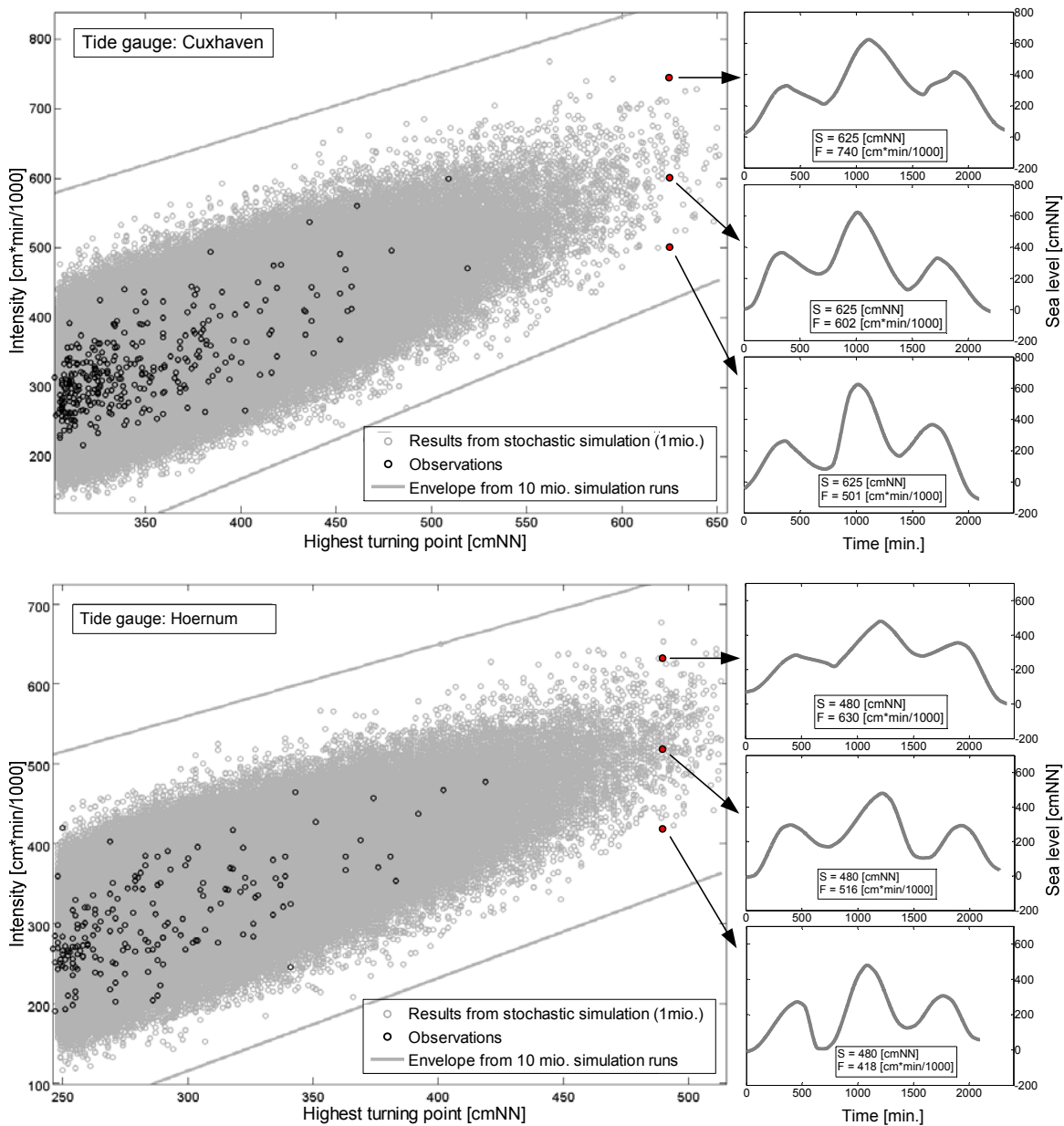
Figure 4-13:   Results from simulating 10 million storm surges, represented by the parameters 'highest turning point' and 'intensity' for the tide gauges of Cuxhaven (top) and Hoernum (bottom) and selected high resolution and stochastically simulated storm surge curves (right).

As each of the grey dots in the figure represents a storm surge event which is available as a time series with a 1-minute resolution, it is easily possible to extract a large number of

scenarios showing different characteristics and being relevant for a risk analysis at the same time (see also Fig. 4-1).

By applying the stochastic model it is possible to provide accurate hydrodynamic boundary conditions for risk assessments in coastal areas. Considering the stochastic model in combination with few numerical model runs or empirical analyses improves the accuracy of the overall results while the required computation time is relatively short. High frequency storm surge curves (at least hourly sea level observations) represent the only input data required to run the model. In addition, some information about physically possible extreme water levels (under current climate conditions) should be taken into account. The model also allows the consideration of possible future sea level changes within the simulations by using the MSL offset method as described in Sect. 1.2.

4.6 Conclusions

In this section, a stochastic storm surge model which simulates a large number of storm surge scenarios is described in detail. The storm surge scenarios may be used as input data for various practical and research-oriented applications. The most important steps of the stochastic simulation are: (1) parameterising the observed events, (2) fitting parametric distributions functions to the resulting parameter time series, and (3) applying empirical filter functions. The methodology leads to reliable results and is at the same time very cheap in computation time, compared to alternative methods that can be used to derive a larger number of storm surge scenarios. The skills of the model are highlighted in the validation section (Sect. 4.4.3) by comparing the simulation results with observations and results from former studies based on hydrodynamic models or empirical analyses. The two important storm surge parameters 'highest turning point' and 'intensity' are considered to present the overall simulation results and to characterise a particular storm surge event. This means that the temporal evolution of extreme water levels is (at least implicitly) taken into account in addition to the maximum water level. The latter is the only parameter that has been analysed in most former studies but is not sufficient to perform integrated risk analyses (e.g. based on the Source-Pathway-Receptor concept). By plotting the two parameters as shown in Fig. 4-13, it is easily possible to extract a specified number of storm surge scenarios with different characteristics from the simulation results, whereas every synthetic storm surge event is available as a time series with a 1-minute resolution.

These storm surge curves can directly be considered for scenario-based risk analyses in coastal areas. They contribute to reducing the uncertainties and improving the overall results.

In addition, the simulated storm surge events can be employed for statistical analyses. In the following Sect. 5 a multivariate statistical model based on Archimedean Copula functions is applied to estimate the exceedance probabilities of storm surge scenarios. The results from the current section are used as the data basis and the two storm surge parameters 'highest turning point' and 'intensity' are taken into account to derive joint exceedance probabilities. This is a major step forward when calculating exceedance probabilities for storm surge scenarios within risk analyses. An approach to extend the bivariate Copula model to the trivariate case is also presented. This allows for taking selected wave parameters into account in addition to the two storm surge parameters.

5 A multivariate statistical model based on Copula functions

5.1 Abstract

In this section an advanced approach to statistically analyse storm surge events is presented. In former studies the highest water level during a storm surge event usually was the only parameter that was used for the statistical assessment. This is not always sufficient, especially when statistically analysing storm surge scenarios for event-based risk analyses. Here, Archimedean Copula functions are applied and allow for the consideration of further important parameters in addition to the highest storm surge water levels. First, a bivariate model is presented and used to estimate exceedance probabilities of storm surges (for two tide gauges in the German Bight) by jointly analysing the important storm surge parameters 'highest turning point' and 'intensity'. Second, another dimension is added and a trivariate fully nested Archimedean Copula model is applied to additionally incorporate the significant wave height as an important wave parameter. With the presented methodology reliable and realistic exceedance probabilities are derived and can be considered (among others) for integrated flood risk analyses contributing to improve the overall results. It is highlighted, that the concept of Copulas represents a promising alternative to face multivariate problems in coastal engineering.

5.2 Introduction

Scenario- or event-based flood risk analyses in coastal areas are often performed by following the so called Source-Pathway-Receptor concept (e.g. Oumeraci, 2004 and Sect. Sect. 1). One of the main challenges consists in estimating the hydrodynamic boundary conditions. Possible future sea level changes have to be taken into account, as well as

storm surge scenarios and wind waves. The latter may coincide with the high storm surge water levels and play an important role for some investigation areas, while they can be neglected for others (e.g. lee of islands). All of the different loading factors for the existent coastal defence structures have to be jointly examined within integrated risk analyses, as performed in the German joint research project XtremRisK (www.xtremrisk.de) for the city of Hamburg and Sylt Island in the German North Sea.

Results from analysing observed mean sea level changes in the German Bight are summarised in Sects. 2 and 3 of the thesis. The interaction between mean sea level changes and changes in storm surge heights (i.e. total water levels arising from a combination of astronomical tides and a meteorologically induced surge component) has recently been investigated by Mudersbach et al. (under review). The present section focuses on the multivariate statistical assessment of storm surge events, including the wave conditions where necessary. Most former studies only considered the storm surge water levels to determine exceedance probabilities (e.g. Jensen et al., 2006; Haigh et al., 2010b; Mudersbach and Jensen, 2010). However, especially for risk analyses, where the complete storm surge curve is used to identify the initial conditions for flood propagation in the hinterland, the temporal behaviour of the storm surge water levels should also be taken into account for the statistical assessment. When exclusively analysing the maximum storm surge water levels, a storm surge event with two or more high tides in a row has the same exceedance probability as a storm surge event with only one high tide and the same maximum water level. At the same time the temporal behaviour of storm surge water levels may significantly affect the potential losses along the coastal defence line or in the hinterland. Cai et al. (2008) for example refer to a flood event, which occurred in North Wales on the 26 February 1990 (namely the Towyn flood) and where defence breaches occurred during the initial high tide, while flooding arose from three successive high tides (see also HR Wallingford, 1990). In a recent study, Ruocco et al. (2011) first ranked flood events that occurred along the south coast of the UK (Southampton and Portsmouth) by looking at the storm surge water levels. Secondly, they reconstructed coastal flooding based on the information from media sources (first of all newspapers). They also report a flood event (from 14 December 1989), which was ranked to be only the 70th highest for Portsmouth, but still resulted in significant flooding due to the long duration of elevated high waters. This highlights the necessity for including such information also into statistical assessments (especially within flood risk analyses) to be able to determine

realistic exceedance probabilities. A storm surge event with a moderate maximum water level, but consisting of two or three high tides in a row, should have a small exceedance probability. The same applies for an extremely high storm surge event, where the maximum water level is only reached for a short time period and the surrounding high tides are much lower.

Hence, more storm surge parameters have to be included within the statistical assessment. This requires the calculation of joint exceedance probabilities. If the parameters are not independent from each other multivariate statistical models have to be applied or the data sets have to be filtered as for example described by Tawn (1988). Many different models, which are first of all bivariate, are described in literature. For example the bivariate (or trivariate) Normal, the bivariate Gumbel or the bivariate Gamma models (see e.g. Kotz and Nadarajah (2000) for an overview). Applications of bivariate models in coastal engineering mostly focussed on the joint analysis of high water levels and wave heights or wave periods (e.g. Coles and Tawn 1994; HR Wallingford 1990 and 2000; Hawkes et al., 2002; Galiatsatou and Prinos, 2007; Hanson and Larson, 2008; Hawkes, 2008) or astronomical tidal water levels and surges (e.g. Pugh and Vassie, 1979; Tawn and Vassie, 1989; Tawn, 1992; Dixon and Tawn, 1994; McMillan et al. 2011).

Most of the multivariate models suffer from the drawback that the marginal parameters need to be independent from each other or that the marginal distributions need to be from the same family. When working with a bivariate Gumbel model, it is for example assumed that both of the considered parameters are Gumbel distributed. However, in reality this assumption does often not apply and one has to deal with dependent marginal parameters with different distributions. In such cases Copula functions, first mentioned by Sklar (1959), may be used. Copulas are very flexible joint distributions. They are able to handle mixed marginal distributions and account for the structure of dependence overlooking the margins. When using Copulas, the dependence function is studied separately from the marginal distributions (Salvadori et al., 2007). Although the theory of Copulas is not new, the number of papers dealing with Copula functions in many different ways has significantly increased over the last decade or so. Mikosch (2006) reports that a Google search for the word 'Copula' resulted in 10,000 responses in 2003, while today - in July 2011 - the same search leads to more than 2.6 million responses. Many of the available journal papers are related to mathematical finance, risk management, insurance, econometrics and hydrology (first of all multivariate hydrological frequency analyses, e.g.

DeMichele and Salvadori, 2003; Favre et al., 2004; Salvadori and De Michele, 2004; Klein et al. 2008; Karmakar and Somonovic, 2009). An interesting website providing an overview of available papers dealing with Copulas in water science is hosted by the 'Statistics in Hydrology Group' (www.stahy.org). The website contains only two references from the year 2003, nine references from 2004 and more than 30 references from 2010, which again highlights the explosion of activity in this field. In contrast, very few authors addressed coastal engineering problems by using bivariate Copulas. So did for example de Waal and van Gelder (2005) and Serinaldi and Grimaldi (2007) to model wave heights and periods. Sto. Domingo et al. (2010) used Copulas to calculate the joint probabilities of storm surge water levels and durations. Some of the ideas forming the basis for the methodology that is presented here in detail are already summarised by Wahl et al. (2010b). The approach described in there has recently been adopted by Salecker et al. (in press) to perform similar analyses (i.e. bivariate statistical storm surge analyses with Copulas) in the Baltic Sea.

One of the advantages of Copulas is given by the possibility to extend the models and add further dimensions. Different authors recently considered higher-dimensional (first of all trivariate) Copula functions with respect to hydrological data sets to perform flood frequency or rainfall frequency analyses, respectively (e.g. Grimaldi and Serinaldi, 2006a, 2006b; Serinaldi and Grimaldi, 2007; Zhang and Singh, 2007). Wong et al. (2010) performed drought analyses and De Michele et al. (2007) analysed sea storms based on a trivariate Copula model by taking the parameters wave height, storm duration and storm direction into account. Pinya et al. (2009) applied a nested Copula model to assess the risk of flooding in a tidal sluice regulated catchment. A comprehensive review of multivariate Archimedean Copula models is provided by Berg and Aas (2007).

Although Copulas have many advantages when addressing multivariate problems and to perform statistical assessments (especially within risk analyses), Mikosch (2006) provides a very critical review on Copulas. This resulted in an extensive expert discussion (Genest and Remillard, 2006; de Vries and Zhou, 2006; Segers, 2006). However, as outlined in the following sections, Copula functions represent a powerful alternative to deal with various multivariate problems in coastal engineering.

Here, for the first time the two important storm surge parameters 'highest turning point' (S) (i.e. the maximum storm surge water level) and 'intensity' (F) (see Fig. 4-12) are taken into account for statistical storm surge analyses. The bivariate model is then extended to

additionally include selected wave parameters. The three main objectives are to: (1) present a bivariate statistical approach based on Copula functions to jointly analyse the two storm surge parameters S and F (including the application of goodness of fit (GoF) tests for the model selection), (2) present a trivariate (nested) Copula model to jointly analyse the two storm surge parameters and the significant wave height H_s (including GoF tests) and (3) present results for selected investigation areas in the German Bight (i.e. Cuxhaven, Hoernum and Westerland). The presented results are used to perform scenario-based risk analyses within the XtremRisK project.

The section is organised as follows: In Sect. 5.3 the considered data sets are introduced. Section 5.4 contains detailed information about the applied methodology based on the Copula theory (Sklar, 1959). The overall results are presented and discussed in Sect. 5.5 and the section closes with a summary of the key findings and the conclusions in Sect. 5.6.

5.3 Data

In Sect. 4, a methodology to stochastically simulate a large number of storm surge scenarios for flood risk analyses has been introduced. Simulated storm surge events cover three tidal cycles and have a temporal resolution of 1-minute. From the study, 10 million storm surge scenarios are available for the tide gauges of Cuxhaven and Hoernum (see Fig. 3-1). These scenarios are used here as a data basis for bivariate (and trivariate) statistical storm surge analyses. The simulation results are based on 314 observed events for Cuxhaven (from 1900 to 2008) and 175 for Hoernum (from 1936 to 2008) (see Sect. 4 and Fig. 5-1).
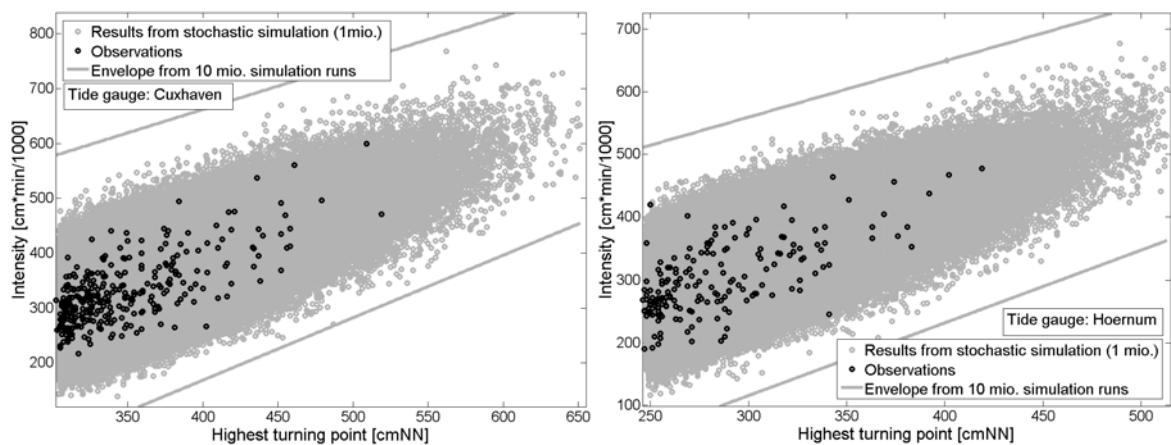
Figure 5-1:   Results from stochastic storm surge simulation as presented in Sect. 4 for the tide gauges of Cuxhaven (left) and Hoernum (right).

In Fig. 5-1 the storm surges are represented by the two parameters 'highest turning point' and 'intensity' (the unit for the intensity has been divided by thousand for presenting purposes). These parameters are also taken into account for the statistical assessment. The observed storm surge events are shown as black dots. One million of the simulated events are shown as grey dots and envelopes calculated from the 10 million storm surge scenarios are displayed for presenting purposes.

In Sect. 5.4.3 a trivariate statistical model is introduced, which allows the inclusion of selected wave parameters in the statistical analyses. Therefore, observational records for different wave parameters are needed. For both investigation areas, Cuxhaven and Hoernum, wind waves do not play an important role due to the locations in an estuary and the lee of an island, respectively. Furthermore, no observational data sets are available. Hence, an empirical model to transfer the simulated storm surge events from the tide gauge of Hoernum to the tide gauge of Westerland is introduced in Sect. 5.4.2. The tide gauge of Westerland is located on the west side of Sylt Island (coordinates: 54°54'31"N, 8°16'16"E), where high wind waves occur due to the exposed location. The tide gauge provides high resolution sea level data for the period from 1988 to 2007 and wave data are available for the same time period from a measuring station near the tide gauge (coordinates: 54°55'2"N, 8°13'18"E; water depth: 13m). The sea level data set is used to compile the empirical transfer model for the storm surges (see Sect. 5.4.2) and the wave measurements are considered for the trivariate (or 3-dimensional) statistical assessment (see Sect. 5.4.3). Figure 5-2 shows a scatter plot of simultaneously measured water levels (referred to the German ordnance datum NN) and significant wave heights H_s.
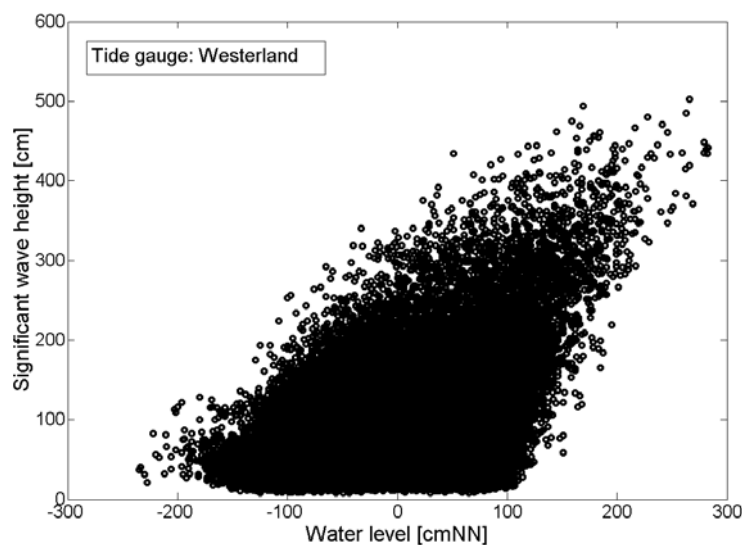
Figure 5-2:   Observed water levels (from tide gauge) and significant wave heights (from wave measurement station) in Westerland on the west side of Sylt Island.

Wave heights of up to 5 m have been observed in Westerland in the past and the scatter plot highlights an existent dependency between the two parameters. High waves tend to coincide with high water levels exacerbating the overall flood risk. This dependency has to be taken into account for the trivariate statistical analyses.

5.4   Methods

5.4.1 Bivariate statistical model and goodness of fit tests

The exceedance probabilities of the available storm surge events are expressed as joint probabilities of the two storm surge parameters S and F. Figure 5-1 shows that these two parameters are not independent from each other. Thus, the simple multiplication of the exceedance probabilities of the margins does not represent the joint probabilities and a multivariate model has to be applied. From testing different parametric distribution functions for the marginal parameters S and F, it was found that the Generalized Pareto distribution (GPD) fits best for the parameter S. This is not surprising, as the GPD has been used in Sect. 4 to simulate this parameter. The parameter F is not directly simulated but is given implicitly by the stochastic storm surge model. The LogNormal distribution is found to be the most appropriate parametric distribution function for this parameter. Hence, one has to deal with dependent marginal parameters with different distributions. As outlined in Sect. 5.2, Copula functions are valuable to analyse such multivariate data sets and are applied in the following.

Before the theoretical background of Copulas is briefly introduced, appropriate univariate marginal distributions for the two storm surge parameters S and F have to be defined. It has been mentioned above, that the GPD has been identified to be the most suitable distribution for S and the LogNormal distribution for F. As the margins are analysed separately from the dependence function when using Copulas, this also allows for taking nonparametric marginal distributions, such as Kernel Density Functions (KDFs) into account. Especially when large numbers of realisations are available for the marginal parameters, as it is the case for the present study, such nonparametric functions lead to good results. The uncertainties are smaller as when fitting certain parametric functions to the available data sets. Here, for both of the parameters S and F the following Gaussian (or Normal) Kernel Density Function $K(x)$ is applied (see e.g. Karmakar and Simonovic, 2008):

$$K(x) = (2\pi)^{-1/2} e^{(x^2)/2}, \quad \text{with} \quad \int_{-\infty}^{\infty} K(x)dx = 1 \qquad (5\text{-}1)$$

To calculate joint probabilities from the marginal distributions, different Copula functions belonging to different Copula families are available. In the relevant literature, the applied Copulas often belong to the Elliptical, the Normal, the t-Student or the Archimedean family. Especially Copula functions belonging to the Archimedean family are often used for hydrological analyses (e.g. Favre et al., 2004) as they are flexible and easy to construct. Here, three Archimedean Copula functions, namely the Clayton, Frank and Gumbel Copulas are considered. These Copulas were chosen as many of the authors mentioned in Sect. 5.2 outlined their applicability for multivariate frequency analyses and more important, the three Copulas cover the full range of tail behaviour. The Clayton Copula has lower tail dependence, while the Frank Copula has no tail dependence and the Gumbel Copula has only upper tail dependence (Schölzel and Friedrichs, 2008).

Sklar (1959) describes the connection between a Copula C and a bivariate cumulative distribution function (cdf) $F_{XY}(x,y)$ of any pair (X,Y) as follows (also known as Sklar's theorem):

$$F_{XY}(x,y) = C[F_X(x), F_Y(Y)] \qquad (5\text{-}2)$$

where $F_X(x)$ and $F_Y(y)$ are the univariate marginal distributions. The bivariate probability density function (pdf) reads as:

$$f_{XY}(x,y) = c[F_X(x), F_Y(y)] f_X(x) f_Y(y) \qquad (5\text{-}3)$$

where $f_X(x)$ and $f_Y(y)$ represent the pdf's of the margins. Let U and V be uniformly distributed random variables defined as $U = F_X(x)$ and $V = F_Y(y)$, then the function $c(u,v)$ (sometimes referred to as the Copula density function) is given by:

$$c(u,v) = \frac{\partial^2 C(u,v)}{\partial u \partial v} \qquad (5\text{-}4)$$

Further important features of Copulas and information about the theoretical background can be found in Nelsen (1999), who provides a detailed introduction to the subject.

The Archimedean Copulas considered for the present study are constructed based on the so-called Copula generator φ: $[0,1] \rightarrow [0,\infty]$, being a strictly monotonically decreasing function with $\varphi(1) = 0$ (e.g. Nelsen, 1999). The general form of a one-parametric Archimedean Copula is:

$$C_\theta(u,v) = \varphi^{-1}[\varphi(u) + \varphi(v)]$$

(5-5)

Table 5-1 contains an overview of the Copula functions used for the present study. Functions of the generators $\varphi(t)$ are displayed, as well as the connection between the Copula parameter θ and the rank correlation Kendall's τ. The latter represents a well-known nonparametric measure of dependence and is calculated from the available observations as:

$$\tau = \binom{N}{2}^{-1} \sum_{j=1}^{N} \sum_{i=1}^{j} sign[(x_i - x_j)(y_i - y_j)]$$

(5-6)

with $sign = 1$ if $[(x_i - x_j)(y_i - y_j)] > 0$, $sign = -1$ if $[(x_i - x_j)(y_i - y_j)] < 0$ and $i,j = 1,2,\ldots,N$ (e.g. Kamarkar and Simonovic, 2009). Another nonparametric measure of dependence is given by Spearman's rank correlation ρ (Spearman, 1904), which is not used for the present study. Table 5-1 shows that Kendall's τ (here, for the storm surge parameters S and F) is the only parameter, which is required (in addition to the marginal distributions) to solve the Copula functions. The values for Kendall's τ are found to be $\tau = 0.43$ [-] for both of the tide gauges Cuxhaven and Hoernum.

With this information the Copula parameters θ (as shown in Tab. 5-1) and joint probabilities for the parameters S and F can be calculated. Alternative methods to derive the Copula parameters θ, such as the maximum pseudolikelihood estimator, are described for example by Genest and Favre (2007). Corresponding to the univariate case, appropriate Copula functions have to be identified based on GoF tests before starting the statistical analyses.

Table 5-1: Archimedean Copula functions considered for the present study and their generator functions, ranges for the Copula parameters θ and connections to Kendall's τ.

Copula function C_θ	Generator $\varphi(t)$**	Range $\theta \in$	Kendall's τ
Clayton (or Cook-Johnson)			
$\left[u^{-\theta} + v^{-\theta} - 1\right]^{\frac{-1}{\theta}}$	$t^{-\theta} - 1$	$[0,\infty)$	$\dfrac{\theta}{\theta + 2}$
Frank			
$-\dfrac{1}{\theta}\ln\left[1 + \dfrac{\left(e^{-\theta u} - 1\right)\left(e^{-\theta v} - 1\right)}{e^{-\theta} - 1}\right]$	$-\ln\left(\dfrac{e^{-\theta t} - 1}{e^{-\theta} - 1}\right)$	$(-\infty,\infty)\backslash\{0\}$	$1 - \dfrac{4}{\theta}\left[1 - D_1(\theta)\right]$ *
Gumbel (or Gumbel-Hougaard)			
$\exp\left\{-\left[(-\ln u)^\theta + (-\ln v)^\theta\right]^{\frac{1}{\theta}}\right\}$	$(-\ln t)^\theta$	$[1,\infty)$	$1 - \theta^{-1}$

* 1. Debye Function $D_1(\theta) = \dfrac{1}{\theta}\int\limits_0^\theta \dfrac{t}{e^t - 1}\,dt$

** $t = u$ or $t = v$

As the margins are analysed separately, the GoF tests aim to identify a Copula function, which is able to capture the existent structure of dependence between the considered parameters. Extensive research efforts have been undertaken in recent years to improve GoF tests for multivariate problems and Copulas, respectively. A comprehensive review including a power study is provided by Genest et al. (2009), as well as by Berg (2009). Some results from sensitivity studies can be found in Berg and Quessy (2009). For the present study, two GoF tests are applied to identify proper Copula functions. The first test is based on a comparison of the theoretical and empirical joint non-exceedance probabilities. The theoretical joint non-exceedance probabilities are calculated with the three Copula functions from Tab. 5-1, where the marginal distributions are KDFs (see Eq. 5-1) derived from the available observations. The empirical joint non-exceedance probabilities are calculated as shown in Eq. (5-7) (see e.g. Yue et al., 1999; Kamarkar and Simonovic, 2009). This is an extension of the approach introduced by Gringorten (1963) to derive unbiased plotting positions for the Gumbel distribution. For univariate statistical storm surge analyses in the German Bight area Gringorten's approach was already used by

Jensen et al. (2006) and Mudersbach and Jensen (2010) to estimate empirical probabilities (alternative approaches for the univariate case are summarised in Stedinger et al., 2008).

$$F_{XY}(x_i, y_i) = P(X \leq x_i, Y \leq y_i) = \frac{\sum_{m=1}^{i} \sum_{l=1}^{i} N_{ml} - 0.44}{N + 0.12}$$

(5-7)

where the pairs (x_m, y_l) are arranged in ascending order with respect to x_m and N_{ml} represents the number of occurrences of (x_m, y_l) with $x_m < x_i$ and $y_l < y_i$, $i = 1, \ldots, N$ and $1 \leq m, l \leq i$. N is the sample size (here: 314 for Cuxhaven and 175 for Hoernum). The simulation results are not considered for this test as the structure of dependence between S and F is found to be the same in the observations and the simulation results (see Fig. 5-1). The root mean squared errors (RMSEs) and the maximum distances (for a Kolmogorov-Smirnov (KS)-test) are calculated from the theoretical and the empirical joint non-exceedance probabilities to identify the most appropriate Copula function (e.g. Zhang and Singh, 2007). The RMSEs and the KS-values are determined for all of the observed events, as well as for rare events with empirical non-exceedance probabilities > 0.8 [1/a] (see Sect. 5.5.1).

A second GoF test is applied. This test compares observed and simulated (with different theoretical Copula functions) pairs of the two marginal parameters (see e.g. Serinaldi and Grimaldi, 2007; Klein et al., 2008). In contrast to most other GoF tests, this test does not calculate any critical value of a statistic. First, large numbers (here: 1 million) of random pairs (u_i, v_i) are generated based on the different theoretical Copula functions shown in Tab. 5-1. With the marginal distributions $F_X(x)$ and $F_Y(y)$ the generated pairs are subsequently transformed into the original units of the considered parameters (here S and F). Finally, the simulated pairs are superimposed by the observed pairs of S and F (or here by pairs of S and F from the stochastic storm surge simulation). From the resulting plots it is easy to identify a theoretical Copula function, which is able to model the structure of dependence between the marginal parameters.

5.4.2 Empirical transfer functions

As it has been mentioned in Sect. 5-3, wind waves do not represent an important loading factor for existent coastal defence structures (i.e. first of all dikes) in the investigation areas Cuxhaven and Hoernum. However, in other areas, for example Westerland on the west side of Sylt Island, high wind waves may coincide with storm surge water levels. For Westerland long records (from 1988 to 2007; see Sect. 5-3) of simultaneously measured wave parameters and water levels are available (data sets from after 2007 were not available at the time of the analyses), but no stochastically simulated storm surge events. To transfer 10 million storm surges from Hoernum to Westerland, an empirical model is introduced in the following.

The model is mainly based on regression functions, which are compiled for the 25 storm surge parameters considered in Sect. 4 to parameterise observed storm surge events consisting of three tides. The parameterisation scheme is based on 19 sea level parameters (i.e. the tidal high and low waters and the water levels one hour before and one hour afterwards) and 6 time parameters (i.e. the time periods between two adjacent high and low waters). The available observations from Westerland and Hoernum include 64 storm surge events, which have been recorded at both sites. From parameterising the 64 storm surge events for Westerland and Hoernum, regression functions are derived for all of the 25 parameters. In addition to the 64 observed storm surge events, selected extreme events from hydrodynamic model runs are considered to build the model (Jensen et al. 2006). Therewith, a wider range of possible values is covered and regression functions can be reliably estimated. Correlation coefficients r are calculated for the 25 parameter time series from Hoernum and Westerland (see Fig. 5-3). All correlation coefficients are significant (on the 99%-significance level from t-test statistics) with most of them being larger than $r = 0.9$ [-]. Slightly weaker correlations are found for the parameters 9 to 11, where parameter 10 is the 'highest turning point' and the parameters 9 and 11 are the surrounding parameters (i.e. the water levels one hour before and one hour afterwards). High frequency variations often occur in the water level time series around the storm surge peaks. These variations mainly result from small wind generated waves, which are poorly damped by the tide gauges. This increases the uncertainties for the affected parameters when parameterising the observed storm surge events. Lowest coefficients (in the order of $r = 0.6$ [-] to $r = 0.8$ [-]) are found for the time parameters (i.e. the parameters 20 to 25).

Uncertainties from automatically parameterising observed storm surge events are in general higher for the time parameters compared to the sea level parameters.
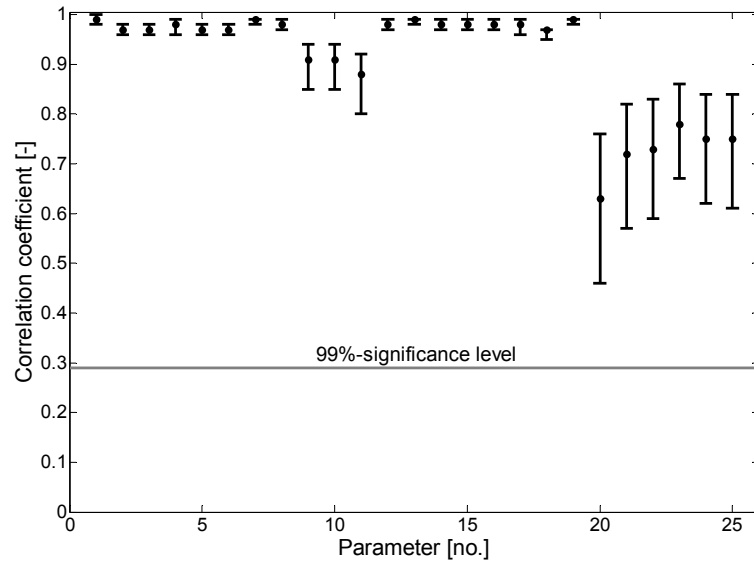
Figure 5-3:   Correlation coefficients for the 25 storm surge parameters and the tide gauges of Hoernum and Westerland with 99%-significance level from t-test statistics.

Based on the 25 regression functions, all of the 25 parameters of a particular storm surge event are transferred from Hoernum to Westerland, where the storm surge curve is reconstructed by applying piecewise cubic hermite interpolation. As an example, for the important parameter 10 the following second order polynomial function is considered as a transfer function:

$$P_{10,Westerland} = 0.0013 \cdot \left(P_{10,Hörnum}\right)^2 + 0.0464 \cdot P_{10,Hörnum} + 113.57 \qquad (5\text{-}8)$$

With the empirical model all 10 million storm surge scenarios are transferred from Hoernum to Westerland. By taking these storm surge events and the available wave measurements into account, a trivariate model as described in the following Sect. 5.4.3 is used to calculate joint probabilities. The value of Kendall's τ for the parameters S and F is found to be $\tau = 0.46$ [-] for the tide gauge of Westerland.

5.4.3 Trivariate statistical model and goodness of fit tests

It has been outlined in the introduction of this section, that for some investigation areas not only storm surge scenarios, but also reasonable wave conditions have to be taken into account for integrated flood risk analyses. Especially during storm surges, high wind waves may occur and potentially lead to damages along the coastal defence line or in the hinterland due to high overtopping rates. Here, a trivariate (or 3-dimensional) model is applied to jointly analyse selected wave parameters and the storm surge parameters S and F. For the present study, the significant wave height H_s is considered as it represents one of the most important wave parameters (alternatively other parameters, such as the wave period can be used). In Sect. 5.2, it has been outlined that one of the advantages of Copulas is given by the possibility of extending the models to the d-dimensional case, where Eq. (5-5) becomes:

$$C(u_1, u_2, ..., u_d) = \varphi^{-1}[\varphi(u_1) + \varphi(u_2).... + \varphi(u_d)]$$

(5-9)

Three higher-dimensional Copula models discussed by Berg and Aas (2007) are briefly introduced in the following. They are subsequently used to calculate exceedance probabilities of combinations of storm surges (represented by the parameters S and F) and wave conditions (represented by H_s). The first model is referred to as fully nested Archimedean Copula construction (FNAC). Figure 5-4 (left) shows the construction scheme for a 4-dimensional Copula, where one dimension is added step by step. The 4-dimensional Copula consists of three bivariate Copulas (C_{11}, C_{21}, C_{31}) with three generators (φ_{11}, φ_{21}, φ_{31}) (note that the subscripts of C and φ do not refer to the dimensions). This approach is restricted in its flexibility, as four parameters are analysed, but only three mutual bivariate dependence structures are freely specified. The remaining Copula and distribution parameters are implicitly given through the construction. In Fig. 5-4 the pairs (u_1, u_3), (u_1, u_4), (u_2, u_3) and (u_2, u_4) all have Copula C_{21} with the related dependence parameter θ_{21} (i.e. all of the mentioned pairs need to have a similar rank correlation). Furthermore, it is required that the degree of dependence decreases with the level of nesting. The same constraints as for the FNAC model also apply for the partially nested construction (PNAC) (Fig. 5-4, middle). First, the parameters (u_1, u_2) and (u_2, u_3) are coupled via Copulas C_{11} and C_{12}, respectively, before the two bivariate Copulas are coupled via a third bivariate Copula C_{21}. Again, the pairs (u_1, u_3), (u_1, u_4), (u_2, u_3) and

(u_2, u_4) all have Copula C_{21} with the related parameter θ_{21}. The third model is referred to as pairwise Archimedean construction (PAC). This model is very flexible as more Copulas than parameters are considered (see Fig. 5-4, right). The Copulas for each pair of variables can be freely chosen and do not even have to belong to the same family. However, the construction is more complicated and requires more computational efforts. For more information on the described models and the theoretical background see Berg and Aas (2007) and the literature referenced therein.
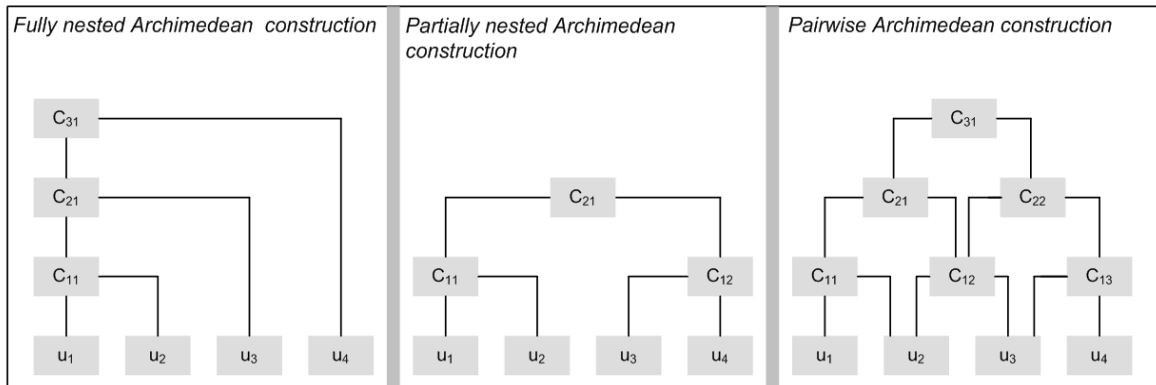
Figure 5-4: Selected models to construct higher-dimensional Copulas.

Here, the parameters S, F and H_s are jointly analysed. The parameters are all cross correlated with each other (see detailed explanation below). This requires the application of a trivariate model and for the present study a fully nested approach (FNAC) as shown in Fig. 5-4 (left) is considered. First, it has to be tested whether the multivariate data set faces the abovementioned criteria for the application of a FNAC model. Hence, it has to be proven, whether the parameter pairs (F, H_s) and (S, H_s) have at least similar rank correlations or not. Further, the values for Kendall's τ have to be smaller than $\tau = 0.46$ [-], which is the rank correlation calculated for the pair (S, F) for the tide gauge of Westerland (see Sect. 5.4.2). It has been mentioned that the degree of dependence must decrease with the level of nesting. To measure the dependence for the parameter pairs (S, H_s) and (F, H_s) wave events which occurred simultaneously with high water levels have to be analysed. Here, a comparable small threshold for the water level of $W = 85$ cm above MHW is chosen to identify storm surge events from the available water level time series for the tide gauge of Westerland. On the one hand, this threshold still represents a high water level, which has been exceeded 95 times (two events have to be at least 30 hours apart from each other) during the 20 years of observations (number of occurrences per year is < 5). On the other hand, a number of 95 events is large enough to capture the existent structure of

dependence between the different parameters. The value for Kendall's τ for the parameters S and F is slightly higher when the smaller threshold is considered ($\tau = 0.48$ [-]) but does not change significantly. Figure 5-5 shows scatter plots for the parameter pairs (F, H_s) and (S, H_s) and it is obvious that both parameter pairs have similar structures of dependence. The values for Kendall's τ are found to be $\tau = 0.36$ [-] for the pair (F, H_s) and $\tau = 0.35$ [-] for the pair (S, H_s). There is no physical reason for the two parameter pairs to have the same (or at least similar) rank correlations, but it is required for the FNAC model (if the rank correlations were different a more complex PAC approach could be used instead of the FNAC model). Here, both criteria for the application of a FNAC model are fulfilled: the pairs (F, H_s) and (S, H_s) have the same Copula (i.e. the same structure of dependence) and the existent dependency is weaker than for the pair (S, F).
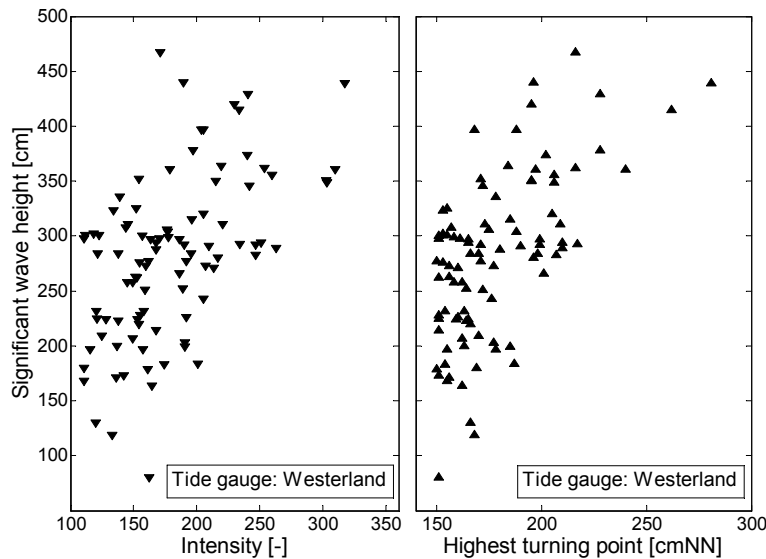
Figure 5-5:   Scatter plots for the parameter pairs (F, H_s) (left) and (S, H_s) (right).

Again, KDFs are used as marginal distributions for the parameters S and F, resulting from transferring 10 million storm surge events from Hoernum to Westerland. The KDFs are shown in Fig. 5-11. For the third parameter H_s, 95 realisations are available and a Generalized Extreme Value distribution (GEV) of the following form is fitted to the data set:

$$GEV(x) = \exp\left[-\left(1 + k \cdot \frac{x-a}{b} \right)^{-1/k} \right]$$

(5-10)

where *a, b* and *k* represent location, scale and shape parameters, respectively. Figure 5-6 shows the results from fitting the GEV (with 95%-confidence levels) to the available data set of H_s. The distribution parameters are estimated with the maximum likelihood approach (e.g. Rao and Hamed, 2000) and the plotting positions are derived by following the approach proposed by Gringorten (1963). A significant wave height of $H_s = 300$ cm has a return period of about 1 year, an event with $H_s = 400$ cm of about 2.7 years and a 100-year event is represented by a significant wave height of about $H_s = 510$ cm.
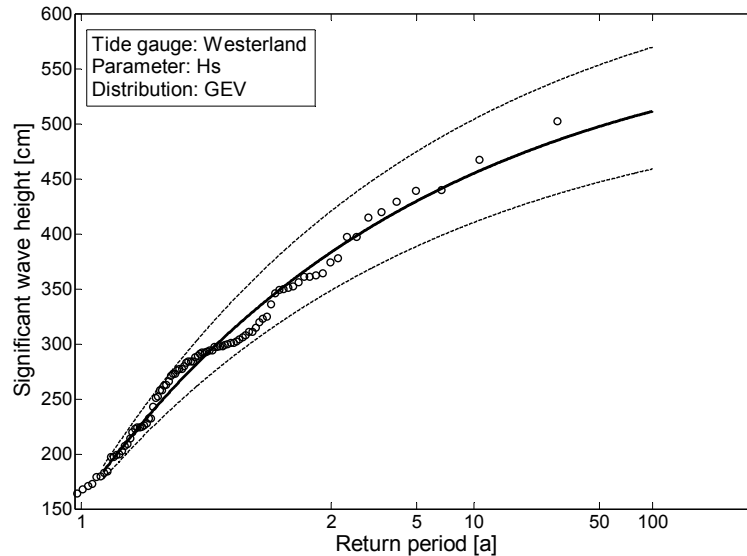
Figure 5-6:   Marginal distribution for the parameter H_s based on a GEV (with 95%-confidence bounds).

Now that all three marginal distributions, as well as the dependence structures between the considered parameters are known, a trivariate FNAC model can be applied to estimate the joint exceedance probabilities. According to the 1- and 2-dimensional cases, GoF tests are applied to identify appropriate Archimedean Copulas for the model. Here, the same GoF tests as described in Sect. 5.4.1 are taken into account. The first test compares theoretical and empirical joint non-exceedance probabilities. Theoretical probabilities are calculated with the Copulas in Tab. 5-1, whereas the Gumbel Copula is used to combine the parameters *S* and *F* and the Clayton, Frank and Gumbel Copulas are tested to incorporate the third parameter H_s. Marginal distributions are KDFs for the parameters *S* and *F* (as in Sect. 5.4.1) and a GEV for the parameter H_s. Empirical joint non-exceedance probabilities are calculated with an extension of Eq. (5-7) to the trivariate case (e.g. Zhang and Singh, 2007), which reads:

$$F_{XYZ}(x_i, y_i, z_i) = P(X \le x_i, Y \le y_i, Z \le z_i) = \frac{\sum_{m=1}^{i}\sum_{l=1}^{i}\sum_{p=1}^{i} N_{mlp} - 0.44}{N + 0.12} \qquad (5\text{-}11)$$

The second GoF test is applied in the same way as described in Sect. 5.4.1, but this time for the parameter pairs (F, H_s) and (S, H_s), which both have a similar structure of dependence and the same bivariate Copula in the FNAC model.

5.5   Results

5.5.1 Bivariate statistical analyses

Results from comparing theoretical and empirical joint probabilities for the parameters S and F are shown in Fig. 5-7 (only for Hoernum) and Tab. 5-2 (for Cuxhaven and Hoernum). The results in Fig. 5-7 highlight that the Gumbel Copula fits best to the data set. The same conclusion is drawn from the results presented in Tab. 5-2, where the RMSEs and the values for the KS-statistic (i.e. the maximum distance between the theoretical and empirical joint probabilities) are shown for Cuxhaven and Hoernum. For both tide gauges the Gumbel Copula leads to the smallest RMSEs and the smallest values for the KS-statistic when all events are taken into account, as well as when only extreme events (return period > 5 years) are analysed. The Gumbel Copula is followed by the Frank Copula, while the Clayton Copula leads to the largest RMSEs and the largest values for the KS-statistic.
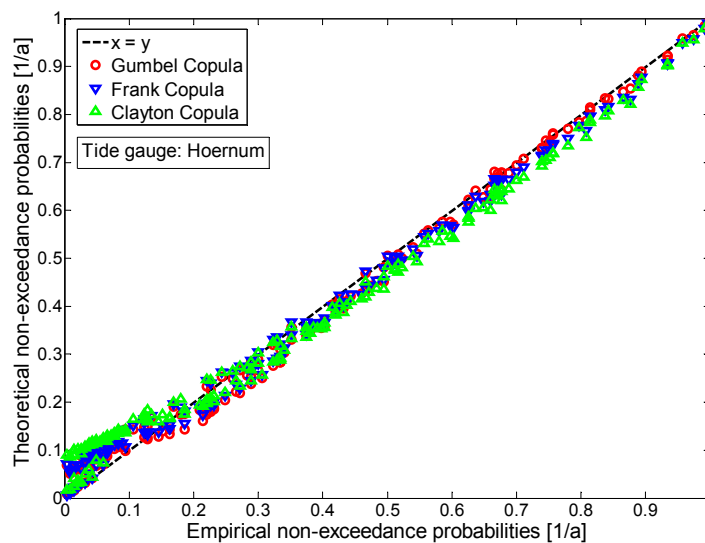
Figure 5-7:   Q-Q-plot for the tide gauge of Hoernum with the theoretical and empirical joint exceedance probabilities of the observed storm surge events.

Table 5-2:   RMSEs and values for the KS-statistic from comparing theoretical and empirical joint probabilities (Cuxhaven | Hoernum).

Function	RMSE	RMSE (extreme events*)	KS-statistic	KS-statistic (extreme events*)
Clayton Copula	0.036 | 0.043	0.033 | 0.032	0.071 | 0.087	0.068 | 0.056
Frank Copula	0.023 | 0.030	0.026 | 0.026	0.062 | 0.068	0.051 | 0.045
Gumbel Copula	0.018 | 0.029	0.011 | 0.012	0.060 | 0.065	0.028 | 0.023

* Events with an empirical non-exceedance probability of $P_u > 0.8$ (equals a return period of 5 years)

Results from a second and graphical based GoF test (see Sect. 5.4.1) are shown in Fig. 5-8 (only for the tide gauge of Hoernum). Again, the test results clearly point to the Gumbel Copula to be the most appropriate one for calculating the joint exceedance probabilities. It is the only Copula being able to model the existent structure of dependence between the parameters S and F with a clear tail dependency in the upper right. The same is found for the tide gauge of Cuxhaven (not shown here).

Thus, the Gumbel Copula as shown in Tab. 5-1 is chosen for both gauges to calculate the joint exceedance probabilities of the available storm surge events (from the parameters S and F). Selected storm surges may directly be considered as scenarios for event-based risk analyses. Therefore, the so-called 'AND' case is considered and it is assumed that both of the parameters S and F exceed a given value. The joint exccedance probabilities are given by:

$$
\begin{aligned}
&P(X > x \wedge Y > y) \\
&= 1 - F_X(x) - F_Y(y) + F_{XY}(x, y) \\
&= 1 - F_X(x) - F_Y(y) + C[F_X(x), F_Y(y)]
\end{aligned}
\tag{5-12}
$$

For other studies, for example when designing reservoirs or performing safety checks, the 'OR' case might also be interesting. It assumes that only one of the parameters exceeds a given threshold, while the other parameter does not (see e.g. Klein et al., 2008). The joint exceedance probabilities are calculated as follows:

$$
\begin{aligned}
&P(X > x \vee Y > y) \\
&= 1 - F_{XY}(x, y) = 1 - C[F_X(x), F_Y(y)]
\end{aligned}
\tag{5-13}
$$

Figure 5-8:   Results from a graphical based GoF test for the tide gauge of Hoernum by considering the Clayton Copula (top), the Frank Copula (middle) and the Gumbel Copula (bottom).

The overall results from statistically analysing the available storm surge events (observations and results from stochastic storm surge simulation) are presented in Fig. 5-9 for Cuxhaven (top) and Hoernum (bottom). For both tide gauges the marginal distributions (i.e. KDFs) are shown in the figure as well the contours of some relevant joint exceedance probabilities calculated with the Gumbel Copula.
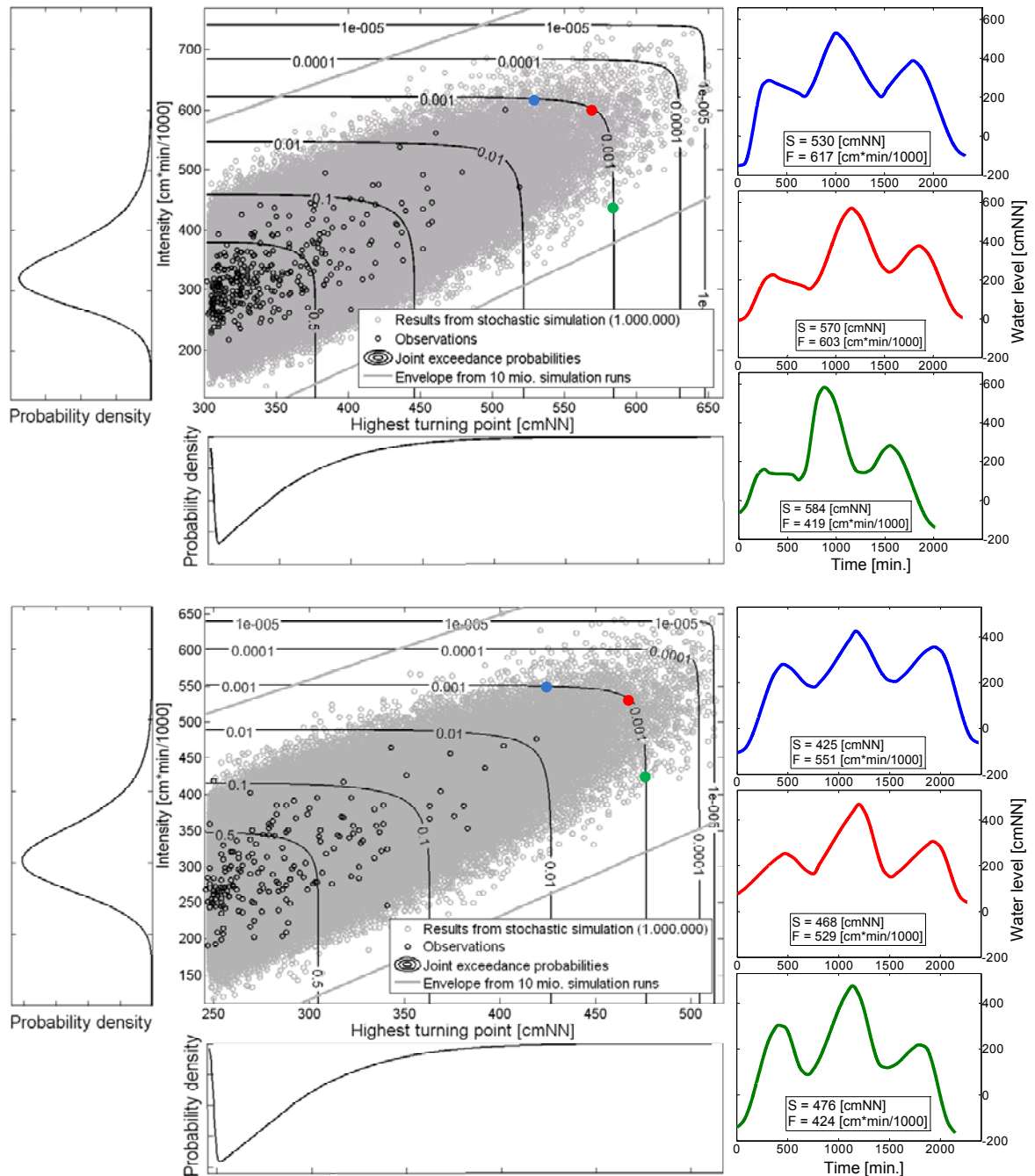
Figure 5-9:   Results from statistically analysing the observed and stochastically simulated storm surge events for the tide gauges of Cuxhaven (top) and Hoernum (bottom) based on KDFs (for the marginal distributions) and the Gumbel Copula and selected simulated storm surge events with a occurrence probability of P_e = 0.001 [1/a] (right).

With the results it is easily possible to estimate the exceedance probability of any given storm surge event (either from stochastic simulation, empirical studies or numerical model runs) by taking into account the two important storm surge parameters 'highest turning point' and 'intensity'.

Furthermore, it is possible to extract a specified number of storm surge events with the same exceedance probability but different values for S and F. Hence, the selected events, although having the same exceedance probability, may have significantly different characteristics and implications in terms of the flood risk. Figure 5-9 (right) shows selected storm surge events for both of the considered tide gauges. All of these storm surges have a joint exceedance probability of $P_e \approx 0.001$ [1/a] (i.e. a return period of 1,000 years) and different values for S and F. For the tide gauge of Hoernum for instance (Fig. 5-9, bottom), the storm surge event shown in the middle panel on the right (red curve) has a 'highest turning point' of S = 468 cmNN and an 'intensity' of F = 529 [cm*min/1000]. The exceedance probabilities for the marginal parameters are found to be $P_{e,S}$ = 0.0016 [1/a] (equals a return period of 625 years) and $P_{e,F}$ = 0.0025 [1/a] (equals a return period of 400 years). If one would mistakenly assume independency between the parameters S and F, the joint exceedance probability would be calculated by simply multiplying the exceedance probabilities of the margins and be $P_{e,independency}$ = 0.000004 [1/a] (equals a return period of 250,000 years). Using this exceedance probability for a risk analysis would result in a significant underestimation of the flood risk. By assuming perfect dependency, the exceedance probability would be $P_{e,dependency}$ = 0.0025 [1/a], resulting in an overestimation of the flood risk. Only analysing the parameter S within a risk assessment also leads to an overestimation of the flood risk.

For both tide gauges the 'highest turning points' of the three selected storm surge events vary by more than 50 cm (Fig. 5-9, right). The events in the upper panels (blue curves) have small values for S, but high values for F and long durations. In contrast, the storm surge curves in the lower panels (green curves) have large values for S and small values for F. This is because the surrounding high water levels (i.e. the first and the third tidal high waters) are comparable low. For some investigation areas (e.g. areas protected by dunes) storm surges with characteristics as shown in the upper panels (i.e. small values for S, high values for F) might have serious implications for the coastal defence line (e.g. risk of erosion) or for the hinterland. For other investigation areas, storm surges with

characteristics as shown in the lower panels (i.e. high values for S, small values for F) might have more devastating consequences.

Analysing various storm surge events with a specified exceedance probability but different characteristics might be useful when performing flood risk analyses for investigation areas where special protection is required (e.g. airports). In Germany for instance, dikes in front of nuclear power plants located in tidal influenced areas had to be designed to withstand a storm surge event with a return period of 10,000 years (KTA 2207, 2004). A design storm surge, causing the highest risk of flooding, can be reliably estimated by analysing a larger number of 10,000-year storm surge events with different characteristics.

5.5.2 Trivariate statistical analyses

Trivariate statistical analyses are performed for stochastically simulated storm surge events (transferred from Hoernum to Westerland and represented by S and F) and the important wave parameter H_s. Table 5-3 shows the results from comparing trivariate theoretical joint probabilities (calculated with a FNAC model as described in Sect. 5.4.3) and trivariate empirical joint probabilities. The storm surge parameters S and F are combined with a Gumbel Copula as described in Sect. 5.4.1 and it is tested which Copula is most appropriate to incorporate H_s into the FNAC model. The results in Tab. 5-3 show that the Gumbel Copula leads to the smallest RMSEs and the smallest values for the KS-statistic, closely followed by the Frank Copula. The Clayton Copula leads to the highest values. Hence, the GoF test suggests the FNAC model to jointly analyse the parameters S, F and H_s to consist of two Gumbel Copulas.

Table 5-3: RMSEs and values for the KS-statistic from comparing theoretical and empirical trivariate joint probabilities (S, F and H_s) for Westerland.

Function	RMSE	RMSE (extreme events*)	KS-statistic	KS-statistic (extreme events*)
Clayton Copula	0.059	0.047	0.147	0.083
Frank Copula	0.039	0.036	0.116	0.061
Gumbel Copula	0.033	0.020	0.106	0.031

* Events with an empirical non-exceedance probability of $P_u > 0.8$ [1/a] (equals a return period of 5 years)

However, conclusions drawn from the second GoF test are different. Figure 5-10 shows that merely the Frank Copula is able to model the existent structures of dependence between the parameter pairs (F, H_s) (left) and (S, H_s) (right).
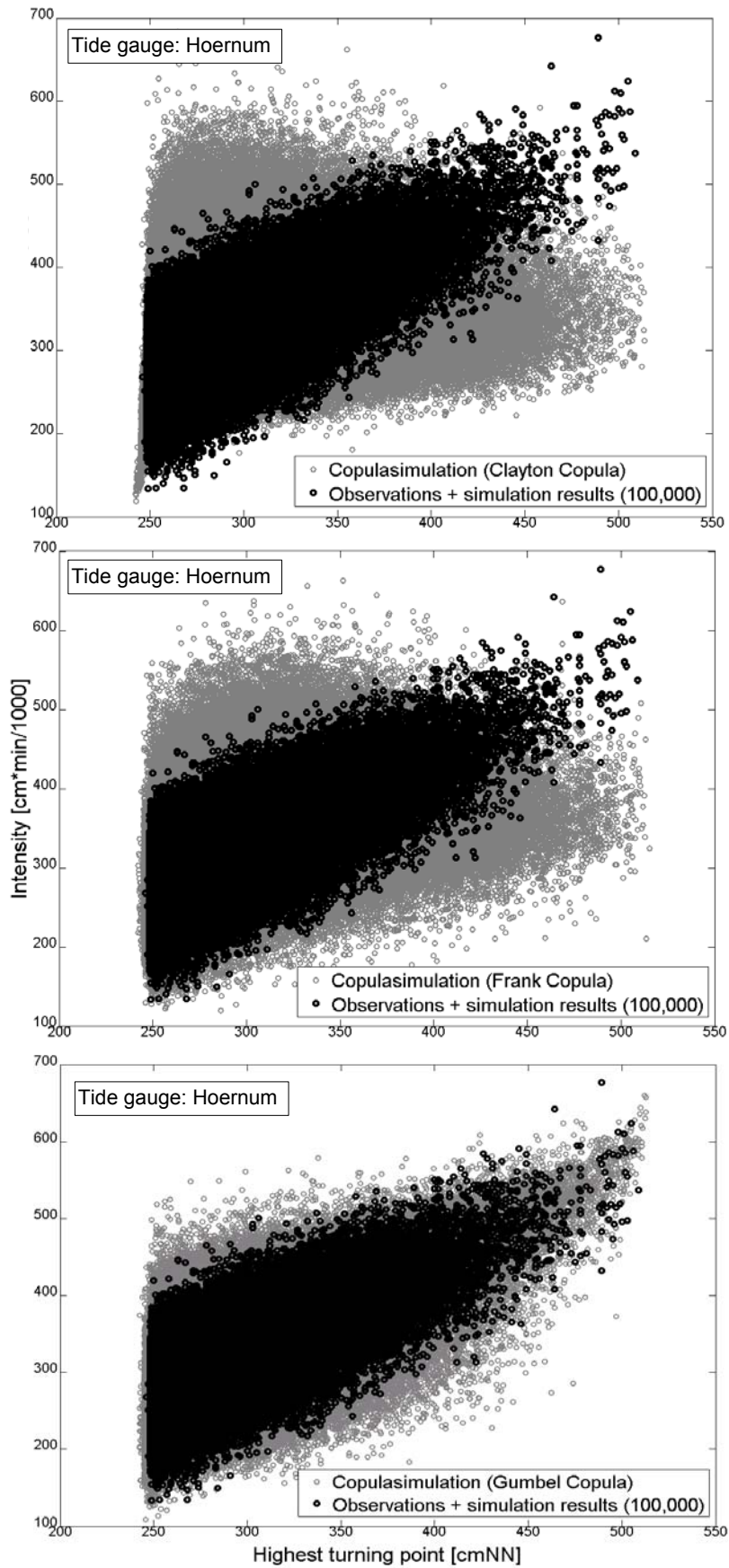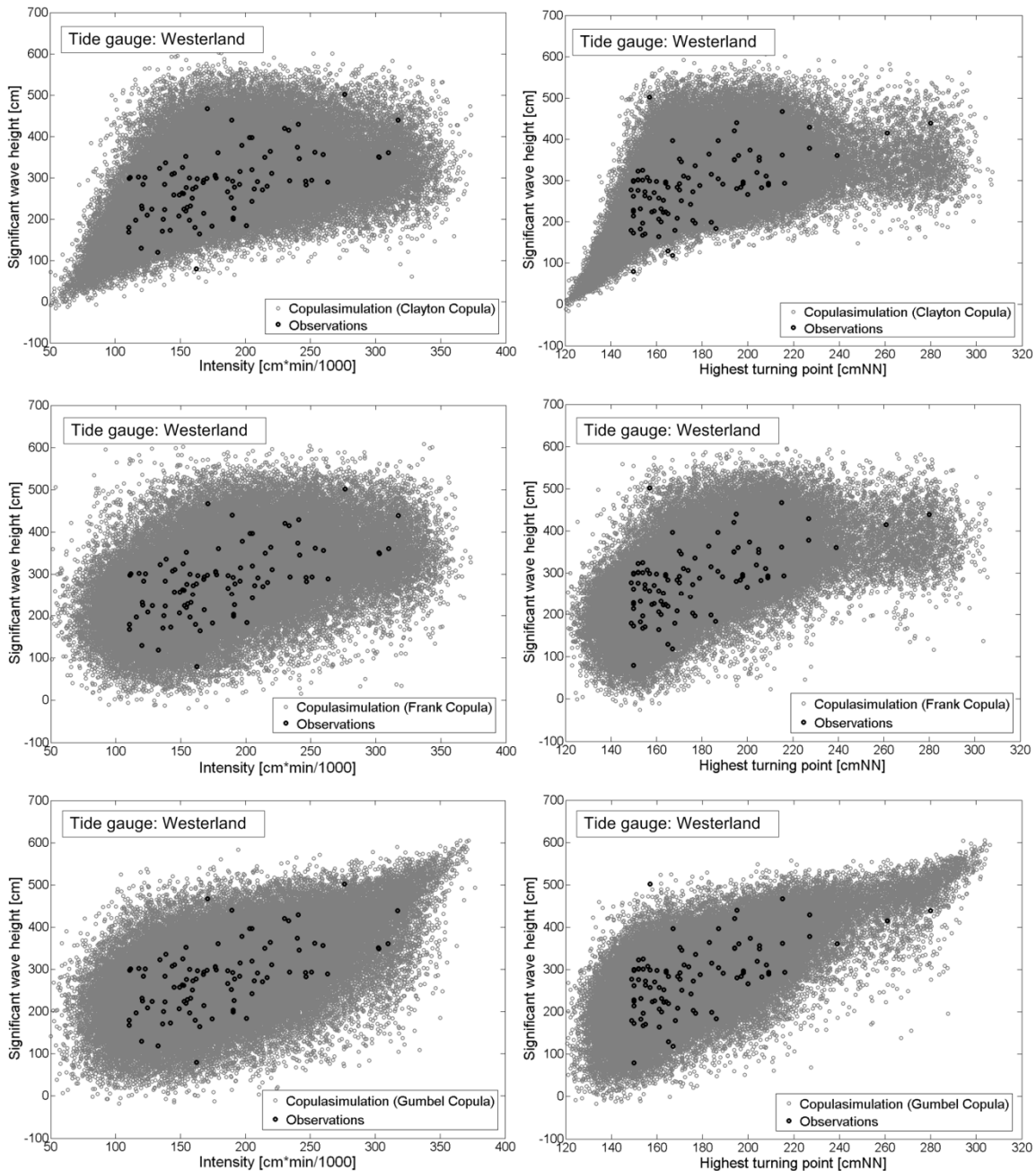

Figure 5-10:   Results from a graphical based GoF test for the tide gauge of Westerland by considering the Clayton Copula (top), the Frank Copula (middle), the Gumbel Copula (bottom) and the parameter pairs (F, H_s) (left) and (S, H_s) (right).

Simulation results from the Clayton Copula show strong tail dependence in the lower left, which is not present in the observations. Simulation results from the Gumbel Copula in contrast show strong tail dependence in the upper right. Such a dependence structure exists

for the parameter pair (S, F) (see e.g. Fig. 5-1), but not for the pairs (F, H_s) and (S, H_s). Furthermore, the lower right panel in Fig. 5-10 shows an outlier in the upper left corner. Hence, this graphical GoF test strongly suggests the Frank Copula could be considered as a second Copula to construct the FNAC model.

As the Frank Copula leads to good results with both GoF tests, the FNAC model is constructed based on a Gumbel and a Frank Copula. First, the parameters S and F are analysed based on a bivariate Gumbel Copula. This Copula is subsequently considered as a marginal distribution and a Frank Copula (as shown in Tab. 5-1) is used to incorporate the parameter H_s into the model.

In Fig. 5-11, results from bivariate and trivariate statistical analyses for the tide gauge of Westerland are compared. The parameters S and F are used for the bivariate analysis (black contours in Fig. 5-11). For the trivariate analysis S, F and a significant wave height of $H_s = 400$ cm (red contours in Fig. 5-11) are considered.
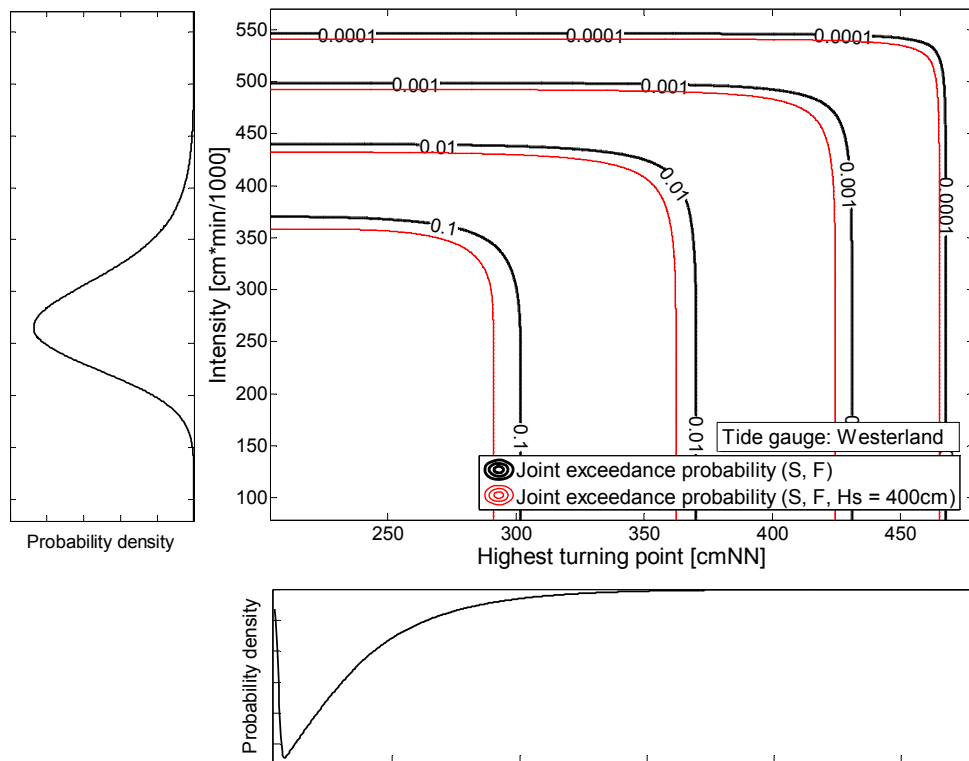
Figure 5-11:   Comparison of the results from bivariate statistical analyses for the parameters S and F and trivariate analyses for the parameters S, F and H_s (with $H_s = 400$ cm).

The exceedance probability for $H_s = 400$ cm is found to be $P_{e,Hs} = 0.37$ [1/a], which equals a return period of approximately 2.7 years (see Fig. 5-6). Figure 5-11 shows that incorporating H_s into the model reduces the exceedance probabilities for specific storm

surge events compared to the bivariate analysis. As an example, a storm surge event with $S = 425$ cmNN and $F = 468$ [cm*min/1000] represents a 1000-year event ($P_e = 0.001$ [1/a]) for the tide gauge of Westerland (with $P_{e,S} = 0.0013$ [1/a] and $P_{e,F} = 0.0035$ [1/a]). When taking into account a significant wave height of $H_s = 400$ cm, the same storm surge event has an exceedance probability of $P_e = 0.00078$ [1/a] (equals a return period of approximately 1280 years). Again, mistakenly assuming the independent case for all three parameters would lead to a significant underestimation of the flood risk ($P_{e,independent} = 0.0000017$ [1/a]; return period approx. 590,000 years). Assuming perfect dependency would lead to a significant overestimation ($P_{e,dependent} = 0.37$ [1/a]; return period approx. 2.7 years).

As it has been outlined in Sect. 5.4.3, Copulas may theoretically be extended to the d-dimensional case to include further parameters into the statistical assessment. However, this implies more constraints (if a FNAC model or a PNAC model is used), higher uncertainties and increased computational requirements. Here, the two important storm surge parameters S and F and the wave parameter H_s are considered. Alternatively the wave period T could be used instead of the wave height H_s.

5.5.3 Uncertainty assessment

Especially when analysing extreme storm surge events, the uncertainties of the statistical assessment are considerable high. In the following, the uncertainties involved in the described methodology are briefly discussed and examples of how to quantify the key uncertainties are provided.

There are two main sources of uncertainties that need to be addressed when applying the presented methodology. First, uncertainties emerge from estimating the structure of dependence or the Copula parameter θ, respectively, from a random sample of the considered parameters. By calculating 95%-confidence bounds of the Copula parameter, uncertainties of the exceedance probabilities for selected storm surge events may be quantified. Taking the storm surge event from the upper panel (blue curve) for Hoernum from Fig. 5-9 as an example, the exceedance probability is found to be $P_e = 0.001$ [1/a] (0.00091|0.00104). The numbers in brackets represent the uncertainty range (95%-confidence level), resulting from varying the Copula parameter ($\theta = 1.83 \pm 0.25$ [-]). For

the trivariate case, uncertainties may be quantified in the same way when a second Copula (with a second Copula parameter θ) is used to incorporate the wave parameter H_s.

A second key uncertainty emerges from the fact that the multivariate statistical analyses in this study are based on stochastically simulated storm surge events. As described in Sect. 4 different filter functions are applied within the simulations, whereas one of these filters affects the statistical analyses presented here. This filter function removes very extreme events (with water levels exceeding a given threshold) from the simulation results. The water levels which have been chosen are considered currently physically possible for the investigation areas. Thresholds of 651 cmNN (as a result from a large number numerical model runs) and 513 cmNN (as a result from extensive empirical studies) are used for Cuxhaven and Hoernum, respectively. Choosing different thresholds would affect the results of the statistical analyses presented here. The uncertainties for the threshold values are 603 cmNN to 673 cmNN for Cuxhaven and 444 cmNN to 537 cmNN for Hoernum (see Sect. 4.4.3). By choosing the upper and lower values as thresholds for the stochastic simulation, the related uncertainties in the statistical analyses may be quantified. Taking the storm surge event in the upper panel (blue curve) for Hoernum from Fig. 5-9 as an example again, the exceedance probability is found to be $P_e = 0.001$ [1/a] (0.00034|0.0011). The numbers in brackets represent uncertainties resulting from varying the thresholds in the stochastic storm surge model. The uncertainty range is much larger compared to the uncertainty range resulting from varying the Copula parameter. Both of the described key uncertainties may affect the results of the statistical assessment at the same time. Thus, they have to be superimposed to capture the whole range of uncertainties and the exceedance probability for the example storm surge from Fig. 5-9 becomes $P_e = 0.001$ [1/a] (0.00025|0.00114).

Further uncertainties result from fitting univariate distribution functions to the marginal parameters and from choosing certain bivariate or trivariate models. These uncertainties are not quantified and only briefly discussed in the following. For the parameters S and F Kernel Density Functions are considered as marginal distributions, assuring a good fit to the available data sets. Uncertainties may arise for very extreme events from instabilities due to the limited number of events. However, when considering 10 million scenarios, storm surges with exceedance probabilities larger than $P_e > 5.0 \cdot 10^{-6}$ [1/a] are not affected. A parametric univariate distribution function (namely the GEV) is used here for the marginal parameter H_s. The uncertainties from fitting the distribution to the data set are

expected to be small compared to the key uncertainties discussed above. Furthermore, moderate wave conditions (in terms of the return periods) are usually taken into account when defining scenarios (storm surges and wave conditions) for integrated risk analyses. Here, a significant wave height of 400 cm and with a return period of approx. 2.7 years is used as an example. Finally, fitting bivariate and trivariate models to the available data sets involves uncertainties. Here, two GoF tests are applied to choose proper Copula functions in order to minimise the uncertainties.

5.6   Conclusions

In this section a Copula based approach to statistically analyse storm surges and wind waves is presented. A bivariate statistical model is applied to jointly analyse the important storm surge parameters 'intensity' and 'highest turning point'. Especially when performing integrated risk analyses, where breach models are applied to identify the initial conditions for flooding of the hinterland and potential losses are quantified, the 'intensity' of a storm surge (as a proxy for the energy input into the defence structures) has significant implications. Many of the bivariate models available from literature suffer from restrictions and constraints regarding the underlying data sets in terms of the dependence or the marginal distributions. Copulas in contrast are very flexible and can handle dependent parameters with mixed marginal distributions. Moreover, it is possible to construct higher dimensional Copula models to incorporate further important parameters. In the present study, the bivariate model is extended to the trivariate case to additionally take into account the significant wave height H_s as one of the most important wave parameters. A fully nested Archimedean Copula approach is applied to construct a trivariate model. Alternatively other wave parameters, such as the wave period, may be analysed instead of (or theoretically also in addition to) the significant wave height. To outline the transferability of the model, results from the bivariate analyses are presented for two different investigation areas in the German Bight (i.e. Cuxhaven and Hoernum). The trivariate analyses focus on the investigation area Westerland on the west side of Sylt Island, for which wind waves represent a considerable loading factor. The results presented in Sect. 5.5 highlight that Copula functions are valuable for statistical assessments (especially within event-based risk analyses), as they are flexible and can analyse a larger number of important parameters. This leads to realistic exceedance probabilities and

contributes to improving the overall results from integrated flood risk analyses, as for example performed within the German XtremRisK project for the city of Hamburg and Sylt Island.

Future work to improve the multivariate model(s) may focus on the incorporation of further GoF tests, especially when higher dimensional Copula models are applied. This assures an objective and reliable model selection. Although Copulas provide valuable features compared to traditional multivariate approaches, the adoption of certain models to certain data sets still includes considerable uncertainties. If more than two parameters are jointly analysed, further higher dimensional models might be taken into account as an alternative to the FNAC model used for the present study. Some of the models discussed in Sect. 5.4.3 (and further approaches described in literature) are more flexible and do not require the marginal parameters to fulfil special criteria as it is the case with the FNAC model. However, the presented results highlight that Copulas represent a promising alternative to address various multivariate problems. While they are nowadays widely used in hydrology (and other research fields), it is hoped that some of the above remarks and examples will contribute to establish Copulas also in the coastal research and engineering sector.

6   Summary and general conclusions

The aim of this research has been to improve our understanding of how to derive reliable hydrodynamic boundary conditions for flood risk analyses in coastal areas under current and possible future climate conditions (see also Sect. 1.5) in the German Bight. This has been accomplished by undertaking four main stages of research, each one addressing a specific objective.

The objective of the first stage has been to introduce advanced methods to construct and analyse MSL time series from high frequency data sets (i.e. at least hourly observations) and high and low water time series from tide gauges in the German Bight. The *k*-factor method (Lassen, 1989) has been further developed and state of the art as well as some new analysis techniques to investigate longer-term MSL changes have been presented in Sect. 2. Linear trends were calculated for different time periods and a more sophisticated approach to analyse non-linear changes in MSL time series (i.e. MCAP and SSA) has been introduced. All methods were applied to the MSL time series of Cuxhaven and Helgoland. Linear trends were calculated with associated standard errors, highlighting that the year to year variability in the German Bight is large compared to most other parts of the North Sea coastline (for example the UK east coast and large parts of the Dutch coastline). Hence, long time series are required to derive meaningful results from linear trend analyses. For the Cuxhaven and Helgoland time series long-term trends were found to be similar to those calculated from a global and a UK sea level reconstruction. Higher trends were estimated from the two German Bight time series for the last 15 years, whereas the standard errors were also large. The MCAP approach was validated against other padding techniques described in literature (Mann, 2004; Jansen et al., 2007; Trenberth et al., 2007) and it has been outlined that it allows the specification of uncertainties when smoothing time series over the whole record length. From analysing the Cuxhaven time series, two periods of sea level rise acceleration were detected at the end of the 19th century (consistent with findings

from other long tide gauge records, e.g. Brest and Liverpool) and over the last approximately three decades of the 20th century.

These findings were mostly confirmed in the second stage of research, where a large number of MSL time series was constructed and analysed (see Sect. 3). A new (and from our current knowledge) homogeneous MSL data set with monthly and annual time series from 13 tide gauges covering the entire German North Sea coastline has been compiled (see Jensen et al. (2010) for detailed information about the data preparation and construction of the MSL time series). This data set served as a basis for the first detailed analysis of observed MSL changes in the German Bight from the mid 19th century to present. Most former studies suffered from missing high frequency data (i.e. at least hourly records) (e.g. Jensen, 1984) or focussed on a small number of tide gauge sites (e.g. Dietrich, 1954). Here, individual MSL time series as well as virtual station time series (comprised from a certain number of individual time series) were analysed with the methods described in Sect. 2. Linear trends were calculated for different time periods and were found to be relatively constant in the order of 2 mm/a in the 19th and 20th century. Higher rates were derived for a time period covering the last decades (i.e. 1971 to 2008; trends were in the order of 3 to 4 mm/a), indicating a recent acceleration of SLR. This was confirmed by applying non-linear smoothing techniques (i.e. SSA and MCAP) to individual and virtual station time series. However, it was found that longer records (e.g. Cuxhaven or Norderney) showed similar periods of accelerated SLR at other times in the 19th and 20th century. Hence, the estimated high recent rates are not as yet particularly unusual. Similar findings were reported for example by Haigh et al. (2011a) from analysing 20th century MSL changes in the English Channel. Global sea levels have also risen at higher rates over the last 15 years (3.5 mm/a; Mitchum et al., 2010) compared to the 20th century (1.7 mm/a; Church and White, 2006), suggesting a recent acceleration in global SLR. In the present study, higher trends of relative SLR were detected for sites along the coastline of Schleswig-Holstein, compared to Lower Saxony. These differences most likely result from spatial variations in velocities of vertical land movement along the coastline (i.e. land subsidence in the case of the German Bight) and in the meteorological forcing. The rates of vertical land movement are not well known up to now due to short or missing CGPS measurements near the tide gauges. A first attempt to derive site specific rates of vertical land movement has been undertaken and the results are presented in Sect. 3. The estimated rates vary from -1.0 mm/a to -0.5 mm/a for most sites (negative

values denote land subsidence). A comparison of a German Bight and a global sea level reconstruction approved the findings reported in Sect. 2 (where only one time series from the German Bight was considered). That is linear long-term trends are similar but temporal patterns of sea level change (e.g. decadal variability) are significantly different. Similar patterns as in the German Bight were found from a northeast Atlantic sea level reconstruction. This highlights the need to work out reliable regional SLR scenarios for regional and local planning purposes or risk assessments, where possible future climate conditions need to be taken into account. The current knowledge about possible future sea level changes on different spatial scales was summarised in Sect. 1.1. The new mean sea level data set could be used to validate the output of regional climate models when compiling regional SLR scenarios. The data set has been transferred to colleagues working on similar topics and has already been used as a basis for further studies (e.g. Albrecht et al., 2011 and accepted; Hein et al., 2011; Dangendorf et al., 2012; Mudersbach et al., under review)

The third stage of research focussed on developing and testing a stochastic model to simulate a large number of high frequency storm surge curves (i.e. total still water levels resulting from the combination of tides and wind surges) (see Sect. 4). Storm surges represent the most important loading parameter for coastal defence structures along the German North Sea coastline. It has been outlined that a larger number of scenarios is required to achieve meaningful results from risk analyses based on the SPR concept. The stochastic model needs observed high frequency storm surge curves as input data and information about maximum possible storm surge heights (under current or future climate conditions) should also be taken into account. As an example, 10 million storm surge curves (each one consisting of three tidal cycles) were simulated for the tide gauges of Cuxhaven and Hoernum. All storm surge events were characterised by two parameters, namely the 'highest turning point' and the 'intensity'. With these parameters the overall simulation results were presented, from which particular storm surge curves (with certain characteristics) can be selected to be used as input data for risk assessments. By undertaking two steps of validation, it has been proven that the stochastic storm surge model leads to reliable results. Its application within risk assessments reduces the uncertainties and the computational requirements, which are usually needed to derive a sufficient number of storm surge scenarios with different characteristics. SLR scenarios

can be taken into account (at present with the MSL offset method, as described in Sect. 1.2) to simulate storm surges for future time steps.

In the fourth stage of research, all relevant loading parameters for coastal structures along the German North Sea coastline (i.e. storm surge and wave parameters) were jointly analysed with different multivariate statistical models (see Sect. 5). Bivariate and trivariate models were constructed from Archimedean Copula functions. With the bivariate model the two important storm surge parameters 'highest turning point' and 'intensity' were examined. From GoF tests the Gumbel Copula was identified to be most appropriate to calculate exceedance probabilities for the available storm surge curves (i.e. the outcome of the stochastic simulation presented in Sect. 4). These exceedance probabilities are more reasonable to be used for risk assessments than those calculated in former studies. Storm surges with a small duration and extremely high water levels as well as storm surges with comparable small water levels and very large durations can potentially cause substantial damages in the hinterland. Hence, both types of storm surge events should have small exceedance probabilities. This is the case when the storm surge intensity is taken into account as shown in Sect. 5, but not when solely analysing the highest storm surge water levels (as in most former studies). The results from the multivariate statistical analyses were presented as contour plots together with the results from the stochastic storm surge simulation presented in Sect. 4. With these plots it easily possible to extract (stochastically simulated) storm surge events with different characteristics but same exceedance probabilities. In a further step, the bivariate model was extended and a trivariate fully nested Archimedean Copula model was constructed to additionally include relevant wave parameters in the statistical assessment. Here, the significant wave height was chosen as a representative wave parameter. It was jointly analysed with the two important storm surge parameters for Westerland on the west side of Sylt Island.

To conclude, with the methods and results presented in this thesis hydrodynamic boundary conditions for flood risk analyses in coastal areas can be estimated more accurately than before. The results from investigating observed mean sea level changes are only valid for the German Bight. However, the applied methods (e.g. SSA and MCAP) are transferable and can be used for similar studies in other regions (see for example Haigh et al., 2011b). The same is true for the multivariate statistical approach, which was used to calculate reliable joint exceedance probabilities. The stochastic storm surge model was developed for the prevailing tidal regime in the German Bight. Thus, it needs to be modified when

applying it to data sets from investigation areas with completely different tidal conditions. The research that was conducted for the thesis developed the following innovations:

- the Monte-Carlo autoregressive padding approach (in combination with Singular System Analysis) to analyse the non-linear behaviour of high variability sea level time series to a higher accuracy than before

- a new and high quality mean sea level data set for the German North Sea area

- results from a first detailed analysis of observed mean sea level changes in the German Bight based on a high quality data set and by applying state of the art (and some advanced) analysis techniques

- a stochastic storm surge model, which allows the simulation of a large number of high frequency storm surge curves based on tide gauge data (results can be used for risk assessments or various other applications)

- multivariate statistical models based on Copula functions, which allow the consideration of all important loading parameters for coastal defence structures (i.e. storm surge water levels and waves) within the statistical assessment (for example when performing integrated risk analyses)

7   Recommendations for further research

The results summarised in the previous sections show that the objectives of the thesis (listed in Sect. 1.5) were mostly accomplished. Nevertheless, the research which has been undertaken suggests different directions for future activities. The main points, which could contribute to further improve our understanding of how to estimate reliable hydrodynamic boundary conditions for flood risk analyses, with a focus on the German North Sea region, are listed in the following eight recommendations:

1. **Digitise analogue (historic) sea level data**

    Hundreds of years of analogue tidal charts (and tables) are available from tide gauges along the German North Sea coastline and have not yet been digitised. Long digital high and low water time series are available for most gauges, whereas high frequency data sets are often not longer than 10 to 15 years. Even the high and low water data sets could be extended backwards to the 19th century for many sites. This involves time consuming investigations of datum shifts (e.g. from replacing the measurement equipment) to create homogeneous data sets. Such data sets could be used to improve the results from MSL analyses, as well as from storm surge analyses (as for example presented in Sect. 4). Haigh (2009) and Haigh et al. (2009) provide similar recommendations referring to tide gauges around the UK.

2. **Separation of vertical land movements from observed sea level changes**

    It has been outlined in Sects. 2 and 3 that velocities of vertical land movement at tide gauge sites along the German coastline are mostly unknown at present. A first attempt has been undertaken to estimate the influence of vertical land movement on observed sea level changes (see Sect. 3.4.4). Continuous GPS measurements near tide gauges are available but to date are relatively short, with many of the records

starting after 2007. Longer records will be available in the future and will allow for a more precise calculation of absolute sea level changes.

3. **Extended study to analyse observed MSL changes from coastlines around the entire North Sea basin and in the Baltic Sea**

Mean sea level analyses presented in this thesis focussed on the comparable small investigation area of the German Bight. A comparison with changes along other parts of the North Sea coastline (including the English Channel) and with observed changes in the Baltic Sea will allow for a better understanding of the spatial patterns of SLR and how the German Bight is influenced by adjacent areas. Achieving reliable results from such a study requires the application of common methods to all available data sets. All analysis techniques used in this study have been automated in MATLAB (see Appendix) and can be applied to MSL time series from other parts of the North Sea (or Baltic Sea) coastline. A study with the focus on analysing observed MSL changes from 30 tide gauges along the entire North Sea coastline is currently under way (Wahl et al., in prep.). Furthermore, White et al. (2005) showed that altimeter products can be used to investigate differences between sea level changes along the coastlines and in the open ocean.

4. **Identify the main contributors for differences in regional or local sea level changes compared to the global average and work out reliable SLR scenarios**

In Sect. 1.1 (and also in Sects. 2 and 3) it has been outlined that regional sea level changes differed from global sea level changes in the past. Hence, regional or local scenarios of possible future sea level changes are urgently needed to work out sustainable management strategies. Such regional scenarios have to account for the main contributors for the differences between regional/local and global changes. For the German Bight, GIA (i.e. land subsidence) and thermal expansion are the main contributors for higher values compared to the global average (Slangen et al., 2011 and pers. comm.; see also Fig. 1-4). The ice contribution is slightly below average, due to Greenland melt. However, it has been mentioned that the spatial resolutions of the climate models, which are nowadays used for global assessments, are still too course to derive meaningful results for specific regions. Hence, models with higher resolutions need to be developed or alternative methods to downscale results from global assessments have to be applied.

5. **Improve results from investigating possible future changes in storminess and wave climate in the German Bight**

The current knowledge about possible future changes in storm surge heights (which are not influenced by MSL changes), as well as the knowledge about possible changes in wave heights and periods need to be improved (see also Sects. 1.2 and 1.3). Especially for the German Bight area, some studies suggest future changes in both loading parameters to be significant. However, the results presented by different authors and derived by applying different methods are not consistent. This refers to spatial patterns, as well as to magnitudes of the estimated changes. More reliable projections are required to allow the consideration of possible future changes within risk assessments (for example when simulating storm surge scenarios, see following paragraph). At first, a crucial step consists in fully exploring the observed changes, as for example reported by Jensen et al. (2008) and Mudersbach et al. (under review); that is significant changes in the mean tidal range along the German North Sea coastline between the 1950s and 1990s.

6. **Optimise the stochastic storm surge model**

The stochastic storm surge model introduced in Sect. 4, was used to simulate many storm surge scenarios for two tide gauges and for present day climate conditions. By using the MSL offset method, the model allows for taking certain SLR scenarios into account when simulating storm surges for future time steps (see Appendix). In the current version, possible future changes in storminess, which are also not well known at present, cannot be considered. However, with more reliable projections available (see previous paragraph), it would be possible to optimise the model in a way that such information are used for the simulations. This could be done for example, by applying non-stationary extreme value approaches, allowing certain distribution parameters to change over time (e.g. Menendez and Woodworth, 2010; Mudersbach and Jensen, 2010).

7. **Optimise the multivariate statistical approach**

The multivariate statistical approach presented in Sect. 5 uses Archimedean Copula functions to jointly analyse relevant loading parameters and to calculate joint exceedance probabilities. Although three different Copula functions are used with GoF tests to choose an appropriate model, uncertainties emerge from fitting certain

models to certain data sets. Other types of Copulas (e.g. Elliptical Copulas, Fairly-Gumbel-Morgenstern Copula) and Copulas with more than one parameter (as it is the case with the three Copulas considered for the present study) are described in literature (e.g. Joe, 1997; Nelsen, 1999). Some of these Copulas are more flexible as they allow for example to analyse the upper tail dependence separately from the lower tail dependence of the considered data set. Hence, the uncertainties from fitting a Copula model to the data set might be reduced. However, in the case of two-parametric models, an additional Copula parameter has to be estimated (which also involves uncertainties) and the calculation of joint exceedance probabilities might become more complex. Further studies should focus on investigating the benefit from considering further Copula functions. This also involves the application of further GoF tests (as for example described by Genest et al., 2009) to allow an objective evaluation of the models. In Sect. 5.5.2 a FNAC model was used to jointly analyse three important loading parameters for coastal defence structures and to calculate joint exceedance probabilities. It has been discussed, that this approach requires the underlying data sets to fulfil certain criteria. For future applications, more flexible methods to construct higher dimensional Copula models (as briefly described in Sect. 5.4.3) could be used in addition or as an alternative to the FNAC model to assure unrestricted alienability of the method.

8. Spatial extension and use of the output of process-based hydrodynamic models

Here the stochastic storm surge model was used to simulate storm surges for two sites and the multivariate statistical approach was used to assess the results. Both the stochastic model and the multivariate statistical analyses have been automated in MATLAB (see Appendix). With these tools, large storm surge samples can be easily generated and analysed for further tide gauges along the German North Sea coastline. This requires some sensitivity studies to evaluate how long high frequency water level time series need to be in order derive meaningful results. The application to other sites would improve the understanding of existing spatial patterns along the coastline and reliable input data for further risk assessments (or other applications) would be available. In addition to observed records, results from long sea level hindcasts derived from hydrodynamic modelling could be included. With such information, it is possible to estimate return period curves for water levels or combinations of water levels and waves for the entire coastline, involving

ungauged areas (e.g. Dixon and Tawn, 1997). For the German Bight area hindcasts for many different parameters derived from numerical model runs are for example available from www.coastdat.de (hosted by the Helmholtz-Zentrum Geesthacht, Centre for Materials and Coastal Research).

The previous list summarises the main points which have been identified within the research for this thesis with a focus on the German North Sea area and makes no claims to completeness. Future challenges related to the research topics discussed in this thesis, but being often more general and with the focus mostly on global assessments, are also discussed for example in the individual chapters of Church et al. (2010).

8   References

Albrecht, F., Wahl, T., Jensen, J. and Weisse, R.: Determining sea level change in the German Bight, Ocean Dynamics, 61, 12, 2037–2050, doi: 10.1007/s10236-011-0462-z, 2011.

Albrecht, F., Weisse, R. and von Storch, H.: Wind and Pressure Effects on past regional Sea-Level Trends and Variability in the German Bight, Ocean Dynamics, accepted.

Ang, A.H.-S. and Tang, W.H.: Probability Concepts in Engineering – Emphasis on Application in Civil & Environmental Engineering, Wiley, 2nd Edition, ISBN: 978-0-471-72064-5, 2007.

Augath, W.: Stand und Weiterentwicklung der Höhenüberwachung der niedersächsischen Nordseeküste, Nachrichten der Niedersächsischen Vermessungs- und Katasterverwaltung 43: 78–92, 1993.

Araújo, I.: Sea level variability: Examples from the Atlantic coast of Europe. PhD thesis, University of Southampton, United Kingdom, 216pp., 2005.

Araújo, I., Pugh, D.T.: Sea levels at Newlyn 1915-2005: Analysis of trends for future flooding risks, Journal of Coastal Research, 24 (sp3), 203-212, 2008.

Beckley, B.D., Lemoine, F.G., Luthcke, S.B., Ray, R.D. and Zelensky, N.P.: A reassessment of global and regional mean sea level trends from TOPEX and Jason-1 altimetry based on revised reference frame and orbits, Geophys. Res. Lett., 34, L14608, doi:10.1029/2007GL030002, 2007.

Bender, J. and Jensen, J.: Generierung synthetischer Hochwasserganglinien, Tagungsband des 1. CoastDoc-Seminars, In: Mitteilungen des Forschungsinstituts Wasser und Umwelt, Vol. 2, ISSN 1868-6613, 2011.

Berg, D. and Aas, K.: Models for construction of multivariate dependence: A comparison study, Europ. J. Finance, 15 (7–8), 639–659, 2007.

Berg, G.: Copula goodness-of-fit testing: an overview and power comparison. Europ. J. Finance, 15 (7–8), 675–701, 2009.

Berg, D. and Quessy, J.-F.: Local sensitivity analyses of goodness-of-fit tests for copulas, Scand. J. Statist., 36, 389–412, 2009.

Bindoff, N.L., Willebrand, J., Artale, V., Cazenave, A., Gregory, J., Gulev, S., Hanawa, K., Le Quéré, C., Levitus, S., Nojiri, Y., Shum, C.K., Talley L.D., Unnikrishnan, A.: Observations: Oceanic climate change and sea level. In: Climate Change 2007: The physical science basis. Contribution of working group I to the Fourth Assessment Report of the Intergovernmental Panel on Climate Change. Editors: Solomon, S., Qin, D., Manning, M., Chen, Z., Marquis, M., Averyt, K.B., Tignor M., Miller H.L. Cambridge University Press, Cambridge, United Kingdom and New York, NY, USA, pp. 385-432, 2007.

Box, G.E.P. and Jenkins, G.M.: Time Series Analysis- forecasting and control, Holden-Day, London, 1976.

Brahms, A.: Anfangs - Gründe der Deich- und Wasser-Baukunst, 2 Bände, Aurich, 1754 und 1757.

Bosello. F., Nicholls, R., Richards, J., Roson, R. and Tol., R.S.J.: Economic Impacts of Climate Change in Europe: Sea-level rise, Climatic Change, DOI: 10.1007/s10584-011-0340-1 (online first), 2011.

Bungenstock, F. and Schäfer, A.: The Holocene relative sea-level curve for the tidal basin of the barrier island Langeoog, German Bight, Southern North Sea. Global and Planetary Change 66(1-2):34-51, 2009.

Burzel, A., Dassanayake, A., Naulin, M., Kortenhaus, A., Oumeraci, H., Wahl, T., Mudersbach, C., Jensen, J., Gönnert, G., Sossidi, K., Ujeyl, G. and Pasche, E.: Integrated flood risk analysis for extreme storm surges, Proc. of the 32nd International Conference on Coastal Engineering, Shanghai, China, 2010.

Cai, Y., Gouldby, B.P., Hawkes, P.J. and Dunning, P.: Statistical simulation of flood variables: incorporating short-term sequencing. J. Flood Risk Management, 1 (1), 3–12, 2008.

Cazenave, A., Dominh, K., Guinehut, S., Berthier, E., Llovel, W., Ramillien, G., Ablain, M. and Larnicol, G.: Sea level budget over 2003–2008: A reevaluation from GRACE space gravimetry, satellite altimetry and Argo. Global and Planetary Change 65:83–88, 2008.

Chen, H. L. and Rao A. R.: Testing Hydrologic Time Series for Stationarity, J. Hydrologic Eng., 7(2), 129–136, doi: 10.1061/(ASCE)1084-0699(2002)7:2(129), 2002.

Chow, V. T.: Handbook of Applied Hydrology, McGraw-Hill Book Company, 1964.

Christensen, J., Hewitson, B., Busuioc, A., Chen, A., Gao, X., Held, I., Jones, R., Kolli, R., Kwon, W.-T., Laprise, R., Rueda, V.M., Mearns, L., Menéndez, C., Räisänen, J., Rinke, A., Sarr, A., Whetton, P.: Regional climate projections. In: Solomon, S., Qin, D., Manning, M., Chen, Z., Marquis, M., Averyt, K., Tignor, M., Miller, H. (Eds.), Climate Change 2007: The Physical Science Basis. Contribution of Working Group I to the Fourth Assessment Report of the Intergovernmental Panel on Climate Change. Cambridge University Press, Cambridge, United Kingdom and New York, NY, USA, 2007.

Church, J.A., White, N.J., Coleman, R., Lambeck, K. and Mitrovica, J.X.: Estimates of the regional distribution of sea level rise over the 1950-2000 period, Journal of Climate 17: 2609-2625, 2004.

Church, J.A. and White, N.J.: A 20th century acceleration in global sea-level rise, Geophys. Res. Lett., 33, L01602, doi:10.1029/2005GL024826, 2006.

Church, J. A., White, N. J., Aarup, T., Wilson, S. W., Woodworth, P. L., Domingues, C. M., Hunter, J. R. and Lambeck, K.: Understanding global sea levels: past, present and future, Sustain Sci, 3(1), 9–22, doi: 10.1007/s11625-008-0042-4, 2008.

Coles, S.: An Introduction to Statistical Modeling of Extreme Values, Springer, ISBN 1-85233-459-2, 2001.

Dangendorf, S., Wahl, T., Hein, H., Jensen, J., Mai, S., and Mudersbach, C.: Mean Sea Level variability and influence of the North Atlantic Oscillation on long-term trends in the German Bight, Water 2012, *4*, 170-19, 2012.

Degen, H. and Lohrscheid, P.: Statisti*k*-Lehrbuch, mit Wirtschafts- und Bevölkerungs-statistik, 2. Auflage, Oldenbourg Wissenschaftsverlag, ISBN 3-486-27240-3, 2002.

De Michele, C., Salvadori, G., Passoni, G. and Vezzoli, R.: A multivariate model of sea storms using copulas. Coast. Eng., 54, 734–751, 2007.

de Vries, C.G. and Zhou, C.: Discussion of "Copulas: Tales and facts", by Thomas Mikosch, Extremes, 9 (1), 23–25, 2006.

De Waal, D.J. and van Gelder, P.H.A.J.M.: Modelling of extreme wave heights and periods through copulas. Extremes, 8, 345–356, 2005.

Dietrich, G.: Ozeanographisch-meteorologische Einflüsse auf Wasserstandsänderungen des Meeres am Beispiel der Pegelbeobachtungen von Esbjerg, Die Küste, 2/2, 130–157, 1954.

Dixon, M.J. and Tawn, J.A.: Extreme sea-levels at the UK A-class sites: optimal site-by-site analysis and spatial analyses for the East Coast, POL Internal Document Number 72, 1995. (available from http://www.pol.ac.uk/ntslf/pdf/id72.pdf)

Dixon, M.J. and Tawn, J.A.: Estimates of extreme sea conditions - final report, spatial analysis for the UK coast, POL Internal Document Number 112, 1997 (avialble from: http://www.pol.ac.uk/ntslf/pdf/id112.pdf).

Domingues, C.M., Church, J.A., White, N.J., Gleckler, P.J., Wijffels, S.E., Barker, P.M. and Dunn, J.R. Improved estimates of upper-ocean warming and multi-decadal sea-level rise. Nature 453:1090-1093. doi:10.1038/nature07080, 2008.

Douglas, B.C.: Global Sea Level Rise, J. Geophys. Res. 96(C4):6981–6992. doi:10.1029/91JC00064, 1991.

EU: Directive 2007/60/EC of the European parliament and of the council of 23 October 2007 on the assessment and management of flood risks, 2007.

Favre, A.-C., El Adlouni, S., Perreault, L., Thiémonge, N. and Bobée, B.: Multivariate hydrological frequency analysis using copulas, Water Resour. Res., 40, W01101, doi:10.1029/2003WR002456, 2004.

Flather, R. and Williams, J.: Climate change effects on storm surges: methodologies and results, ECLAT-2 Workshop Report, No 3, In: Beersma, J., Agnew, M., Viner, D., Hulme, M. (Eds.), Climate Scenarios for Water-related and Coastal Impact, pp. 66–78, 2000.

FLOODsite: Language of Risk - Project Definitions, Report T32-04-01, HR Wallingford, 2005

FLOODsite: Integrated Flood Risk Analysis and Management Methodologies, project website: http://www.floodsite.net, 2009.

Firing, Y. and Merrifield, M.A.: Extreme sea Level Events at Hawaii: Influence of Mesoscale Eddies, Geophysical Research Letters, 31:L24306, 2004.

Führböter, A. und Jensen, J.: Säkularänderungen der mittleren Tidewasserstände in der Deutschen Bucht, Die Küste, 42, 78–100, 1985.

Gaslikova, L.: High-resolution wave climate analysis in the Helgoland area, Helmholtz-Zentrum Geesthacht Center for Materials and Coastal Research (former GKSS Research Center), Doctoral Thesis, 2006. (available from: http://www.earthsystemschool.de)

Genest, M. and Remillard, B.: Discussion of 'Copulas: Tales and Facts', by Thomas Mikosch, Extremes, 9, 27–36, 2006.

Genest, C. and Favre, A.-C.: Everything you always wanted to know about copula modeling but were afraid to ask, J. Hydrol. Eng., 12(4), 347–368, 2007.

Genest, C., Rémillard, B. and Beaudoin, D.: Goodness-of-fit tests for copulas: A review and a power study, Insurance Math. Econom, 44, 199–213, 2009.

Ghil, M., Allen, M.R., Dettinger, M. D., Ide, K., Kondrashov, D., Mann, M. E., Robertson, A. W., Saunders, A., Tian, Y., Varadi, F. and Yiou, P.: Advanced spectral methods for climatic time series, Rev. Geophys., 40(1), 1003, doi:10.1029/2000RG000092, 2002.

Golyandina, N. K., Nekrutkin, K. and Zhiglëiìavskiæi, A. A.: Analysis of time series structure. SSA and related techniques, Chapman & Hall/CRC (Monographs on statistics and applied probability, 90), Boca Raton, Florida, 2001.

Gönnert, G., Isert, K., Giese, H. and Plüß, A.: Charakterisierung der Tidekurve, Die Küste, 68, 101–141, 2004.

Gönnert, G., Buß, Th. and Thumm, S.: Coastal Protection in Hamburg due to climate change. An example to design an extreme storm surge event, Proceedings of the First International Conference "Coastal Zone Management of River Deltas and Low Land Coastlines", Alexandria, Egypt, 2010.

Grabemann, I. and Weisse, R.: Climate change impact on extreme wave conditions in the North Sea: an ensemble study, Ocean Dyn., 58, 199−212, 2008.

Greenwood, P.E. and Nikulin, M.S.: A Guide to Chi-Squared Testing, John Wiley and Sons Inc., New York, ISBN: 047155779X, pp. 280, 1996.

Grimaldi, S. and Serinaldi, F.: Design hyetographs analysis with 3-copula function, Hydrolog. Sci. J., 51(2), 223−238, 2006a.

Grimaldi, S. and Serinaldi, F.: Asymmetric copula in multivariate flood frequency analysis, Adv. Water Resour., 29(8), 1115–1167, 2006b.

Gringorten, I. I.: A plotting rule for extreme probability paper. J. Geophys. Res., 68, No. 3, 813–814, 1963.

Grinsted, A., Moore, J.C. and Jevrejeva, S.: Reconstructing sea level from paleo and projected temperatures 200 to 2100 AD, Clim Dyn., published online first, doi: 10.1007/s00382-008-0507-2, 2009.

Günther, H., Rosenthal, W., Stawarz, M., Carretero, J., Gomez, M., Lozano, I., Serrano, O. and Reistad, M.: The wave climate of the Northeast Atlantic over the period 1955-1994: the WASA wave hindcast, Glob. Atmos. Oc. Syst., 6, 121–164, 1998.

Haigh, I.D.: Extreme sea levels in the English Channel 1900 to 2006, University of Southampton, School of Civil Engineering and the Environment, Doctoral Thesis, 214pp., 2009.

Haigh, I.D., Nicholls, R.J. and Wells, N.C.: Mean sea-level trends around the English Channel over the 20th century and their wider context. Continental Shelf Research 29:2083-2098, 2009.

Haigh, I.D., Nicholls, R.J. and Wells, N.C.: Assessing changes in extreme sea levels: Application to the English Channel, 1900–2006. Continental Shelf Research, 30 (9), 1042–1055, doi:10.1016/j.csr.2010.02.002, 2010a.

Haigh, I.D., Nicholls, R.J. and Wells, N.C.: A comparison of the main methods for estimating probabilities of extreme still water levels, Coast. Eng., 57 (9), 838–849, 2010b.

Haigh, I.D., Nicholls, R.J. and Wells, N.C.: Rising sea levels in the English Channel 1900 to 2100, Proc. of the ICE – Maritime Engineering, 1622 (2), 81–92, 2011a.

Haigh, I.D., Eliot, M., Pattiaratchi, C. and Wahl, T.: Regional changes in mean sea level around Western Australia between 1897 and 2008, Proc. of the Coasts & Ports Conference 2011, Perth, Australia, 2011b.

Hein, H., Mai, S. and Barjenbruch, U.: What tide gauges reveal about the future sea level, Proc. of the acqua alta 2011, Hamburg, 2011. (available from: http://acqua-alta.de/fileadmin/design/acqua-alta/pdf/abstracts/paper/13_10/Hein_Harmut_full_papers.pdf)

Holgate, S. J.: On the decadal rates of sea level change during the twentieth century, Geophys. Res. Lett., 34, L01602, doi:10.1029/2006GL028492, 2007.

Holgate, S. J., Jevrejeva, S., Woodworth, P. L. and Brewer, S. C.: Comment on: „A Semi-Empirical Approach to Projecting Future Sea-Level Rise", Science, 317, 5846, 1866–1867 DOI: 10.1126/science.1140942, 2007.

Hoozemans F.M.J., Marchand M. and Pennekamp H.A.: A global vulnerability analysis: vulnerability assessment for population, coastal wetlands and rice production on a global scale, 2nd edn. Delft Hydraulics, Delft, The Netherlands, 1993.

Horton, R., Herweijer, C., Rosenzweig, C., Liu, J., Gornitz, V. and RuaneA.C.: Sea level rise projections for current generation CGCMs based on the semi-empirical method, Geophys. Res. Lett., 35, L02715, doi:10.1029/2007GL032486, 2008.

Houston, J.R. and Dean, R.G.: Sea-level acceleration based on U.S. tide gauges and extensions of previous global-gauge analyses, J Coast Res, doi: 10.2112/JCOASTRES-D-10-00157.1, 2011.

Howard, T. and Lowe, J.: Interpreting century-scale changes in southern North Sea storm surge climate derived from coupled model simulations, J. Clim., 23, 6234–6247. doi:10.1175/2010JCLI3520.1, 2010

HR Wallingford: Joint probability of waves and water levels on the North Wales coast, HRWallingford Report EX 2331, 1990.

Hurrell, J.W.: Decadal trends in the North Atlantic Oscillation: regional temperatures and precipitation. Science 269, 676–679, 1995.

Hutchinson, T.P. and Lai, C.D.: The engineering statistician's guide to continuous bivariate distributions, Rumsby Scientific Pub., ISBN: 0646024132, pp. 346, 1991.

IKÜS: Aufbau eines integrierten Höhenüberwachungssystems in Küstenregionen durch Kombination höhenrelevanter Sensorik (final report). Online available from: http://tu-dresden.de, 2008.

Jansen, E., Overpeck, J., Briffa, K. R., Duplessy, J.-C., Joos, F., Masson-Delmotte, V., Olago, D., Otto-Bliesner, B., Peltier, W. R., Rahmstorf, S., Ramesh, R., Raynaud, D., Rind, D., Solomina, O., Villalba, R. and Zhang, D.: Palaeoclimate. In: Climate Change 2007: The Physical Science Basis. Contribution of Working Group I to the Fourth Assessment Report of the Intergovernmental Panel on Climate Change [Solomon, S., Qin, D., Manning, M., Chen, Z., Marquis, M., Averyt, K. B., Tignor, M. and Miller, H. L. (eds.)]. Cambridge University Press, Cambridge, United Kingdom and New York, NY, USA, 2007.

Jensen, J.: Änderungen der mittleren Tidewasserstände an der Nordseeküste, Mitteilungen Leichtweiß-Institut der TU Braunschweig, Heft 83, 1984.

Jensen, J.: Über instationäre Entwicklungen der Wasserstände an der Deutschen Nordseeküste, Mitteilungen des Leichtweiß-Instituts für Wasserbau der Technischen Universität Braunschweig, 88, Technische Universität Braunschweig, 1985.

Jensen, J., Mügge, H.-E. and Schönfeld, W.: Analyse der Wasserstandsentwicklung und Tidedynamik in der Deutschen Bucht, Die Küste, Heft 53, 1992.

Jensen, J., Mudersbach, C., Bork, I., Müller-Navarra, S.H., Koziar, Ch. and Renner, V.: Modellgestützte Untersuchungen zu Sturmfluten mit sehr geringen Eintrittswahrscheinlich-keiten an der Deutschen Nordseeküste, Die Küste, Heft 71, Boyens Medienverlag, Heide i. Holstein, 2006.

Jensen, J. and Mudersbach, C.: Zeitliche Änderungen in den Wasserstandszeitreihen an den Deutschen Küsten, in: Glaser R., Schenk, W., Vogt, J., Wießner, R., Zepp, H. and Wardenga, U. (Hrsg.), Berichte zur Deutschen Landeskunde, Themenheft: Küstenszenarien, Band 81, Heft 2, S. 99-112, Selbstverlag Deutsche Akademie für Landeskunde e.V., Leipzig, 2007.

Jensen, J. and Müller-Navarra, S.: Storm Surges on the German Coast, Die Küste, 74, 92–125, 2008.

Jensen, J., Wahl, T. and Mudersbach, Ch.: Sea Level Variations at the German North Sea and Baltic Sea Coastlines, Proc. of the 7th International Conference on Coastal and Port Engineering in Developing Countries (PIANC COPEDEC VII), Dubai, 2008.

Jensen, J., Frank, T., Wahl, T. and Dangendorf, S.: Analyse von hochaufgelösten Tidewasserständen und Ermittlung des MSL an der deutschen Nordseeküste (AMSeL), final project report, University of Siegen, Siegen, 2010. (available from: http://www.uni-siegen.de/fb10/fwu/wb/forschung/projekte/amsel/amsel_kfki_bericht_abschlussbericht_gesamt.pdf)

Jevrejeva, S., Grinsted, A., Moore, J.C. and Holgate, S.: Nonlinear trends and multiyear cycles in sea level records, J. Geophys. Res., 111, C09012, doi:10.1029/2005JC003229, 2006.

Jevrejeva, S., Moore, J.C., Grinsted, A. and Woodworth, P.L.: Recent global sea level acceleration started over 200 years ago?, Geophys. Res. Lett., 35, L08715, doi:10.1029/2008GL033611, 2008.

Jevrejeva. S., Moore, J.C. and Grinsted, A.: How will sea level respond to changes in natural and anthropogenic forcings by 2100?. Geophys. Res. Lett., 37, L07703. doi:10.1029/2010GL042947, 2010.

Joe, H.: Multivariate Models and Dependence Concepts, Chapman & Hall, London, 1997.

Kahaner, D., Moler, C., Nash, S.: Numerical Methods and Software, Prentice Hall, 1988.

Karmakar, S. and Simonovic, S.P.: Bivariate flood frequency analysis: Part 1 - Determination of marginals by parametric and nonparametric techniques, J. Flood Risk Management, 1, 190–200, 2008.

Karmakar, S. and Simonovic, S.P.: Bivariate flood frequency analysis: Part 2 - A copula-based approach with mixed marginal distributions, J. Flood Risk Management, 2 (1), 32–44, 2009.

Katsman, C.A., Hazeleger, W., Drijfhout, S.S., van Oldenborgh, G.J., Burgers, G.J.H.: Climate scenarios of sea level rise for the northeast Atlantic Ocean: a study including the effects of ocean dynamics and gravity changes induced by ice melt Climatic Change, 2008.

Katsman, C.A., Sterl, A., Beersma , J.J., van den Brink, H.W., Hazeleger, W. and 15 co-authors: Exploring high-end scenarios for local sea level rise to develop flood protection strategies for a low-lying delta - the Netherlands as an example, Climatic Change, DOI 10.1007/s10584-011-0037-5, 2011.

Kauker, K. and Langenberg, H.: Two models for the climate change related development of sea levels in the North Sea - a comparison, Clim. Res., 15, 61–67, 2000.

Kendall, M.: A New Measure of Rank Correlation, Biometrika 30 (1-2): 81–89, doi:10.1093/biomet/30.1-2.81, JSTOR 2332226, 1938.

Klein, B., Pahlow, M., Hundecha, Y., Gattke, C. and Schumann, A.: Probabilistic Analysis of Hydrological Loads to Optimize the Design of Flood Control Systems, 4th International Symposium on Flood Defence: Managing Flood Risk, Reliability and Vulnerability, Toronto, Canada, 2008.

Klein, B.: Ermittlung von Ganglinien für die risikoorientierte Hochwasserbemessung von Talsperren, PhD thesis, Schriftenreihe Hydrologie & Wasserwirtschaft Ruhr- Universität Bochum, Vol. 25, 2009.

Kopp, R., Simons, F., Mitrovica, J., Maloof, A. and Oppenheimer, M.: Probabilistic assessment of sea level during the last interglacial stage, Nature 462, 863–867, 2009.

Kortenhaus, A., Buss, T., Sulz, O., Marengwa, J. and Lehmann, H.-A.: Storm Surge Protection Walls in Germany, Die Küste, 74, 200–211, 2008.

Kotz, S. and Nadarajah, S.: Extreme Value Distribution - Theory and Applications, Imperial College Press, Imperial College Press, London, 2000.

KTA 2207: Schutz von Kernkraftwerken gegen Hochwasser, Fassung 11/2004, 2004.

Lambeck, K., Woodroffe, C.D., Antonioli, F., Anzidei, M., Gehrels, W.R., Laborel, J. and Wright, A.J.: Paleoenvironmental records, geophysical modeling, and reconstruction of sea-level trends and variability on centennial and longer timescales, In: Understanding Sea-Level Rise and Variability (eds. J. A. Church, P. L. Woodworth, T. Aarup and W. S. Wilson), Wiley-Blackwell, Oxford, UK. doi: 10.1002/9781444323276.ch5, 2010.

Lang, M., Ouarda, T.B.M.J. and Bobee, B.: Towards operational guidelines for over-threshold modelling, J. Hydrol, 225, 103–117, 1999.

Langenberg, H., Pfizenmayer, A., von Storch, H. and Sündermann, J.: Storm-related sea level variations along the North Sea coast: natural variability and anthropogenic change, Cont. Shelf. Res., 19, 821–842, 1999.

Lassen, H.: Örtliche und zeitliche Variationen des Meeresspiegels in der südöstlichen Nordsee, Die Küste, 50, 65-96, 1989.

Lentz, H.: Fluth und Ebbe und die Wirkungen des Windes auf den Meeresspiegel, Otto Meissner, Hamburg, 1879.

Lowe, J., Gregory, J. and Flather, R.: Changes in the occurrence of storm surges around the United Kingdom under a future climate scenario using a dynamic storm surge model driven by the Hadley Centre climate models, Clim. Dyn., 18, 179–188, 2001.

Lowe, J. and Gregory, J.: The effects of climate change on storm surges around the United Kingdom, Phil. Trans. R. Soc., A 363, 1313–1328, doi:10.1098/rsta.2005.1570, 2005.

Lowe, J. A., Howard, T. P., Pardaens, A., Tinker, J., Holt, J., Wakelin, S., Milne, G., Leake, J., Wolf, J., Horsburgh, K., Reeder, T., Jenkins, G., Ridley, J., Dye, S., Bradley, S.: UK Climate Projections science report: Marine and coastal projections. Met Office Hadley Centre, Exeter, UK, 2009.

Lowe, J.A., Woodworth, P.L., Knutson, T., McDonald, R.E., McInnes, K.L., Woth, K., von Storch, H., Wolf, J.A., Swail, V., Bernier, N.B., Gulev, S., Horsburgh, K.J., Unnikrishnan, A.S., Hunter, J.R. and Weisse, R.: Past and Future Changes in Extreme Sea Levels and Waves. In: J.A. Church, P.L. Woodworth, T. Aarup und W.S. Wilson (eds): Understanding Sea level Rise and Variability, Wiley-Blackwell, 326–375, 2010.

Lüders, K.: Über das Ansteigen der Wasserstände an der deutschen Nordseeküste, Zentralbl. d. Bauverw., H. 50, 1936.

Mai, S.: Klimafolgenanalyse und Risiko für eine Küstenzone am Beispiel der Jade-Weser-Region, Mitteilungen des Franzius-Instituts für Wasserbau und Küsteningenieurwesen, Heft 91, 2004.

Mann, H.B.: Nonparametric Test Against Trend, Econometrica, Journal of the Econometric Society, 13, 245–259, 1945.

Mann, M.E.: On smoothing potentially non-stationary climate time series, Geophys. Res. Lett., 31, L07214, doi:10.1029/2004GL019569, 2004.

Mann, M.E.: Smoothing of climate time series revisited, Geophys. Res. Lett., 35, L16708, doi:10.1029/2008GL034716, 2008.

Markau, H.-J. (2003): Risikobetrachtung von Naturgefahren - Analyse, Bewertung und Management des Risikos von Naturgefahren am Beispiel der sturmflutgefährdeten Küstenniederungen Schleswig-Holsteins, Dissertation, Christian-Albrechts-Universität, Kiel

McGranahan, G., Balk, D. and Anderson, B.: The rising tide: assessing the risks of climate change and human settlements in low elevation coastal zones, Environ. Urbanisation 19, 17–37, 2007.

McKee Smith, J., Cialone, M.A., Wamsley, T.V. and McAlpin, T.O.: Potential impact of sea level rise on coastal surges in southeast Louisiana. Ocean Engineering, 37-1, pp. 37-47, 2010.

Meehl, G.A., Stocker, T.F., Collins, W.D., Friedlingstein, P., Gaye, A.T., Gregory, J.M., Kitoh, A., Knutti, R., Murphy, J.M., Noda, A., Raper, S.C.B., Watterson, I.G., Weaver, A.J. and Zhao, Z.-C.: Global Climate Projections. In: Climate Change 2007: The Physical Science Basis. Contribution of Working Group I to the Fourth Assessment Report of the Intergovernmental Panel on Climate Change [Solomon, S., Qin, D., Manning, M., Chen, Z., Marquis, M., Averyt, K.B., Tignor, M. and Miller, H.L. (eds.)]. Cambridge University Press, Cambridge, United Kingdom and New York, NY, USA, 2007.

Meier, D.: The Historical Geography of the German North-Sea Coast: a Changing Landscape, Die Küste, 74, 18–30, 2008.

Menéndez. M. and Woodworth, P.L.: Changes in extreme high water levels based on a quasi-global tide-gauge dataset, J Geophys Res, 115:C10011, doi:10.1029/2009JC005997, 2010.

Merrifield M.A., Merrifield S.T. and Mitchum GT.: An anomalous recent acceleration of global sea level rise, Journal of Climate, 22, 5772-5781, Doi:10.1175/2009JCLI2985.1, 2009.

Mikosch, T.: Copulas: Tales and facts, Extremes, 9, 3–20, doi: 10.1007/s10687-006-0015-x, 2006.

Miller, L. and Douglas, B.C.: Gyre-scale atmospheric pressure variations and their relation to nineteenth and 20th century sea level rise. Geophys. Res. Lett., 34, L16602. doi:10.1029/2007GL030862, 2007.

Milne, G.A., Gehrels, W.R., Hughes, C.W. and Tamisiea, M.E.: Identifying the causes of sea-level change, Nat Geosci 2, 471–478, 2009.

Mitchum, G.T., Nerem, R.S., Merrifield, M.A. and Gehrels, W.R.: Modern Sea-Level-Change Estimates, In: Understanding Sea-Level Rise and Variability (eds. J. A. Church, P. L. Woodworth, T. Aarup and W. S. Wilson), Wiley-Blackwell, Oxford, UK. doi: 10.1002/9781444323276.ch5, 2010.

Mitrovica, J.X., Tamisiea, M.E., Davis, J.L. and Milne, J.L.: Recent mass balance of polar ice sheets inferred from patterns of global sea level change. Nature 409, 1026–1029, 2001.

Mitrovica, J.X., Gomez, N., and Clark, P.U.: The Sea-Level Fingerprint of West Antarctic Collapse, Science, 323, 753, doi: 10.1126/science.1166510, 2009.

Mudersbach, C. and Jensen, J.: Non-stationarities in time series and its integration in extreme value statistics for risk management issues, Proc. of the 31st Int. Conf. on Coastal Engineering (ICCE), Hamburg, Germany, 2008.

Mudersbach, C. and Jensen, J.: Non-Stationarities in Time Series and its Integration in Extreme Value Statistics for Risk Management Issues, Proc. of the 31st International

Conference on Coastal Engineering, Vol. 2, pp. 4109–4120, World Scientific, Singapore, 2008.

Mudersbach, C. and Jensen, J.: Extremwertstatistische Analyse von historischen, beobachteten und modellierten Wasserständen an der deutschen Ostseeküste, Die Küste, Heft 75, Boyens Medienverlag, Heide i. Holstein, 2009.

Mudersbach, C.: Untersuchungen zur Ermittlung von hydrologischen Bemessungsgrößen mit Verfahren der instationären Extremwertstatistik – Methoden und Anwendungen auf Pegelwasserstände an der Deutschen Nord- und Ostseeküste, Mitteilungen des Forschungsinstituts Wasser und Umwelt der Universität Siegen, Band 1, ISSN 1868-6613, 2010.

Mudersbach, C. and Jensen, J.: Non-stationary extreme value analysis of annual maximum water levels for designing coastal structures on the German North Sea coastline, J. Flood Risk Management, 3, 52–62, doi: 10.1111/j.1753-318X.2009.01054.x, 2010.

Mudersbach, C., Wahl, T., Haigh, I.D., and Jensen, J.: Trends in extreme high sea levels along the German North Sea coastline compared to regional mean sea level changes, Cont. Shelf Res., under review (submitted in June 2011).

Müller-Navarra, S. H. and Giese, H.: Improvements of an empirical model to forecast wind surge in the German Bight, DHZ, 51, 4, 385–405, 1999.

Nakićenović, N., and Swart, R. (eds.): Special Report on Emissions Scenarios: A special report of Working Group III of the Intergovernmental Panel on Climate Change, Cambridge University Press, ISBN 0-521-80081-1, 978-052180081-5, 2000.

Nelsen, R.B.: An introduction to copulas. Lecture Notes in Statistics, 139, Springer, New York, 1999.

Nicholls R.J.: Coastal flooding and wetland loss in the twenty-first century: changes under the SRES climate and socioeconomic scenarios. Glob Environ Change 14(1):69–86, 2004.

Nicholls, R.J. and A.C. de la Vega-Leinert: Implications of sea-level rise for Europe's coasts: An introduction. Journal of Coastal Research 24, 285-287, 2008.

Nicholls, R.J.: Planning for the impacts of sea level rise. Oceanography 24(2):144–157, doi:10.5670/oceanog.2011.34, 2011.

Nicholls, R.J., Marinova, N., Lowe, J.A., Brown, S., Vellinga, P., de Gusmão, D., Hinkel, J. and Tol, R.S.J.: Sea-level rise and its possible impacts given a 'beyond 4°C world' in the twenty-first century, Phil. Trans. R. Soc. A., 369, 161–181, doi: 10.1098/rsta.2010.0291, 2011.

Oumeraci, H.: Sustainable coastal flood defences: scientific and modelling challenges towards an integrated ris*k*-based design concept, Proc. First IMA International Conference on Flood Risk Assessment, IMA - Institute of Mathematics and its Applications, Session 1, Bath, UK, 9–24, 2004.

Oumeraci, H., Jensen, J., Gönnert, G., Pasche, E., Kortenhaus, A., Naulin, M., Wahl, T., Thumm, S., Ujeyl, G., Gershovich, I. and Burzel, A.: Flood Risk Analysis for a Megacity: The German XtremRis*K*-Project, European and Global Communities combine forces on Flood Resilient Cities, Paris, France, 2009.

Pardaens, A.K., Gregory, J.M., Lowe, J.A.: A model study of factors influencing projected changes in regional sea level over the twenty-first century, Clim Dyn., 36:2015–2033, doi:10.1007/s00382-009-0739-x, 2011.

Peltier, W. R.: Global Glacial Isostasy and the Surface of the Ice-Age Earth: The ICE-5G(VM2) model and GRACE, Ann. Rev. Earth. Planet. Sci., 32, 111–149, doi: 10.1146/annurev.earth.32.082503.144359, 2004.

Petersen, M. und Rohde, H.: Sturmflut. Die großen Fluten an den Küsten Schleswig-Holsteins und in der Elbe. Wachholtz Verlag, Neumünster, 1977.

Pfeffer, W., Harper, J. and O'Neel, S.: Kinematic constraints on glacier contributions to 21st-century sea-level rise. Science 321, 1340–1343, 2008.

Pugh, D.: Changing Sea Levels: Effects of Tides, Weather and Climate, 265 pp., Cambridge Univ. Press, New York, 2004.

Pullen, T., Allsop, N.W.H., Bruce, T., Kortenhaus, K., Schüttrumpf, H. and van der Meer, J.W.: EurOtop – Wave Overtopping of Sea Defences and Related Structures: Assessment Manual, Die Küste, 73, 193 pp., 2007.

Purvis M.J, Bates P.D and Hayes C.M.: A probabilistic methodology to future coastal flood risk due to sea level rise, Coastal engineering, 55 (12), pp 1062-1073, 2008.

Rahmstorf, S.: A Semi-Empirical Approach to Projecting Future Sea-Level Rise, Science, 315, 5810, 368–370, doi: 10.1126/science.1135456, 2007.

Rahmstorf, S., Cazenave, A., Church, J. A., Hansen, J. E., Keeling, R. F., Parker, D. E. and Somerville, R. C. J.: Recent Climate Observations Compared to Projections, Science, 316, 709, doi: 10.1126/science.1136843, 2007.

Rao, A.R. and Hamed, K.H. : Flood frequency analysis, CRC Press, New York, 2000.

Reeve, D.: Risk and Reliability: Coastal and hydraulic engineering, Spon Press, ISBN: 978-0-415-46755-1, 2010.

Rohde, H.: Die Pegel auf Helgoland, Die Küste, 49, 125–141,1990.

Rohling, E., Grant, K., Hemleben, C., Siddall, M., Hoogakker, B., Bolshaw, M. and Kucera, M.: High rates of sea-level rise during the last interglacial period, Nat. Geosci. 1, 38–42, doi:10.1038/ngeo.2007.28, 2008.

Ruocco, A.C., Nicholls, R.J., Haigh, I.D. and Wadey, M.: Reconstructing coastal flood occurrence combining sea level and media sources: a case study of the Solent, UK since 1935, Natural Hazards, doi: 10.1007/s11069-011-9868-7, online first, 2011.

Salecker, D., Gruhn, A., Schlamkow, C. and Fröhle, P.: Parameterization of storm surges as a basis for assessment of risks of failure for coastal protection measures, Proc. of the 5th International short conference on applied coastal research (SCACR), Aachen, Germany, in press.

Salvadori, G. and De Michele, C.: Frequency analysis via copulas: theoretical aspects and applications to hydrological events. Water Resources Research, 40:W12511, doi: 10.1029/2004wr003133, 2004.

Salvadori, G., De Michele, C., Kottegoda, N.T., and Rosso, R.: Extremes in nature: An approach using copulas, ISBN: 1402044143, Springer, 2007.

Schölzel, C. and Friederichs, P.: Multivariate non-normally distributed random variables in climate research – introduction to the copula approach, Nonlinear Proc. Geophys., 15, 761–772, 2008.

Schöne, T., Schön, N. and Thaller, D.: IGS Tide Gauge Benchmark Monitoring Pilot Project (TIGA): scientific benefits, Journal of Geodesy, 83, 3/4, 249–261, 10.1007/s00190-008-0269-y, 2009.

Schumann, A.: Hochwasserwahrscheinlichkeiten in Theorie und Praxis. In: Blöschl und Merz (Hrsg.): Forum für Hydrologie und Wasserbewirtschaftung; Heft 30.11, ISBN: 978-3-941897-79-3, 2011.

Schüttrumpf, H.: Sea dikes in Germany, Die Küste, 74, 189–199, 2008.

Schulte-Rentrop, A. and Rudolph, E.: A sensitivity study of storm surges under climate change in the Elbe Estuary, Proc. of the acqua alta 2011, Hamburg, 2011. (available from: http://acqua-alta.de/fileadmin/design/acqua-alta/pdf/abstracts/paper/11_10/Schulte-Rentrop _full_paper_engl.pdf)

Segers, J.: Discussion of "Copulas: Tales and facts", by Thomas Mikosch, Efficient estimation of copula parameters, Extremes, 9 (1), 51–53, 2006.

Serinaldi, F. and Grimaldi, S.: Fully nested 3-copula: procedure and application on hydrological data, J. Hydrol. Eng., 12 (4), 420–430, 2007.

Shennan, I.: Holocene sea-level changes in the North Sea Region. In: Tooley MJ, Shennan I (Eds.) Sea-level changes, Blackwell, Oxford, pp 109–151, 1987.

Shennan, I. and Horton, B.: Holocene land- and sea-level changes in Great Britain., Journal of quaternary science, 17 (5-6). pp. 511-526, 2002.

Sklar, A.: Fonction de répartition à n dimensions et leurs marges. Publications de Institut de Statistique Université de Paris, 8, 229–231, 1959.

Slangen, A.B.A., Katsman, C.A., van de Wal, R.S.W., Vermeersen, L.L.A., and Riva, R.E.M.: Towards regional projections of twenty-first century sea-level change based on IPCC SRES scenarios, Clim. Dynam., doi:10.1007/s00382-011-1057-6, 2011.

Spearman, C.: The proof and measurement of association between two things, Amer. J. Psych. 15, 72-101, 1904.

Stedinger, J.R., Vogel, R.M. and Foufoula-Georgiou, E.: Frequency Analysis of Extreme Events, Chapter 18, Handbook of Hydrology, D. Maidment (ed.), McGraw-Hill, Inc., New York, 1993.

Sterl, A., van den Brink, H., de Vries, H., Haarsma, R. and van Meijgaard, E.: An ensemble study of extreme storm surge related water levels in the North Sea in a changing climate, Ocean Sci. 5, 369–378, 2009.

Sto. Domingo, N.D., Paludan, B., Madsen, H., Hansen, F., Mark, O.: Climate change and storm surges: Assessing impacts on your coastal city through MIKE flood modeling, International MIKE by DHI Conference "Modelling in a world of change", Copenhagen, 2010.

Teferle, F.N., Bingley, R.M., Williams, S.D.P., Baker, T.F. and Dodson, A.H.: Using continuous GPS and absolute gravity to separate vertical land movements and changes in sea-level at tide-gauges in the UK. Philosophical Transactions of the Royal Society of London, A, 364 (1841). 917–930. 10.1098/rsta.2006.1746, 2006.

Tomczak, G.: Die Sturmfluten vom 9. und 10. Februar 1949 an der deutschen Nordseeküste, Ocean Dynamics , Vol. 3, No. 3/4, p. 227–240, DOI: 10.1007/BF02026795, 1950.

Töppe, A. and Brockmann, T.: Tidewasserstände am Pegel Bensersiel seit 1825. Mitteilungen des Leichtweiss-Instituts für Wasserbau, H. 120, Braunschweig, 1992.

Trenberth, K.E., Jones, P.D., Ambenje, P., Bojariu, R., Easterling, D., Klein Tank, A., Parker, D., Rahimzadeh, F., Renwick, J.A., Rusticucci, M., Soden, B. and Zhai, P.: Observations: Surface and Atmospheric Climate Change. In: Climate Change 2007: The Physical Science Basis. Contribution of Working Group I to the Fourth Assessment Report of the Intergovernmental Panel on Climate Change [Solomon, S., Qin, D., Manning, M., Chen, Z., Marquis, M., Averyt, K.B., Tignor, M. and Miller, H.L. (eds.)]. Cambridge University Press, Cambridge, United Kingdom and New York, NY, USA, 2007.

Uhlig, G. and G. Sahling, G.: Long-term studies on Noctiluca scintillans in the German Bight, Population dynamics and red-tide phenomena 1968-1988, Netherlands Journal of Sea Research, 25, 101–112, 1990.

Van Gelder, P.H.A.J.M., Mai, C. V., Wang, W., Shams, G., Rajabalinejad, M. and Burgmeijer, M.: Data management of extreme marine and coastal hydro-meteorological events, J. Hyd. Res., 46(2), 191–210, 2008.

Vellinga, P., Katsman, C.A., Sterl, A., Beersma, J.J., Church, J.A., Hazeleger, W., Kopp, R.E., Kroon, D., Kwadijk, J., Lammersen, R., Lowe, J., Marinova, N., Oppenheimer, M., Plag, H.P., Rahmstorf, S., Ridley, J., von Storch, H., Vaughan, D.G., van der Wal, R.S.W., Weisse, R.: Exploring high- end climate change scenarios for flood protection of The Netherlands, International scientific assessment carried out at request of the delta committee, Scientific Report WR-2009-05, KNMI/Alterra, The Netherlands, 2008.

Vermeer, M. and Rahmstorf, S.: Global sea level linked to global temperature. doi: 10.1073/pnas.0907765106, 2009.

von Storch, H. and Reichardt, H.: A scenario of storm surge statistics for the German Bight at the expected time of doubled atmospheric carbon dioxide concentration, J. Clim., 10, 2653–2662, 1997.

von Storch, H., Gönnert, G. and Meine, M.: Storm surges – an option for Hamburg, Germany, to mitigate expected future aggravation of risk. Env. Sci. Pol. 11: 735–742, 2008a.

von Storch, H., Zorita, E. and González-Rouco, F.: Relationship between global mean sea-level and global mean temperature in a climate simulation of the past millennium, Ocean Dynamics, 58, 3/4, 227–236, 10.1007/s10236-008-0142-9, 2008b.

Wahl, T., Jensen, J. and Frank, T.: Changing Sea Level and Tidal Dynamics at the German North Sea Coastline, Proc. of the Coastal Cities Summit 2008 – Values and Vulnerabilities, St. Petersburg, Florida, USA, 2008.

Wahl, T., Jensen, J. and Mudersbach, C.: A multivariate statistical model for advanced storm surge analyses in the North Sea, Proceedings of the 32nd International Conference on Coastal Engineering, Shanghai, China, 2010.

Wahl, T., Frank, T. and Jensen, J.: Regional patterns of sea level change in the German North Sea related to global patterns – Are IPCC projections reliable for regional planning purposes, 34th IAHR world congress, Brisbane, Australia, 2011.

Wahl, T., Haigh, I., Albrecht, F., Dillingh, D., Jensen, J., Nicholls, R., Weisse, R., Woodworth, P.L.: Observed mean sea level changes around the North Sea coastline from the mid 19th century to present (in prep.).

WASA-Group.: Changing waves and storms in the Northeast Atlantic?, Bull. Am. Meteorol. Soc., 79, 741–760, 1998.

Watson, P.J.: Is there evidence yet of acceleration in mean sea level rise around mainland Australia?, Journal of Coastal Research, 27, 368–377, 2011.

Weisse, R. and Günther, H.: Wave climate and long-term changes for the southern north sea obtained from a high-resolution hindcast 1958-2002, Ocean Dyn. 57, 161–172, doi:10.1007/s10236e006e0094ex, 2007.

Weisse, R. and von Storch, H.,: Marine climate and climate change. Storms, wind waves and storm surges, Springer-Verlag, Berlin, Heidelberg, New York, 220 pp., 2010.

Weisse, R., von Storch, H., Niemeyer, H.D. and Knaack, H.: Changing North Sea storm surge climate: An increasing hazard?, Ocean and Coastal Management, doi:10.1016/j.ocecoaman.2011.09.005, 2011.

White, N.J., Church, J.A. and Gregory, J.M.: Coastal and global averaged sea level rise for 1950 to 2000, Geophys. Res. Lett., 32, L01601, doi:10.1029/2004GL021391, 2005.

Wieland, P.: Küstenfibel – Ein Abc der Nordseeküste, Westholsteinische Verlagsgesellschaft Boyens & Co., Heide, ISBN 3-8042-0494-5, 1990.

Wong, G., Lambert, M.F., Leonard, M. and Metcalfe, A.V.: Drought Analysis Using Trivariate Copulas Conditional on Climatic States, Journal of Hydrologic Engineering, 15 (2), 129–141, 2010.

Woodworth, P.L.: High waters at Liverpool since 1768: the UK's longest sea level record, Geophys. Res. Lett., 26(11), 1589–1592, 1999.

Woodworth, P.L. and Blackman, D.L.: Evidence for systematic changes in extreme high waters since the mid-1970's." Journal of Climate, 17(6): 1190–1197, 2004.

Woodworth, P.L.: Some important issues to do with long-term sea level change. Phil. Trans. R. Soc. A 2006 364, 787-803. doi: 10.1098/rsta.2006.1737, 2006.

Woodworth, P.L., White, N.J., Jevrejeva, S., Holgate, S.J. and Gehrels, W.R.: Evidence for the accelerations of sea level on multi-decade and century timescales, Int. J. Climatol. 29(6), 777–789, doi: 10.1002/joc.1771, 2009a.

Woodworth, P.L., Teferle, F.N., Bingley, R.M., Shennan, I. and Williams, S.D.P.: Trends in UK mean sea level revisited, Geophys. J. Int., 176(22), 19–30, doi: 10.1111/j.1365-246X.2008.03942.x, 2009b.

Woodworth, P.L., Pouvreau, N. and Wöppelmann, G.: The gyre-scale circulation of the North Atlantic and sea level at Brest. Ocean Sci. 6:185-190. doi:10.5194/os-6-185-2010, 2010.

Woodworth, P.L., Menendez, M., Gehrels, W.R.: Evidence for Century-time scale Acceleration in mean sea levels and for recent changes in extreme sea levels. Surveys in Geophysics, Surveys in Geophysics, 32 (4/5), 10.1007/s10712-011-9112-8, 2011.

Wöppelmann, G., Pouvreau, N. and Simon, B.: Brest sea level record: A time series construction back to the early eighteenth century, Ocean Dynamics, 56(5-6), 487–497, doi: 10.1007/s10236-005-0044-z, 2006.

Wöppelmann, G., Martin-Miguez, B., Bouin, M.-N. and Altamimi, Z.: Geocentric sea-level trend estimates from GPS analyses at relevant tide gauges world-wide, Global and Planetary Change, 57, 396–406, 2007.

Wöppelmann, G., Pouvreau, N., Coulomb, A., Simon, B. and Woodworth, P.L.: Tide gauge datum continuity at Brest since 1711: France's longest sea-level record, Geophys. Res. Lett., 35, L22605, doi:10.1029/2008GL035783, 2008.

Wöppelmann, G., Letetrel, C., Santamaria, A., Bouin, M.-N., Collilieux, X., Altamimi, Z., Williams, S.D.P. and Martin-Miguez, B.: Rates of sea-level change over the past century in a geocentric reference frame, Geophys. Res. Lett., 36, L12607, doi: 10.1029/2009GL038720, 2009.

Woth, K., Weisse, R. and von Storch, H.: Climate change and North Sea storm surge extremes: an ensemble study of storm surge extremes expected in a changed climate projected by four different regional climate models. Ocean Dyn., 56, 3–15, doi:10.1007/s10236e005e0024e3, 2006.

Yue, S., Ouarda, T.B.M.J., Bobee, B., Legendre, P. and Bruneau, P: The Gumbel mixed model for flood frequency analysis, J. Hydrol., 226 (1&2), 88–100, 1999.

Zeiler, M., Schwarzer, K., Bartholomä, A. Ricklefs, K.: Seabed Morphology and Sediment Dynamics, Die Küste, 74, 31–44, 2008.

Zhang, K., Douglas, B.C. and Leatherman, S.P.: Twentieth-century storm activity along the U.S. east coast. Journal of Climate, 13, 1748-1761, 2000.

Zhang, L. and Singh, V.P.: Trivariate flood frequency analysis using the Gumbel-Hougaard copula, J. Hydrol. Eng., 12(4), 431–439, 2007.

Appendices

A.1   Technical implementation

Most of the analyses presented in this thesis were performed and automated in MATLAB, a widely used technical computing environment distributed by MathWorks. In the following, the most important tools, which have been developed for the different types of analyses, are briefly introduced. This compilation is not meant as a detailed user manual, but provides an overview of how the different analyses steps have been conducted.

Mean sea level analyses

All relevant MATLAB functions and script files, which have been used to investigate mean sea level data from the German Bight, are shown in the flow chart of Fig. A-1. The analyses presented in Sects. 2 and 3 are based on the available high frequency data sets and time series of tidal high and low waters. First, these time series need to be read into MATLAB. As the data sets were provided by different agencies, the format was not consistent.

Import_timeseries.m reads time series with different temporal resolutions and different formats (six different formats are considered) into MATLAB.

Debug_timeseries.m performs standard quality checks, whereas suspicious data need to be visually inspected and possibly removed.

Based on the available high frequency data sets (i.e. at least hourly observations), *MSL_hf.m* calculates monthly MSL and *k*-factor values (and other parameters, such as mean tidal high and low waters and mean tidal range).

The *k*-factor time series are then tested with *k_stationary.m* for stationarity.

Non-stationary behaviour of the time series needs to be taken into account when constructing MSL values from tidal high and low water time series with the *k*-factor approach by applying *MSL_lf.m*.

Long and homogeneous MSL time series for specific sites are constructed by combining the results from *MSL_hf.m* and *MSL_lf.m*.

Finally, MSL time series for individual tide gauges (or virtual station time series) are analysed with *TS_stat.m*, as described in detail in Sect. 2.
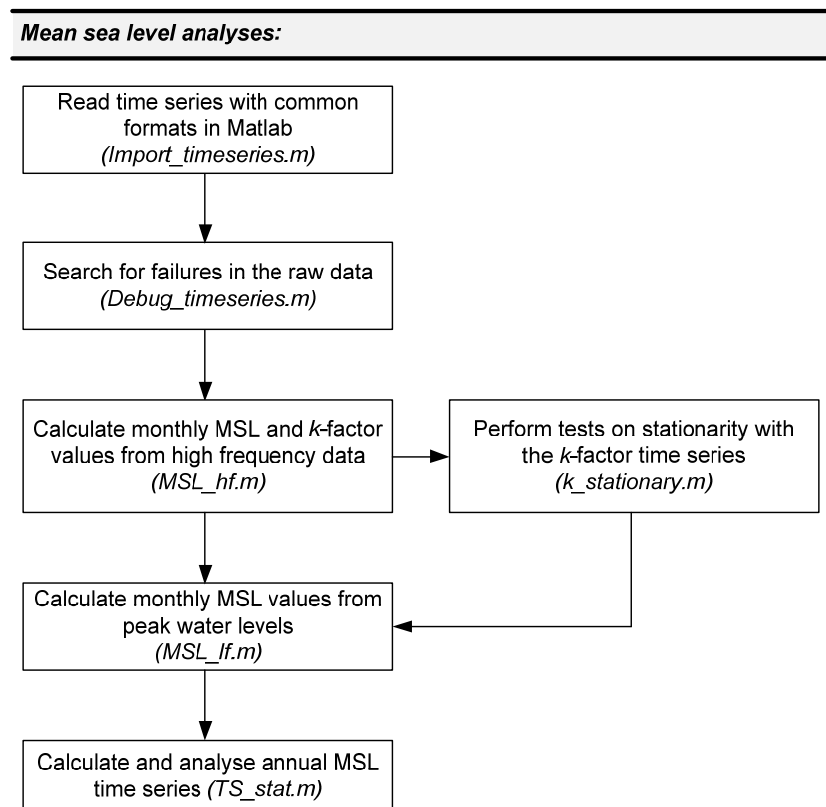

Figure A-1:   Flow chart with MATLAB functions and script files for mean sea level analyses.

Stochastic storm surge simulation

All relevant computational steps to stochastically simulate storm surge scenarios were described in detail in Sect. 4. Fig. A-2 shows the implementation procedure.

At first, an appropriate threshold value is identified from a tidal high water time series with *Thresh_Xtremes.m*.

With the selected threshold value, independent storm surge events are identified from the tidal high water time series with *XtremeEvents.m*.

Storm surge events, which are not yet digitally available, need to be digitised with a suitable software product (e.g. Didger, distributed by Golden Software). For time periods with digital high frequency data sets, identified storm surge events are directly extracted from the time series with *ExtractXtremes.m*.

ParaXtremes.m is subsequently used to parameterise all observed storm surge events (consisting of three tidal cycles).

ParaXtremes.m calls the subroutine *SmoothXtremes.m*. The latter uses a low pass filter to smooth high frequency sea level time series, which assures an accurate estimation of the 25 parameters described in Sect. 4.
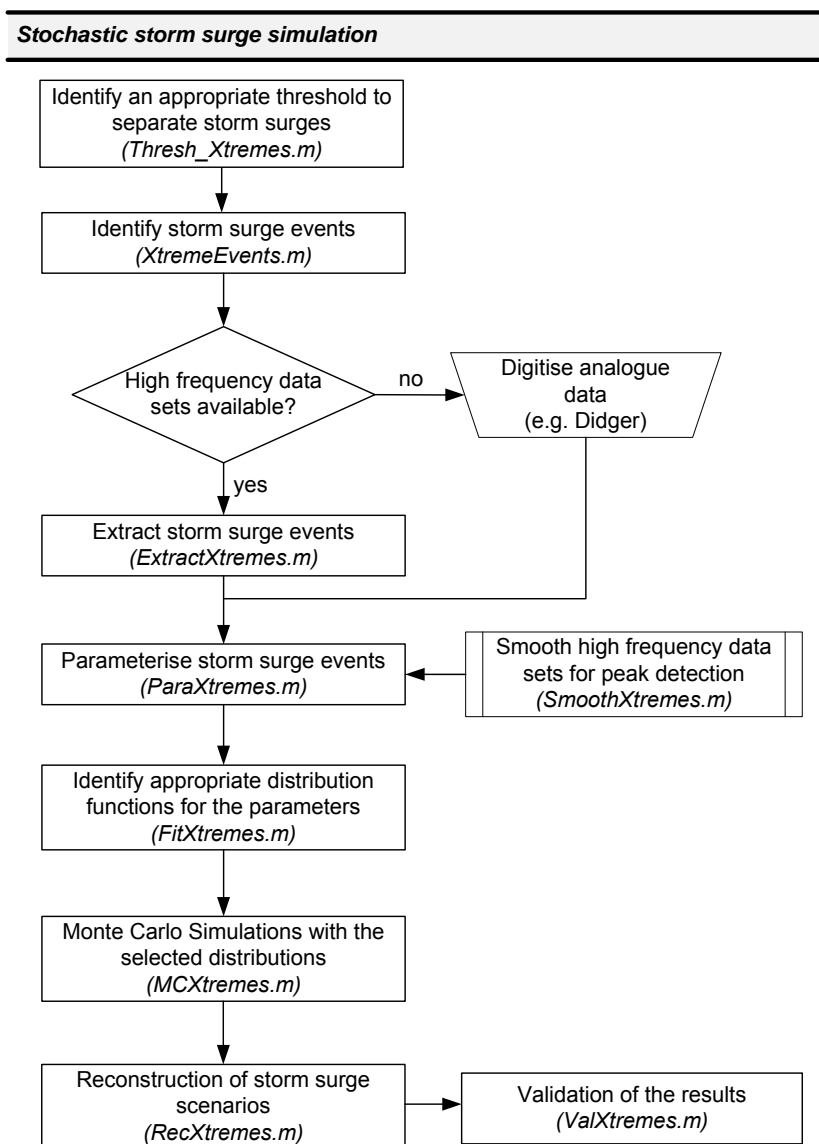

Figure A-2:   Flow chart with MATLAB functions and script files for the stochastic simulation of storm surge scenarios.

The next step consists in fitting different univariate distribution functions to the parameter time series (i.e. the output of *ParaXtremes.m*). *FitXtremes.m* uses different distribution functions and a GoF test to select a proper model for each of the parameters.

The selected distributions are subsequently used by *MCXtremes.m* to run Monte-Carlo simulations (possible future changes in MSL can be taken into account with the MSL-offset method).

Based on the simulation results, *RecXtremes.m* constructs many storm surge scenarios. Two steps of validation (see Sect. 4) can be undertaken with *ValXtremes.m*.

Multivariate statistical analyses

Bivariate and trivariate Copula models were described in Sect. 5 and applied to the simulation results from Sect. 4 to calculate joint exceedance probabilities. Fig. A-3 shows the implementation with MATLAB.

Initially, two GoF tests are applied to identify suitable Archimedean Copula functions. *GoF_EmpCop.m* uses the empirical Copula and calculates RMSEs to identify a proper bivariate or trivariate model. A graphical based GoF test can be performed with *GoF_SimCop.m*.

Once, appropriate Copula functions are identified, joint exceedance probabilities can be calculated with *Stat2DXtremes.m* for the bivariate case and with *Stat3DXtremes.m* for the trivariate case (with a FNAC model).
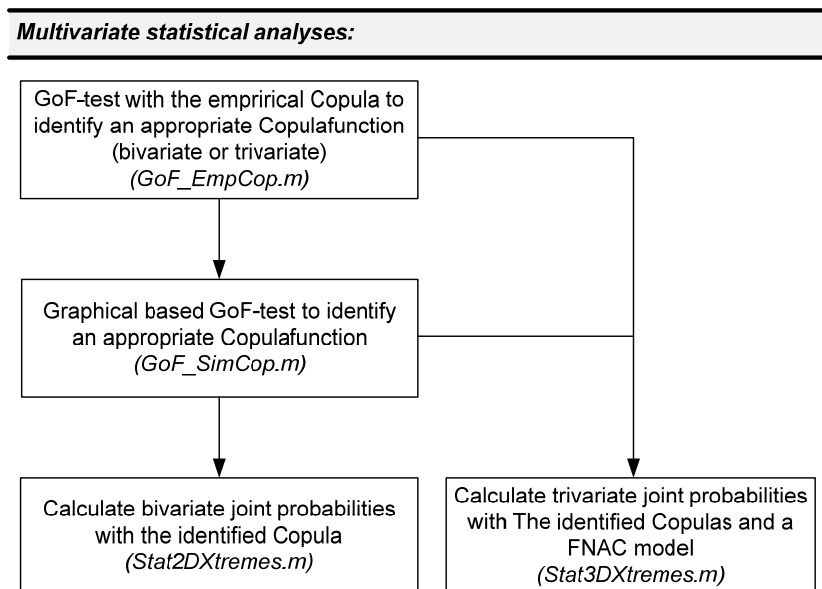

Figure A-3:   Flow chart with MATLAB functions and script files for multivariate statistical analyses.